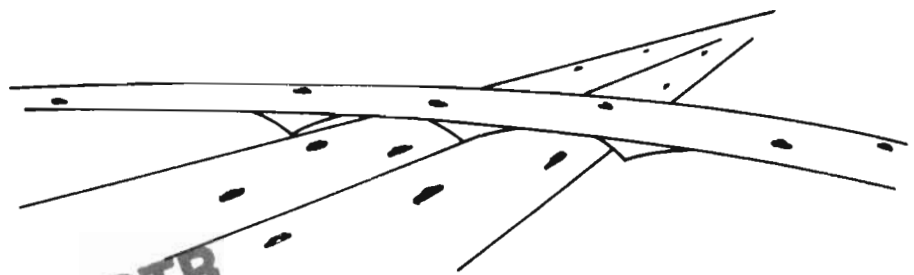


Lec



FOR LOAN ONLY CTR

# DEPARTMENTAL RESEARCH

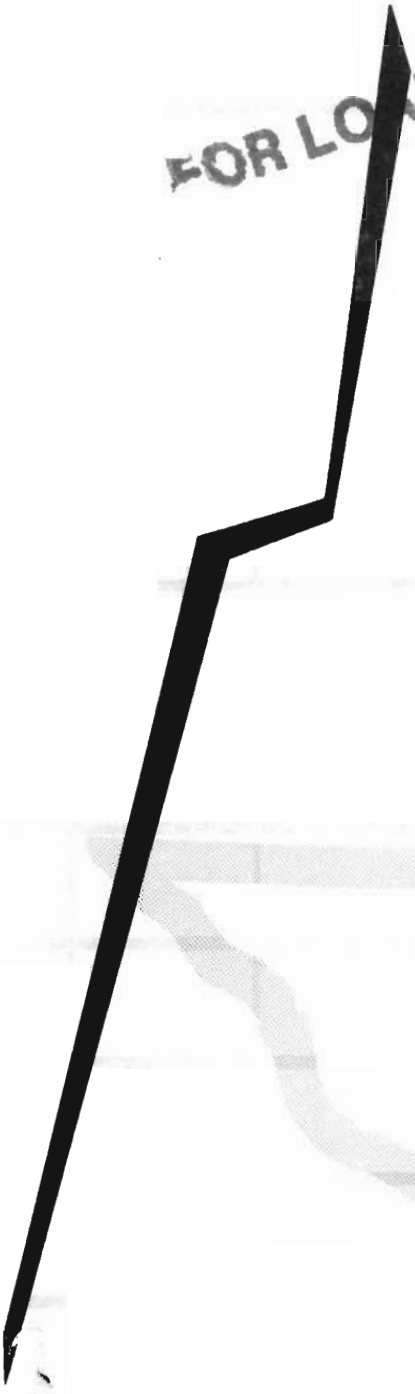
Report Number 62 - 1

## DETERMINING AND EVALUATING The STRESSES OF AN IN-SERVICE Continuously Reinforced Concrete Pavement

By M. D. Shelby  
and B. F. McCullough

For Presentation  
at the  
42nd Annual Meeting of the  
Highway Research Board

TEXAS HIGHWAY DEPARTMENT





L009373

DETERMINING AND EVALUATING  
THE  
STRESSES OF AN IN-SERVICE  
CONTINUOUSLY REINFORCED CONCRETE PAVEMENT

by

M. D. Shelby - Research Engineer

B. F. McCullough - Design Engineer



Research Section  
Highway Design Division  
TEXAS HIGHWAY DEPARTMENT

1962

## TABLE OF CONTENTS

	Page
ABSTRACT . . . . .	ii
DEFINITIONS . . . . .	iii
I. INTRODUCTION . . . . .	1
Background . . . . .	1
Design . . . . .	4
Steel . . . . .	4
Concrete . . . . .	5
II. SCOPE OF EXPERIMENT . . . . .	6
Choice of Site . . . . .	6
Nature of Experiment . . . . .	6
Discussion of Variables . . . . .	9
III. FIELD INSTALLATION AND READING PROCEDURE . . . . .	15
General Construction Procedures . . . . .	15
Field Installation . . . . .	15
Procedure for Field Readings . . . . .	17
IV. METHOD OF ANALYSIS . . . . .	19
General Approach . . . . .	19
Statistical Analysis . . . . .	19
V. CRACK PATTERN OBSERVATION . . . . .	21
Test Sections . . . . .	21
Study Sections . . . . .	26
VI. STRESSES IN REINFORCEMENT . . . . .	29
Effect of Cement Type . . . . .	29
Cyclic Nature of Stresses . . . . .	33
Steel Stress Distribution . . . . .	45
Wheel Load Tests . . . . .	50

TABLE OF CONTENTS, Continued

VII.	CONCRETE MOVEMENT . . . . .	54
	Movement at a Transverse Crack . . . . .	54
	Distribution of Movement . . . . .	57
VIII.	DISCUSSION OF RESULTS . . . . .	61
	Discussion of Factors Affecting Steel Stress . . . . .	61
	Formation of Cracks . . . . .	65
IX.	CONCLUSIONS . . . . .	69
	ACKNOWLEDGEMENTS . . . . .	71
	BIBLIOGRAPHY . . . . .	72
	APPENDIX A . . . . .	74
	APPENDIX B . . . . .	84
	APPENDIX C . . . . .	91

## A B S T R A C T

The determination of an optimum percentage of longitudinal steel in a continuously reinforced concrete pavement, for a given region, is a pressing problem facing highway engineers. To arrive at a satisfactory solution, in-place performance tests are required to check out theoretical formulae used to design these pavements. In Walker County, Texas, an area of moderate climate, the Texas Highway Department constructed an experimental continuous pavement to compare the relative performance of 0.5 per cent and 0.6 per cent longitudinal steel (yield stress of 50,000 psi). This comparison was made on the basis of performance under traffic, the transverse crack spacing, the transverse crack width and stresses in the concrete and steel due to the wheel loads as well as those due to the environmental conditions of the area.

To date both steel percentages, 0.5 per cent and 0.6 per cent, have performed satisfactorily on this project. Other factors such as cement type, time of placement, concrete properties, and the average crack spacing were found to influence steel and concrete stresses more than the steel percentage as long as slab continuity is maintained. The magnitude of effect for each of these factors is presented in the report. In addition, an empirical equation based upon a statistical analysis of the data collected during this experiment is presented. This equation shows the interrelation of each of the influencing factors and the magnitude of effect on steel stress during the early stages of the pavement life.

## DEFINITIONS

1. Slab - The portion of a continuously reinforced concrete pavement placed during one consecutive period of paving operations, such as a day. The length of the slab would be measured between consecutive transverse construction joints.
2. Slab Segment - The portion of a slab between any two consecutive transverse cracks in the pavement.
3. Test Section - A slab or part of a slab used to determine crack pattern development.
4. Study Section - The portion of a slab used to investigate the variation of a crack pattern due to other variables.
5. Test Area - The area within a slab where strain and/or movement measurements are conducted.
6. Average Crack Spacing - The average length of the slab segments within a designated test section.
7. Cycle - Any 24 hour period of time in the life of a pavement during which measurements of movement, strain, etc. are performed. The cycles are numbered consecutively with the first cycle starting with the initial placement of concrete.
8. Plugs - Gage plugs installed in concrete to provide reference points from which to measure minute movements between any two adjacent plugs.
  - a. Opening - distance between any two adjacent plugs increasing.
  - b. Closing - distance between any two adjacent plugs decreasing.

## I. INTRODUCTION

### Background

This paper is a part of a continuing study by the Texas Highway Department pertaining to the development and testing of continuously reinforced concrete pavement in Texas. (A part of the previous work conducted by the Texas Highway Department in this field was presented earlier in a Highway Research Board publication (1).

The study contained in this report pertains to an experimental continuously reinforced concrete pavement consisting of 11.3 miles of new location on Interstate Highway 45, (Project No. I 45-2(3)102) in Walker County, Texas. The project begins at the Walker-Montgomery County Line and traverses a rural area to a point approximately two miles south of Huntsville, Texas. Figure 1.1 shows the location and general layout of the project. The highway is a divided type facility consisting of two lanes in each direction. A typical section of the pavement structure on the project is shown in Figure 1.2. Beginning at the surface and moving downward, the pavement consists of a uniform eight inch slab 24 feet wide that was placed monolithically. An open graded sandstone material was used as the subbase layer, while the top six inches of the natural sand-clay soil was treated with three per cent lime (by weight) to form a stabilized layer and act as a moisture barrier to minimize moisture variations in the lower clay strata.

The ADT count on this section of roadway was approximately 5300 vehicles per day in 1960. A large percentage of this traffic consists of trucks, since this highway serves as the main artery between the Houston and the Dallas metropolitan areas. Therefore, numerous axle loads of excessive magnitude are experienced each day on this section. An analysis of loadometer data and traffic counts by the new AASHO method revealed the roadway had a traffic factor of 760 equivalent applications of an 18,000 pound axle load per day in 1960 (2).

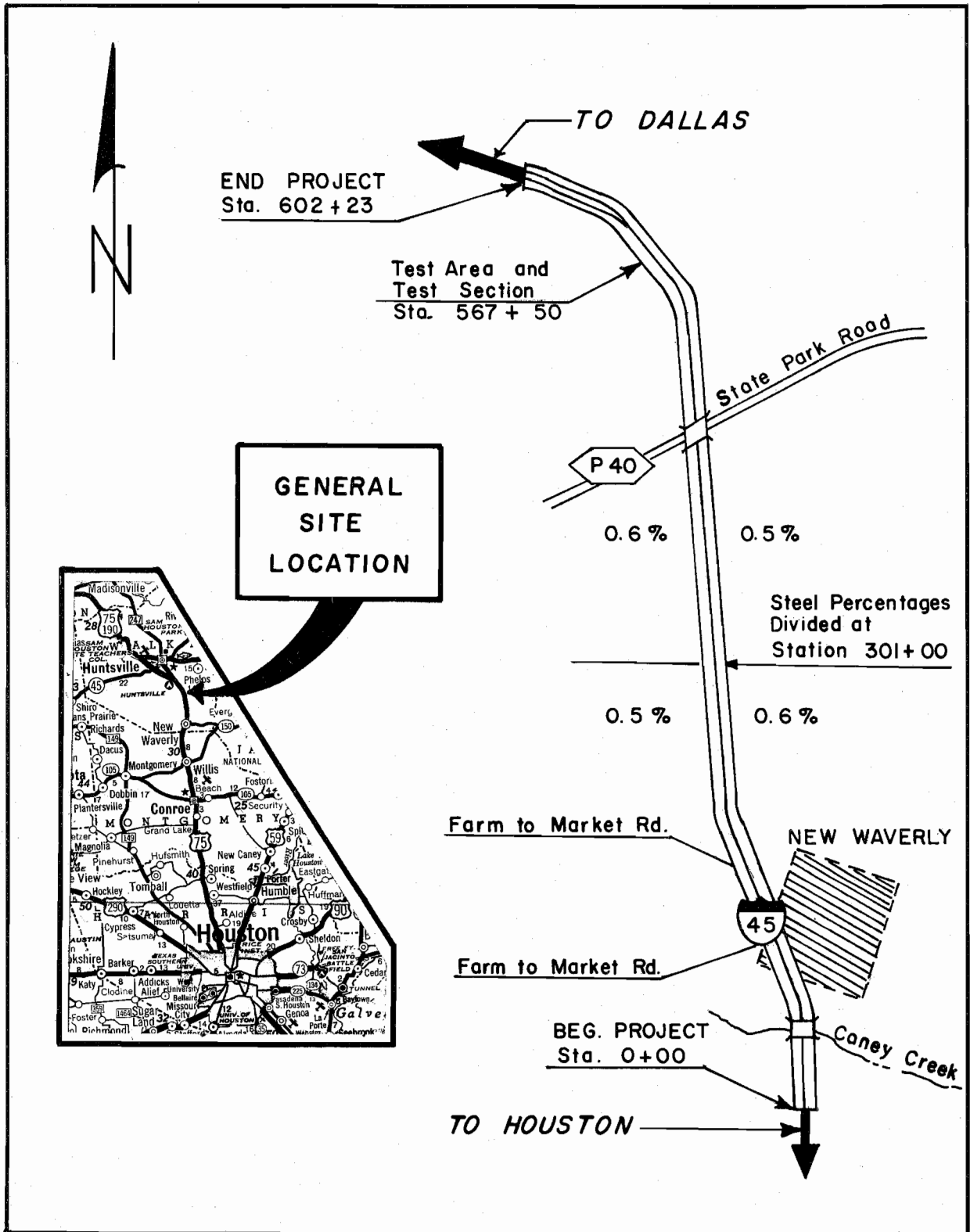
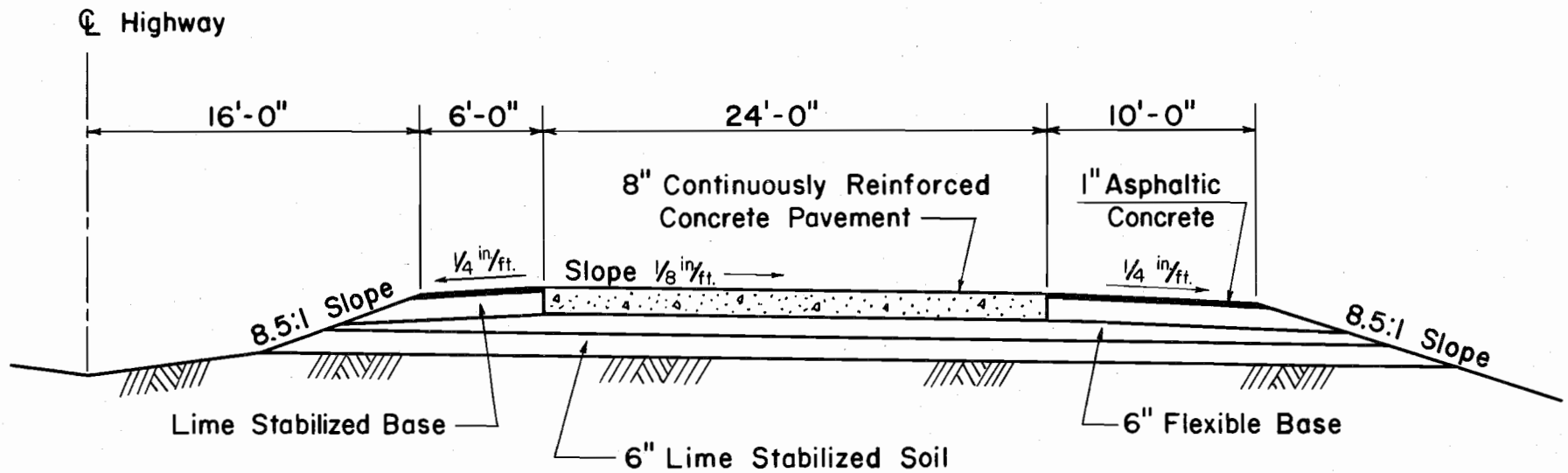


Fig. 1.1 LOCATION AND LAYOUT OF WALKER COUNTY PROJECT





**TYPICAL HALF SECTION FOR WALKER COUNTY PROJECT**

Fig. 1.2

Huntsville is located in the Southeastern part of the state which is an area of moderate rainfall and temperature. The winters are generally mild, broken by intermittent cold spells. The average yearly rainfall for the area is 45 inches while the average monthly temperature ranges from 51° F in January to 84° F in August.

### Design

An attempt was made in the design of the continuously reinforced concrete pavement on this project to arrive at a balanced stress condition between the steel and the concrete; this concept has been pointed out in recent technical papers (3). Therefore, the plans and specifications called for several unique design features to incorporate and investigate these concepts. One feature was the use of two different percentages of longitudinal steel in the concrete pavement to obtain comparative service. Another feature is the use of a controlled flexural strength specification for the concrete.

Steel. The plans called for one-half of the pavement to have 0.5 per cent longitudinal steel and the other one-half to have 0.6 per cent longitudinal steel for the purpose of making an analytical evaluation of the effect of steel percentage on performance. In order to eliminate the possibility of the unequal traffic flow on the two roadways affecting the comparison, each directional roadway was divided equally between the two steel percentages. The north end of the northbound roadway and the south end of the southbound roadway contained 0.5 per cent longitudinal steel, and the opposite ends of each of these roadways contained 0.6 percent longitudinal steel (see Figure 1.1).

The longitudinal steel for the 0.5 per cent design consisted of number 5 round bars at 7 1/2 inch centers, and number 5 round bars at 6 1/2 inch centers for the 0.6 per cent design. The longitudinal bars for both designs were located at mid-depth of slab. While the designs

are referred to as the 0.5 per cent or 0.6 per cent design, the actual percentages are 0.52 per cent and 0.59 per cent. The specifications required the use of a hard grade steel or the equivalent thereof for the longitudinal reinforcing steel, whereas intermediate grade steel was permissible for transverse bars. The transverse steel throughout the project consisted of number 4 round bars at spacings of 24 inches center to center.

Concrete. In order to prevent the design of concrete mixes that tended to produce excessive concrete strengths, a maximum flexural strength was specified in addition to the normal minimum. The specification called for the concrete to be designed with the intention of producing a flexural strength within a range of 550 psi to 675 psi at the age of seven days. The optimum design flexural strength was specified as 600 psi at the age of seven days.

A minimum cement factor of four sacks per cubic yard was allowed on this project. This represents a 20 per cent reduction from the normal minimum of five sacks per cubic yard generally prescribed. As an aid to strength control and for durability purposes, the use of two to five per cent entrained air was mandatory on this project.

## II. SCOPE OF EXPERIMENT

### Choice of Site

After a study of the project plans and a survey of the project, a location near the north end of the project was selected as the most feasible test area from the standpoint of reducing the extraneous variables to a minimum. The test area was located on a tangent section with a relatively flat grade to eliminate any possible effect of curvature or slope on the results. During the initial considerations, it was decided that the two roadways should not be placed over a week apart and should be placed during the summer months in order to minimize differential weather conditions. The first condition required the site to be near a location where the paving train would switch roadways and reverse directions. The site selected was to be placed in the month of August, a time period that would present relatively uniform weather conditions during the early life and progressively more severe conditions during the first year.

### Nature of Experiment

The field experiment was planned with the objective of determining and evaluating variations in: (1) strains in concrete and steel, (2) crack patterns and (3) crack widths due to variations in longitudinal steel percentages and climatic conditions. The ultimate goal of the experiment was the correlation and determination of the interrelation between these variables. In addition, a secondary study was initiated to study the temperature gradient of the concrete pavement during climatic cycles. Table 2.1 gives a resumé of the tests performed, instrumentation, and the reading procedures used during the experiment. As a follow-up to the previous table, Table 2.2 outlines the boundary conditions and parameters related to each measured variable. In essence, these two tables give the method of measurement and the dependent and independent variables used to attain the objectives and goals of the experiment.

TABLE 2.1  
RESUME OF VARIABLES MEASURED

<u>Variable Measured</u>	<u>Method of Measurement</u>	<u>Comments</u>
1. Steel Strain	SR-4 Electrical Strain Gages, Type A-4, Paper Back	Placed on selected steel bars in such manner as to measure transverse and longitudinal distribution of steel strains - hourly reading for observation period.
2. Concrete Strain	Berry Strain Gage with 20 inch gage length	Brass plugs placed in concrete surface at 20 inches center to center - hourly readings for observation period.
3. Crack Width	Microscope with Graduated Eyepiece - 20 power	Hourly readings made at a selected location over a crack during the observation period.
4. Slab Temperature	Stainless steel temperature bulbs connected to a Honeywell recording thermometer	Bulbs placed in the slabs in such manner as to determine temperature gradient, and obtain mid-depth temperature. Continuous readings during observation period.
5. Crack Pattern Development	Adjacent test sections in both roadways (each one about 2,000 feet long)	Periodic observations made for crack pattern development.
6. Crack Pattern Variation	Study sections 400-500 feet long throughout project.	Periodic observations of the crack pattern.
7. Concrete Properties	Lab tests and field tests	Strength tests - flexural, tensile, compression, shrinkage, elasticity and air entrainment.
8. Steel strain due to wheel load	Same as No. 1	Static and dynamic tests. Static test consist of placing wheel load at crack and at various points away from crack.

TABLE 2.2  
SCOPE OF EXPERIMENT - VARIABLES, BOUNDARY CONDITIONS,  
AND PARAMETERS

List of Parameters and Boundary Conditions

1. Weather conditions during placement of slab
2. Weather cycles, i.e. winter, summer, rainfall, etc.
3. Slab thickness
4. Subgrade, subbase, construction control, etc.
5. Concrete pavement curing procedure
6. Steel type
7. Cement type
8. Concrete properties
9. Age
10. Temperature
  - a. Slab
  - b. Air
11. Average crack spacing of slabs
12. Positions of measurement in slab
  - a. Vertical
  - b. Horizontal - transverse or longitudinal
13. Axle load
14. Steel percentage
15. Concrete strains

Outline of Experiment

Variable Measured (Dependent Factors)	Boundary Conditions* (Fixed Factors)	Parameters* (Changeable Factors)
1. Steel strain	1-6, 12a	7-11, 12b, 13, 14
2. Concrete strain	1-6, 12a	7-11, 12b, 14
3. Crack width	1-6, 12a	7-11
4. Slab temperature gradient	1, 3-7, 12b	2, 8, 9, 10b, 12a
5. Crack pattern development	1-8	9, 14
6. Variation in crack pattern	3-7	1, 8, 9, 14
7. Steel strain due to wheel loads	1-11	12b

\*Numbers listed in the column refer to the numerical sequence of parameters and boundary conditions shown above.

### Discussion of Variables

Figure 2.1 depicts the general layout of the steel and concrete strain test area. In order to simplify the installation of testing equipment, the instrumentation was placed in the median. All leads were brought to a storage box in the median through rubber and metal conduits placed six inches beneath the subbase surface. All pavement instrumentation was placed in the inside lane on both roadways. Figures 2.2 and 2.3 give a more detailed layout of the instrumentation used in each of the two roadways to appraise the first three dependent variables in Table 2.1, i.e. steel strain, concrete strain, and crack width.

The steel strains were measured by the use of waterproofed SR-4 electrical strain gages. (For a detailed description of the waterproofing procedure, refer to Appendix B.) Figures 2.2 and 2.3 portray the number and relative position of the gages. These gages were positioned so that longitudinal strain distribution along the bar and transverse strain distribution at a crack could be determined. Bar C, using Gages No. 1 through No. 7, was installed for determining longitudinal strain distribution. The distance of ten feet between Gage No. 1 and Gage No. 6 was believed to be sufficient distance to allow another transverse crack to form, hence the steel strain distribution between cracks could be determined. The gages at the preformed crack (No. 6, No. 9, and No. 11 on Figure 2.2) on Bars A, B, and C allow the transverse strain distribution at a crack to be determined. The gages on Bars A and B located away from the crack give a check on the initial longitudinal strain distribution away from the crack. Strain readings were made by using a variable resistance in a Kelvin double bridge circuit. The variable resistance has a sensitivity of one micro-inch of strain, and a range from one to 15,000 micro-inches. To alleviate errors induced by contact resistance in the switching panel and temperature effects on lead wires, dual leads were used in the wiring. The circuit for the bridge is

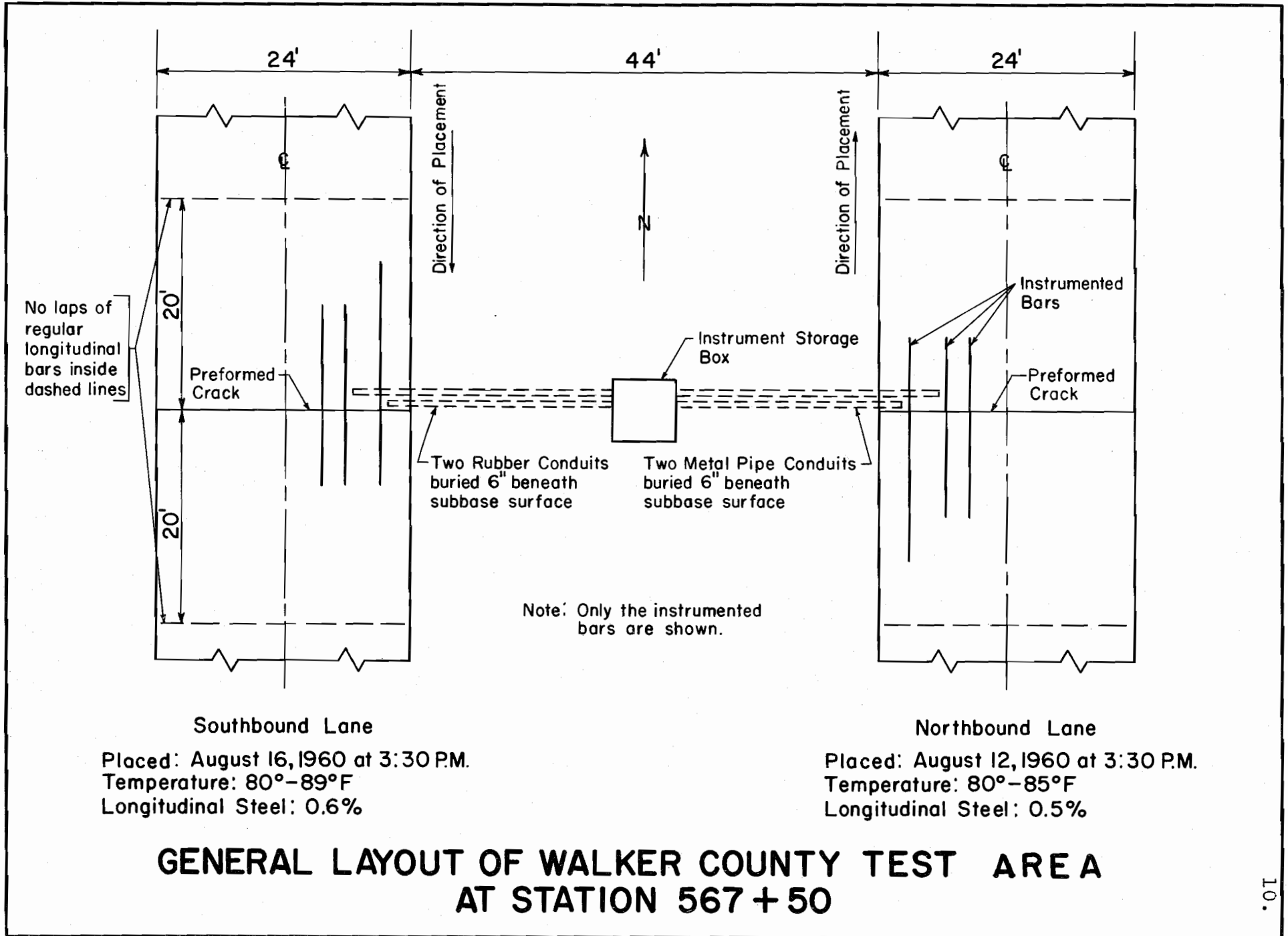
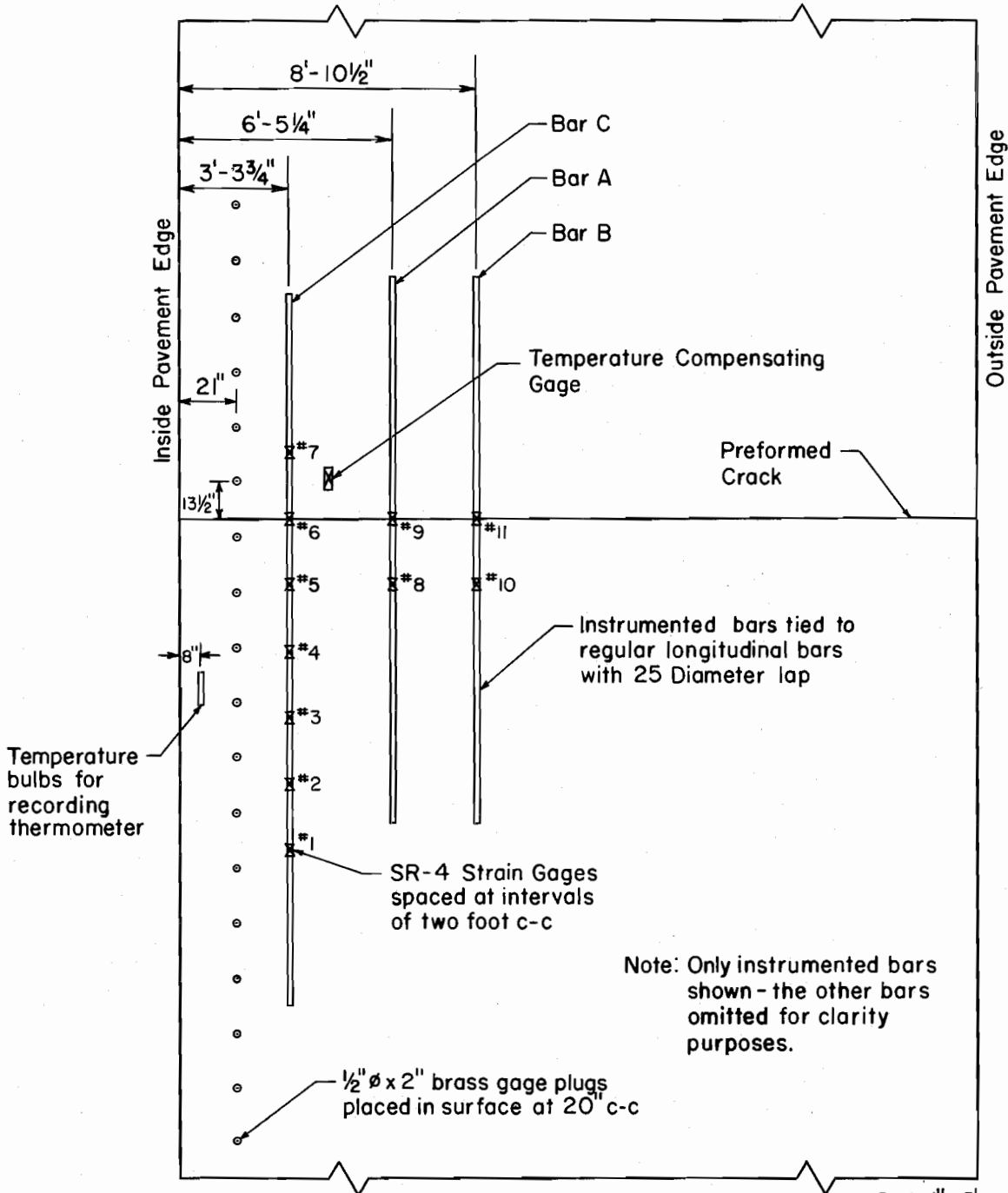


Fig. 2.1

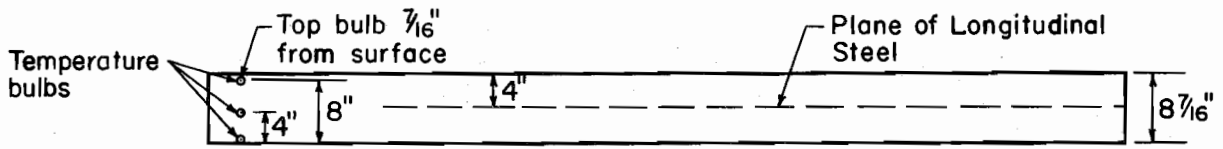




Note: Only instrumented bars shown - the other bars omitted for clarity purposes.

PLAN VIEW

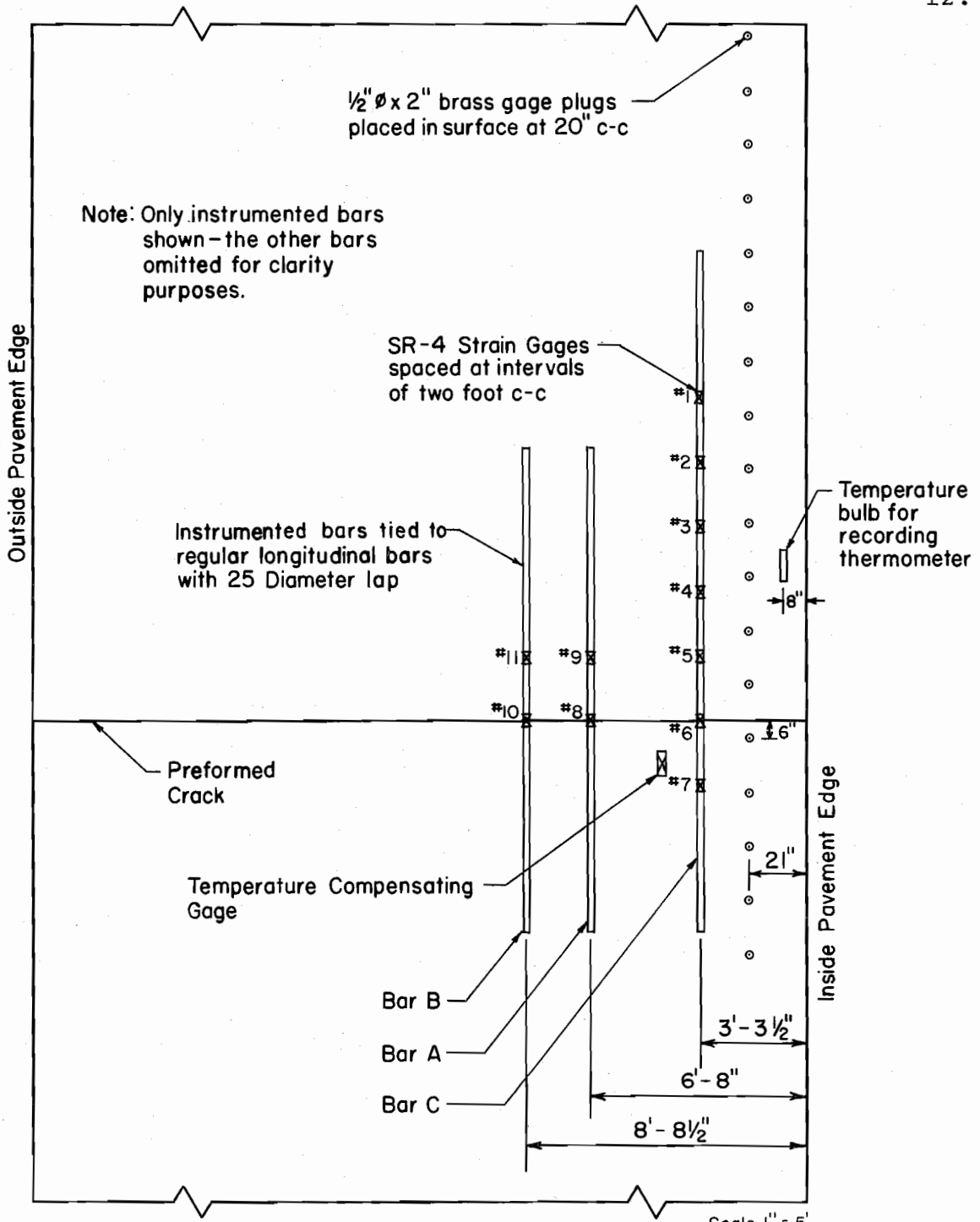
Scale 1" = 5'



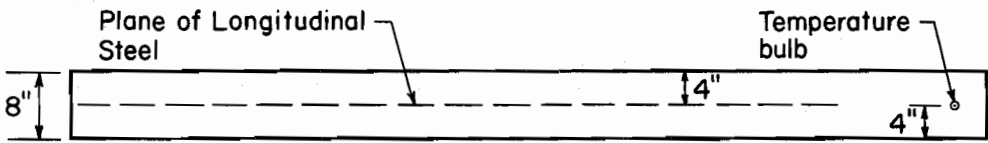
END VIEW

**DETAILED LAYOUT OF INSTRUMENTATION FOR PAVEMENT WITH 0.5% LONGITUDINAL STEEL (NBL) - WALKER COUNTY**

Fig. 2.2



PLAN VIEW



END VIEW

**DETAILED LAYOUT OF INSTRUMENTATION FOR PAVEMENT WITH 0.6% LONGITUDINAL STEEL (SBL) - WALKER COUNTY**

Fig. 2.3

schematically shown in Figure B.4 in Appendix B. The construction and calibration of the bridge has been reported elsewhere by Gersch and Moore (4). For the purpose of detecting "zero drift" due to instrument leads and variable battery voltage, a special reading procedure was used. A reading was taken on each gage in the series, then the position of the active and temperature gage in the circuit was reversed. This procedure gave a resistance reading greater and a resistance reading less than the zero resistance for each gage; hence, any movement of the zero reading could be detected.

The second variable, concrete strains, was measured on brass gage plugs placed in the surface of the concrete at 20 inch centers by the use of a Berry Strain Gage. See Figures 2.2 and 2.3 for the layout of the gage plugs. The gage used is capable of detecting movements as small as 0.0002 inch which gives a strain sensitivity of 10 micro-inches over a 20 inch gage length.

The third dependent variable, width of the crack at the surface, was determined by the use of a twenty power microscope. The microscope's eyepiece had a built in scale graduated in increments 0.001 inch with a range of 0.0 to 0.1 of an inch. The microscope was positioned in the identical spot each time a reading was taken in order to obtain comparable data.

The instrumentation for studying the temperature, the fourth dependent variable, was arranged with the goal of obtaining mid-depth temperatures for stress considerations, and determining temperature distribution through the slab. The latter study was made only in the northbound roadway. Stainless steel temperature bulbs were placed in the slab, and connected to a Honeywell Continuous recording Thermometer placed in the median.

The fifth dependent variable - crack pattern development - was evaluated by the use of a slab for each percentage of steel. These two slabs, hereafter referred to as test sections, are approximately 2500 feet long.

Each of the instrumentation sites, or test areas, are located within these test sections. The sixth dependent variable - variation in crack pattern - was studied by judiciously selecting eight short section of roadway to encompass as many parameters as possible. These short section hereafter referred to as "study sections" are 500-600 feet long.

The seventh variable - steel strain variation due to wheel loads - was evaluated through the use of a loaded truck and the strain gage installation. The load tests consisted of two phases: (1) static loading and (2) dynamic loading. Data concerning the test are presented in Table B.1 in Appendix B.

Due to the Contractor's supply problems, another variable entered the test during the construction operations. A Type III cement (high early strength) was used in the NBL, whereas a Type I cement (normal) was used in the SBL. Therefore, the stresses in the two roadways could not be compared initially without taking this factor into consideration.

### III. FIELD INSTALLATION AND READING PROCEDURES

#### General Construction Procedures

The experiment was organized in such a manner that the installation of the instrumentation could be made with no interruption of the normal paving operations. The steel bars used for instrumentation were obtained from the Contractor's stockpile and instrumented prior to construction, therefore, the test site is as representative of the general construction practices used throughout the project as possible.

The concrete was placed in accordance with Item 320, "Concrete Pavement", of the Texas Highway Department Standard Specifications (1951). The pavement was placed uniformly - full width (24 feet) and full depth. The bar mats were assembled and tied on the subbase immediately in front of the paving train. Bar chairs placed at approximately three foot centers on alternating transverse bars were used to hold the bar mats at the desired elevation. Waterproof paper curing of the concrete pavement was required for a period of three days after placement. The paving train consisted of a mechanical concrete spreader, a 34E dual drum mixer, transverse screeds, longitudinal float, hand finishing with straight edges, followed by a belting for a non-skid surface. Figures 3.1 to 3.3 portray general construction procedures on the project. Due to the hardness of the coarse aggregate, the Contractor elected to form the longitudinal joint during the normal paving operations.

#### Field Installation

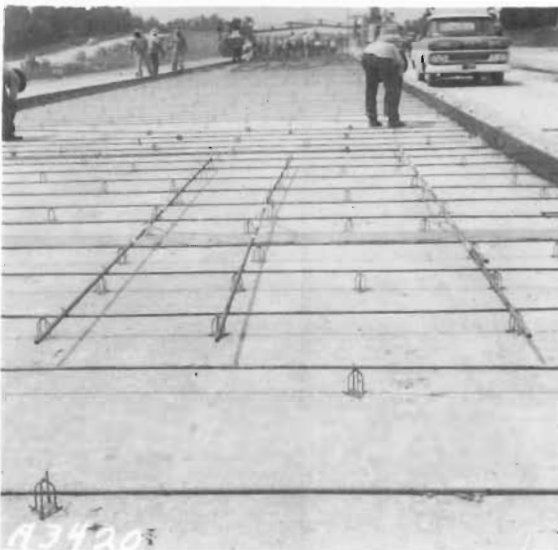
Due to the nature of the Contractors' operations, the majority of the instrument installation for each test area had to be made on the day of concrete placement. The conduits containing the wire leads for the instrumentation were buried prior to placing the forms; and the steel was positioned and the leads pulled through the conduit after the passage of the subgrade planer. After the instrumented bars were placed in



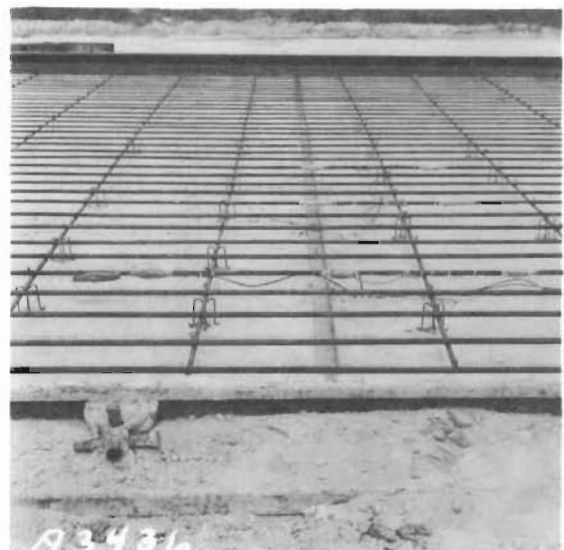
CONCRETE SPREADER AND MIXER BOOM  
Fig. 3.1



STRAIGHTEDGING CREW  
Fig. 3.2



PLACEMENT OF REINFORCING STEEL  
Fig. 3.3



NOTE STRAIN GAGES AND METAL ANGLES  
FOR PREFORMING CRACKS  
Fig. 3.4

the mat and tied, the resistance and resistance to ground of each gage was checked. Each strain gage on the steel bars, as well as the temperature bulbs, were covered with concrete by hand before the concrete spreader passed. For the purpose of controlling the formation of a transverse crack, a two inch by two inch galvanized metal angle was nailed to the subbase for the full pavement width (see Figure 3.4). The gage plugs used for measuring concrete movement were installed in the surface of the pavement immediately after the passage of the longitudinal finishing float.

A comparison of conditions during the placing operations reveals that both test areas were placed at the same time of day (3:30 PM) and at approximately equal air temperatures. This condition was felt to be a necessity if the data from the two test areas were to be compared. The curing paper was layed on both test areas at approximately 6:00 PM on the respective days of placement.

#### Procedure for Field Readings

Preliminary investigations had indicated that if the steel and concrete strain measurements were to be of any value, a number of readings would be required for the gages during each cycle (5). The strain had been found to be in a constant state of change; therefore, the significance of an isolated reading would be difficult to interpret. In this study, an attempt was made to acquire a set of strain readings at least every two hours, and in no case did the number of readings drop to less than six strain readings per 24 hour period. Several sets of strain readings were taken near the time of sunrise and during the mid-afternoon (between 3:00 PM and 6:00 PM) since these two periods represented the periods of maximum and minimum strain in a cycle. Intermediate points between the maximum and minimum values served the purpose of revealing the characteristics of the change.

In an effort to obtain an orderly arrangement for studying the data, consecutive numbers were given to each cycle during which strain measurements were taken. The first cycle after placement of the test site in the northbound lanes - the first to be placed - was designated as cycle number one. Since the southbound roadway was not placed until four days later, the initial readings were not taken in the southbound roadway until the fifth cycle. Both concrete strain and steel strain readings were taken in the northbound roadway for the first eight days of the pavement life, and hence the first three days in the southbound roadway. After these initial cycles, the concrete strain measurements were discontinued and only measurements of the steel strains were made. These subsequent measurements amounted to seven additional cycles for each roadway. It might be noted that the steel strain readings were taken over a wide spread of weather conditions which allows the results of the experiment to be applied over a wide set of conditions.



#### IV. METHOD OF ANALYSIS

##### General Approach

For background information pertaining to an explanation of the method used in analyzing the data obtained during this experiment, refer again to Table 2.2. Each variable in the table was studied for the standpoint of observing the effect of each parameter (changeable factors) on the dependent variable. For example, each of the measured parameters that could possibly affect the magnitude of steel strain such as temperature, cement type, average crack spacing, age, etc. was investigated separately. This was accomplished by investigating the effect of temperature while holding the other parameters constant insofar as possible. Then an attempt was made to combine the effect of these parameters on the dependent variable.

##### Statistical Analysis

A statistical approach was used in analyzing much of the data since numerous readings were taken during the course of the experiment. The degree of interrelationship between any two factors was determined by regression analysis techniques. The type of analysis was ideal for using an electronic computer since this equipment results in a much greater speed of calculation and enables a much broader scope of study.

A linear regression analysis was generally found as the type most adaptable to the data, which tended to confirm preliminary suppositions. The linear regression analysis results simply in a line describing the average relationship between two variables under consideration that is derived by the method of "least squares". The first order equation (linear) used in this report was the following form:

$$Y = a + b x \quad \dots \dots \dots (4.1)$$

where:

Y = the dependent or "predicted" variable,  
x = the independent or "predicting" variable,  
a,b = correlation constants.

In addition to determining the regression equation, the coefficient of determination (d) was also calculated for each equation to serve as a guide in the reliability of the analysis. This coefficient simply gives a measure of the explained variation of the dependent variable due to the effect of a variation in the independent variable (6). For example, a coefficient of determination of 0.91 for a steel-strain slab temperature regression analysis simply means that for the data analyzed 91 per cent of the change in steel strain can be attributed to changes in the slab temperature. Naturally, the higher the coefficient, the better the correlation. Values of 0.90 and greater indicate there is an excellent degree of correlation between the two variables. The coefficient of determination is obtained by squaring the coefficient of correlation.

## V. CRACK PATTERN OBSERVATIONS

Earlier in the report it was pointed out that a slab consisting of a complete day's placement of concrete for each percentage of steel was selected for the purpose of observing the crack pattern development and comparing the performance of the two steel percentages. In addition to these two test sections, eight study sections were selected for the purpose of analyzing the wide variation in average crack spacing found over the project. The studies of the data will be presented as "Test Sections" and "Study Sections" respectively.

### Test Sections

As shown in Table 2.2, the two slabs, or test sections, were used to evaluate the effect of age and steel percentage on the development of the crack pattern. In this section, the study is made from the standpoint of the average crack spacing of the slab. The average crack spacing is obtained by simply dividing the length of the slab under consideration by the number of cracks within the slab. Periodic surveys of the test sections were taken on the basis of counting the number of cracks within each station. Table 2.2 enumerates the boundary conditions involved on these test sections.

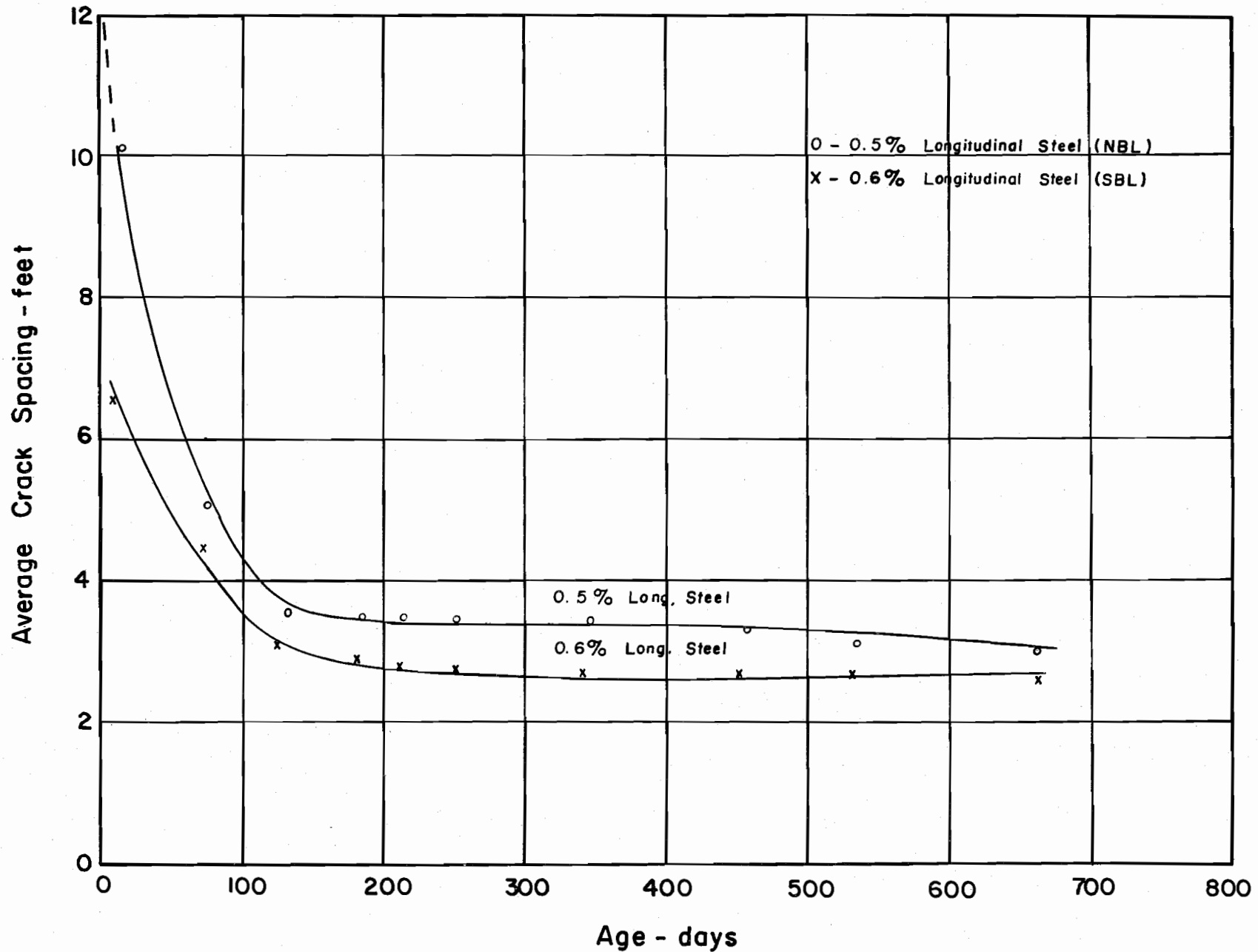
Data pertaining to the average crack spacing was difficult to attain during the first ten days since paper curing was used during the construction operations. The paper remained on the pavement surface from three to ten days depending on the rate of paving. Therefore, data for the test section during the early ages was collected by simply pulling back the paper in localized areas and recording the number of cracks. This operation was performed between sundown and sunrise to avoid any possible effect on the curing. The average crack spacing for the slab during this early period was obtained by extrapolating the values found for the short sections.

Effect of Age. Figure 5.1 shows the effect of age on the average crack spacing for both of the test sections during the first year. The average crack spacing shown on the figure is based on the entire slab length. As has been shown by other studies, the crack spacing decreases with age, but the degree of change is striking (7).

The decrease in average crack spacing from an age of ten days to 200 days is 67 per cent for the northbound roadway (0.5 per cent) and 57 per cent for the southbound roadway (0.6 per cent). This exceeds the total percentage change experienced in other states during the first five years (7). The spacing decreased rapidly during the early age, and reached a leveling out point at about 125 days. Indications are that this pavement has attained its final crack spacing. In essence, these pavements have attained a desired crack spacing during the first year of life.

Per Cent Steel. Figure 5.1 can also be used to compare the effect of steel percentage on the average crack spacing of a slab. As would be expected, there is an inverse relation between the average crack spacing and the per cent of longitudinal steel, but the relation is changing with time. Note that at an age of ten days, there is an average crack spacing differential of 4.6 feet between test sections, which is a 70 per cent difference in terms of the spacing for the 0.6 per cent section. At an age of 200 days, the difference is 0.7 of a foot or 25 per cent in terms of the spacing for the 0.6 per cent section.

It is apparent on these test sections that age is tending to nullify the effect of the two different percentages of longitudinal steel. With all other things being equal (flexural strength, curing conditions, etc.), this observation would probably hold true on other sections as long as there is a sufficient percentage of steel to satisfy the design conditions. Although there is still a 25 per cent difference in crack spacing for

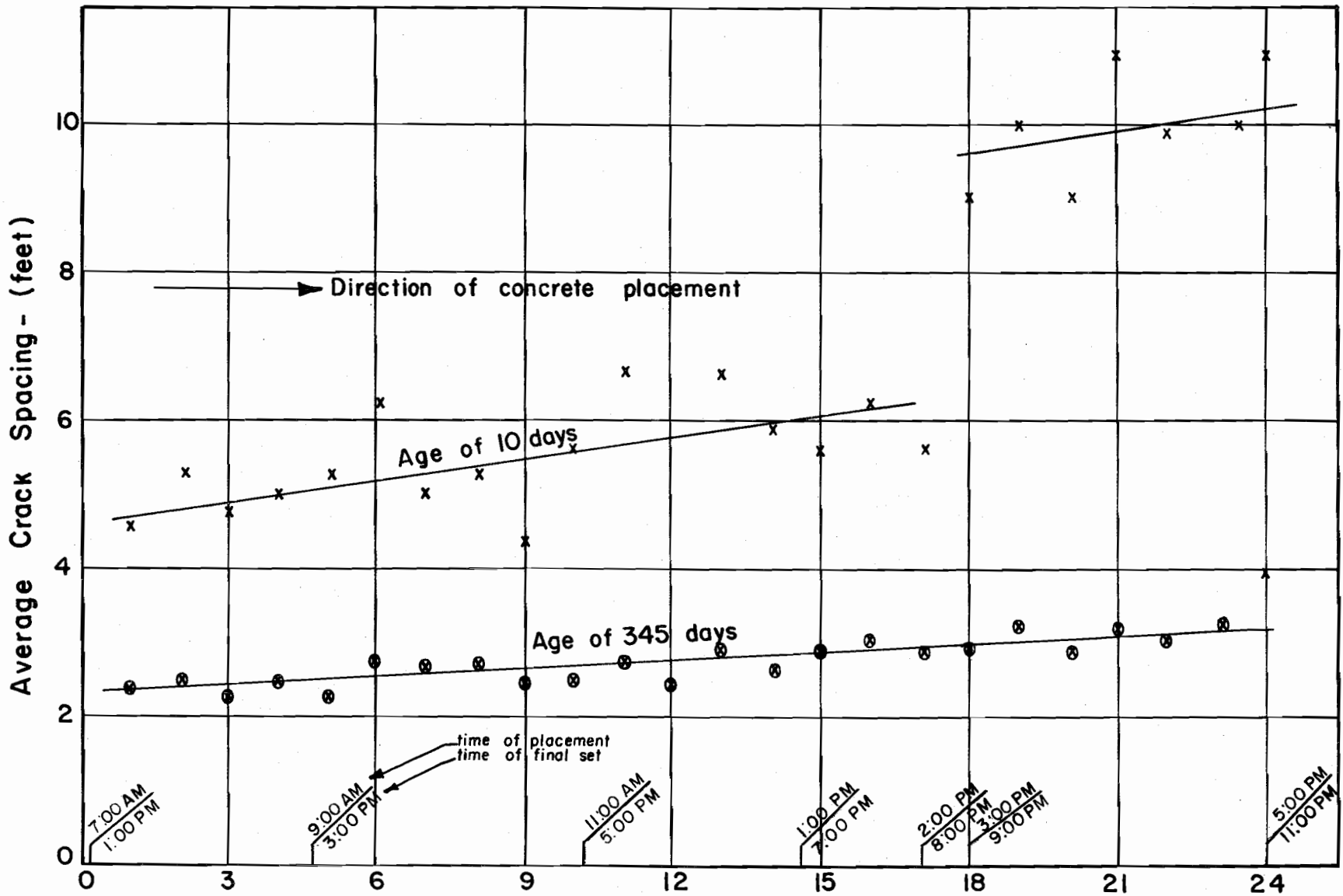


RELATIONSHIP BETWEEN AGE AND THE AVERAGE CRACK SPACING ON THE TEST SECTIONS

Fig. 5.1

a 0.1 per cent change in longitudinal steel, the relative magnitude of the difference is small. In addition to the fact that age is nullifying the effect of steel percentage, the crack spacing on both sections is well below what was considered as an optimum design maximum of six to eight feet.

Distribution of Crack Spacing. A study of the average crack spacing within each station (100 foot sections) indicated there was an uniform variation in the magnitude of the average crack spacing with distance along the slab. The average crack spacing increased in the direction of concrete placement for a given day's placement. This observation held true for both steel percentages. Figure 5.2 portrays the average crack spacing at intervals of 100 feet along the southbound slab (0.6 per cent) at the ages of 10 days and 345 days. Note in comparing the two lines that age appears to be nullifying the effect of location on the average crack spacing. At 10 days, the average crack spacing within a slab increased at a rate of 0.096 feet per station in the direction of placement, whereas the rate had reduced to 0.036 feet per station at 345 days. The top line - the relation at age of 10 days - shows a wide differential at a distance of 1700 feet from the start of the pour. The crack spacing at this point becomes much wider in relation to those experienced in the first 1700 feet. One explanation for this could be the delay in paving operations experienced at this location. In addition to distance, the time of placement based on construction records is presented on the figure along with the approximate time the concrete attained its final set. The time of final concrete set was taken at six hours after placement based upon other investigations of Texas cements (8). An examination of the temperature-time records revealed that this delay caused the final set of the concrete to occur at a time when the drop in the air temperature had started to level off. Hence, the latter part of the slab experienced very little thermal reduction from its setting temperature during the first night. Therefore, the concrete



Distance along Slab From Start of Placement (in stations)  
**EFFECT OF RELATIVE POSITION WITHIN A SLAB  
 ON THE AVERAGE CRACK SPACING - SBL (0.6%)**

Fig. 5.2

in this section had a longer period to build up strength before the thermal reduction in the next cycle was experienced. This resulted in fewer cracks in this section of slab during the initial cycles. A number of cycles occurred before this unbalanced condition was stabilized. Note that uniformity of distribution was present at an age of 345 days.

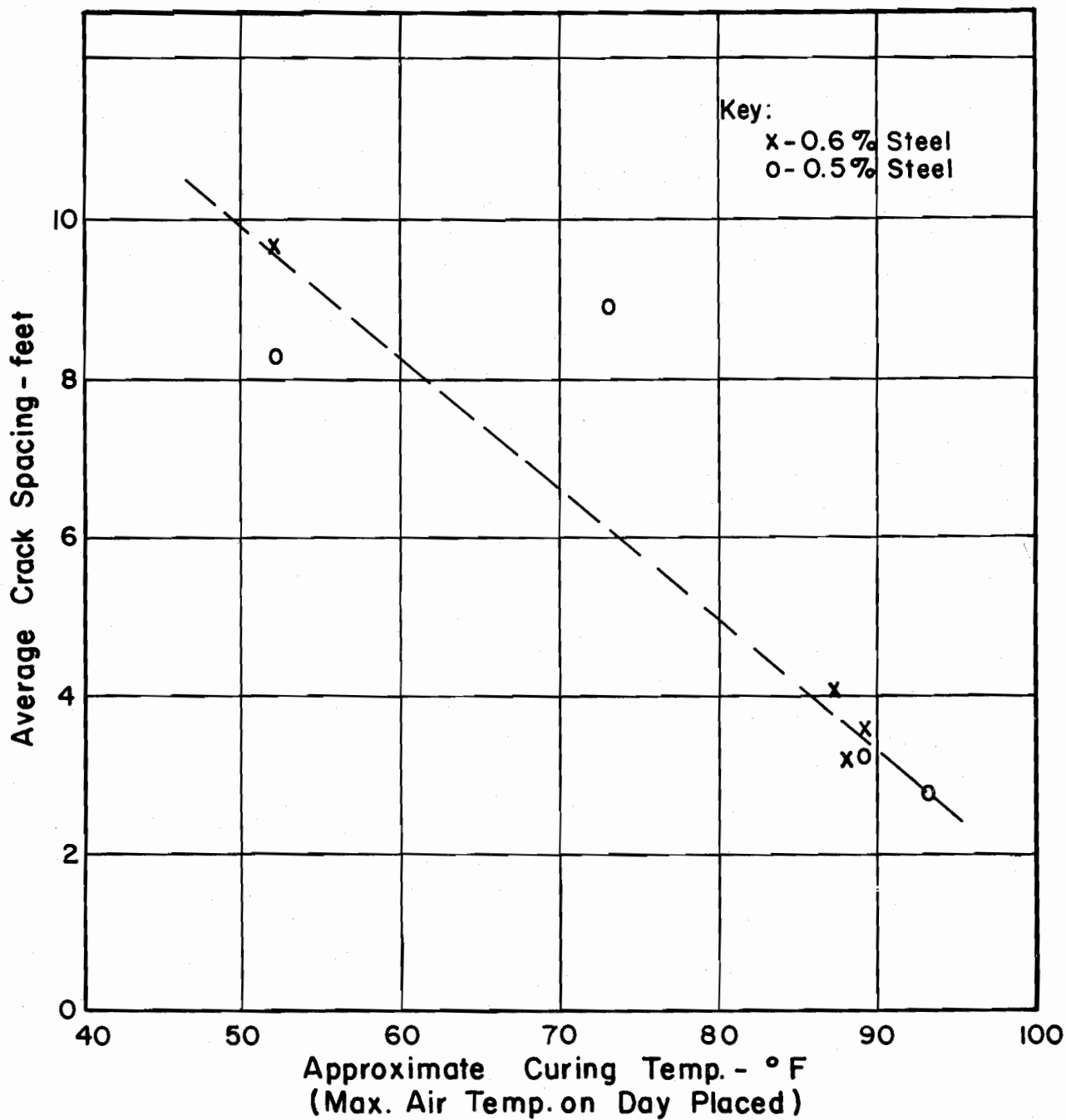
### Study Sections

In an effort to determine the reason for a wide variation in crack spacing experienced over the project, eight "study sections" were selected at various locations on the project. Each of the "study sections" had the following boundary conditions: (1) 500-600 feet long, (2) placed prior to mid-afternoon, and (3) located on level sections or relatively slight grades. In addition, the termini of all "study sections" were located 100 feet or more from the nearest transverse construction joint to eliminate the effect of any possible end action. The locations were selected in such manner that within a "study section" the range of flexural strengths did not exceed 40 psi.

When analyzing the data, it became apparent that an insufficient number of study sections was selected. In essence, an attempt was made to evaluate the effect of four variables (age, average flexural strength, percent steel, and curing temperature) on the average crack spacing with only eight "study sections". Generally it was not possible to hold three of the variables constant and vary the fourth due to the lack of data.

Curing Temperature. The curing temperature selected for the purpose of this analysis was the maximum air temperature recorded by the U. S. Weather Bureau on the day of placement. Figure 5.3 shows there is an inverse relation between the average crack spacing and the curing temperature. This observation agrees with the results of other investigations. Note the curing





**AVERAGE CRACK SPACING VERSUS APPROXIMATE CURING TEMPERATURE FOR STUDY SECTIONS**

Fig. 5.3

temperature has a pronounced effect on the crack spacing in that a reduction of 40° in the maximum curing temperature results in an increase of 4.5 feet in the average crack spacing.

Per Cent Steel. Each of the factors referred to thus far contain both the 0.5 per cent and 0.6 per cent longitudinal steel "study sections". It is apparent from all these studies that the differences between the other variables are more significant in influencing the crack pattern than the 0.1 per cent difference in longitudinal steel present in the project.

## VI. STRESSES IN REINFORCEMENT

For the purpose of analyzing the stresses in the longitudinal steel, data were collected in the form of strain. These strain measurements were made at hourly intervals during the first eight days and three days after placement in the northbound roadway (0.5 per cent) and southbound roadway (0.6 per cent) respectively. After these initial measurements, hourly strain measurements were recorded through a 24 hour period at periodic intervals during the first year of life.

The strain measurements were converted to stress on the basis of the procedure outlined in Appendix C. The steel stresses were then studied from the standpoint of cement type, cyclic behavior, and distribution along the longitudinal bars.

### Effect of Cement Type

A study of the strain versus time plots for the gages located at the transverse control cracks on both pavements showed that the northbound roadway had a much higher strain immediately after the crack occurred than the southbound roadway. A comparison of the strain variation was made by computing the ratio of steel strains at the transverse cracks in each of the roadways as follows:

$$\text{Ratio, } R = \frac{\text{Increase in Steel Strain in NBL @ Failure}}{\text{Increase in Steel Strain in SBL @ Failure}} \dots (6.1)$$

$$R = 4.3$$

In other words, the longitudinal steel of the northbound roadway (0.5 per cent) had approximately four times as much stress at the crack after the concrete failed in tension (crack formed) as the southbound roadway (0.6 per cent). Identical weather conditions during the early life precludes this as a possibility for the high ratio, and rational reasoning would not credit the magnitude of the ratio solely to the small difference

in the longitudinal steel percentage. This reasoning leads to the possibility that the major part of this difference is due to the two types of cement used. Since Type III cement (high early strength) was used in the northbound roadway, whereas, Type I cement (normal) was used in the southbound roadway, it might be tentatively surmised that the use of Type III cement with continuously reinforced concrete pavement can produce undesirable results.

Figure 6.1 gives a graphic portrayal of the effect of cement type on steel stresses during the early curing period. The dashed portion of each of the relations is the change in the steel stress conditions at the time of pavement cracking. Note the change in stress magnitude in both cases. Upon cracking, the stress in the steel goes from approximately 500 psi to 4,500 psi with Type I cement, a difference of 4,000 psi. With the Type III cement, the stress in the steel goes from 2,000 psi to 20,000 psi, a difference of 18,000 psi. The cracking in concrete with a Type III cement is of an explosive nature.

As background for an explanation of the extreme differential in stress levels, the following observations should be retained from Figure 6.1. First, the failure in Type I occurs at approximately 14 hours, whereas the failure in Type III does not occur until an age of 33 hours - which is in the second 24-hour cycle. For an understanding of the forces involved in a continuous pavement, before and after cracking, examine the simplified free-body diagrams in Figure 6.2. It is pointed out here that periods of concrete contraction are the ones of major concern with this type of pavement.

On the left side of the picture, the conditions before cracking in the top portion of the picture and after cracking at the bottom are presented. On the right, the free body or force diagram for each of these conditions (neglecting the effect of subbase friction) is shown. Note that in the force diagram

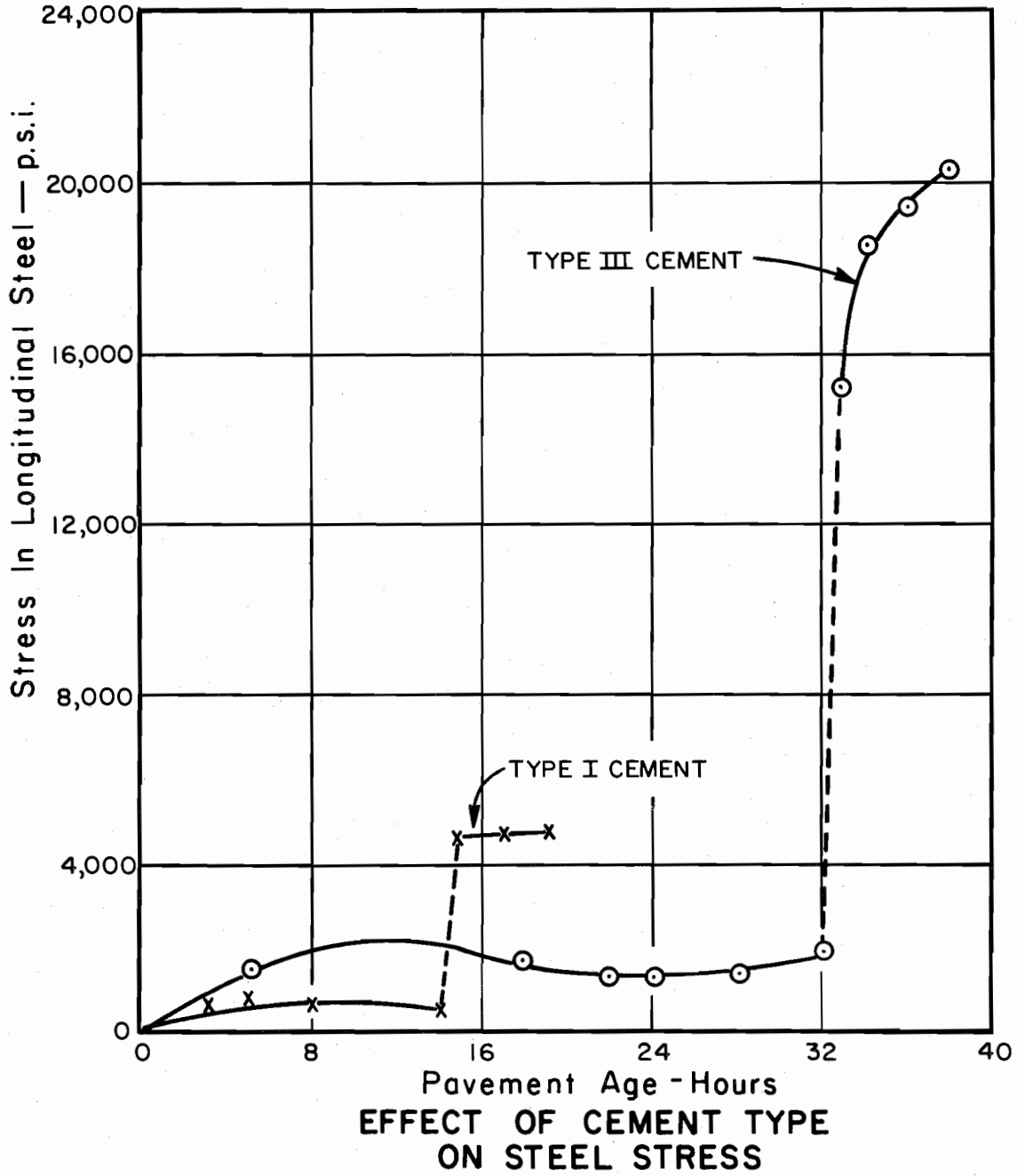
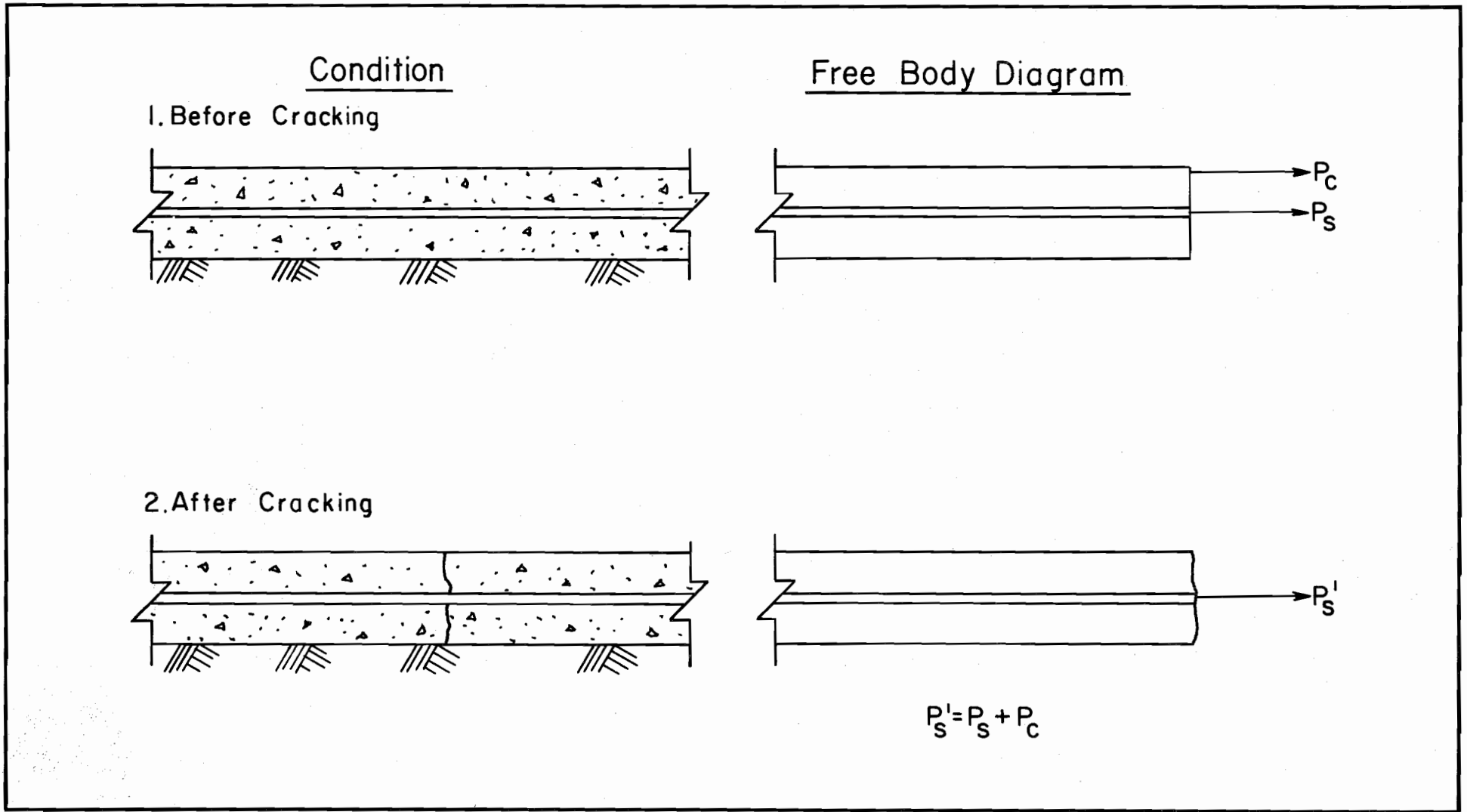


Fig. 6.1



STUDY OF FORCE CONDITIONS  
BEFORE AND AFTER  
CONCRETE CRACKING

Fig. 6.2

for the period prior to cracking, the forces developed in the pavement by volumetric changes are carried by the concrete and the steel. After the crack occurs, the concrete cannot carry tensile forces, therefore, the steel must carry the total force developed. Hence, the tensile stress in the steel will always be greater at a crack than in the interior of a slab.

Now with the concept of the steel carrying the total force at a crack (from Figure 6.1), and the observation from Figure 6.2 that the concrete cracked at 14 hours with Type I cement and at 33 hours with Type III cement, an explanation of the observed differential stress levels is forthcoming. The basic difference between Type I and Type III cement is that Type III attains its strength much more rapidly than Type I, especially during the first 72 hours.

At the time of fracture, the Type I cement had attained a strength of only 40 psi and the Type III had attained a strength of 220 psi (9). This means that approximately 2,500 pounds of force were dropped into each steel bar when the Type I cement was used, whereas up to 11,000 pounds of force were dropped into each bar with the Type III. Hence, the reason for the difference in steel-stress levels for the two cement types after cracking.

#### Cyclic Nature of Stresses

The stresses experienced in each of the operating gages located at the preformed cracks in each roadway were of a cyclic nature. Figures A.1 through A.9 in Appendix A portray the variation of stress with time experienced at each of the gages. It was noted that the stresses generally ranged between a maximum and minimum during each 24 hour period. These daily maximum and minimum stresses were not constant, but varied with time. In addition to these observations, also note that the lesser steel percentage had a smaller minimum strain in addition to the logical higher maximum

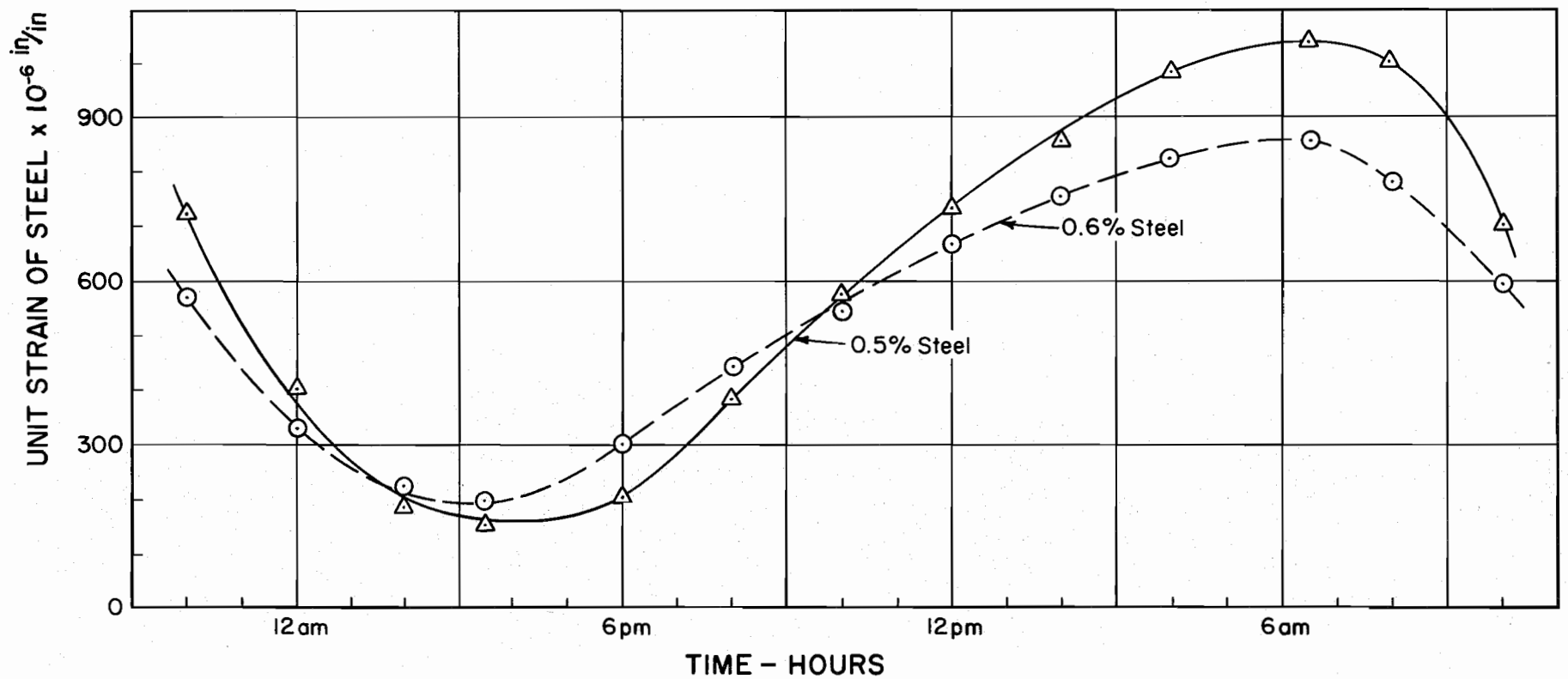
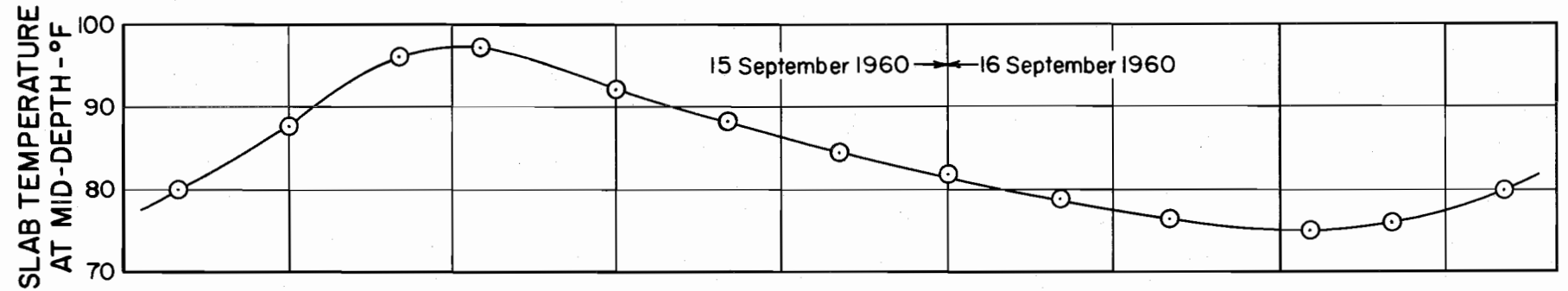
strain. The data presented in the stress-time relations were accumulated under a wide variety of weather conditions, such as: air temperature extremes ranging from 25° F to 95° F, summer and winter seasons, dry to humid atmospheric conditions, sunny and cloudy days. Therefore, any relations derived would encompass a variety of weather conditions.

With these general observations in mind, first, an investigation was conducted to determine the factors influencing each cycle. Next, the possible factors affecting the variation in maximum and minimum stress between cycles were investigated.

A comparison of the stress-time relation reveals the maximum stress generally occurs during the period of minimum temperature and vice versa. This agrees with the observation of an inverse relation between steel stress and temperature made in the past during other investigations (10). Figure 6.3 compares the typical fluctuation in steel stress and temperature during a daily cycle. As would be rationalized, the data shows under normal atmospheric conditions the maximum strain for the cycle will be experienced just before the sun rises, and the minimum strain experienced during mid-afternoon. Since air temperature measurements and slab temperature measurements at various depths were taken for each of the cycles, the question is "which of the temperatures most accurately reflect the changes in steel stresses". After selecting the most appropriate temperature, this temperature could be used in all the other analyses.

Comparing Strain-Temperature Correlations at Various Depths. In the northbound roadway, a constant record of the slab temperature near the top, near the bottom, and at the mid-depth of the slab was kept along with strain measurements (see Figure 2.2). In an attempt to determine which temperature offered the best correlation, a linear regression equation predicting steel strain in terms of temperature at the various depths





**RELATION BETWEEN STEEL STRAIN AND SLAB TEMPERATURE AT MID-DEPTH DURING A TYPICAL CYCLE**

Fig. 6.3

was calculated for the first eight cycles. In addition, the average of the three temperatures - top, mid-depth, and bottom - was used to predict the steel strain.

Table 6.1 gives the coefficient of determination for the strain-temperature relations at different slab depths for Gage Nos. 6 and 11 in the northbound roadway. These two gages were selected since they were located at the preformed crack, and furthermore, they showed the greatest variations in strain. An examination of the table reveals the best correlation is obtained by using the average of three temperatures. This observation also tends to verify conclusions arrived at during other investigations (10). The mid-depth also gives excellent correlation and in actuality there is very little difference in the degree of correlation between the mid-depth temperature and the average of the three temperatures.

The reason for this observation is evident after a study of the slab temperature - time relationships. Generally, the slab temperature at the top of the pavement attains its minimum and maximum magnitude for a cycle approximately two hours before the temperature at mid-depth, whereas the converse is true for the bottom temperature. Hence, the average temperature nullifies this time lag and gives the best correlation. The temperature at the mid-depth also gives excellent correlation since it is approximately the same as the average temperature.

Effect of Temperature on Steel Stress. Since the average slab temperature gives the best correlation, it was used to study the effect of temperature on steel stress in each of the cycles for each of the roadways. As reported in the preceding section, a linear equation was used to predict the steel stress at a crack in terms of the average slab temperature. Using the format of Equation 4.1, the stress-temperature equation is

TABLE 6.1

COMPARING CORRELATION OF SLAB TEMPERATURE AT  
VARIOUS DEPTHS WITH STEEL STRAIN<sup>1</sup>

CYCLE NO.	COEFFICIENT OF DETERMINATION FOR LINEAR REGRESSION ANALYSIS							
	GAGE 6 (NBL) <sup>2</sup>				GAGE 11 (NBL) <sup>2</sup>			
	Slab Temperature				Slab Temperature			
	Mid- depth	Top	Bottom	Average	Mid- depth	Top	Bottom	Average
1	0.283	0.137	0.483	--	0.041	0.049	0.005	--
2	0.695	0.776	0.362	--	0.417	0.594	0.138	--
3	0.935	0.498	0.511	0.920	0.838	0.756	0.183	0.902
4	0.957	0.945	0.849	0.980	0.878	0.959	0.782	0.938
5	0.918	0.881	0.744	0.973	0.832	0.898	0.635	0.914
6	0.991	0.784	0.725	0.983	0.974	0.812	0.674	0.980
7	0.900	0.913	0.564	0.987	0.992	0.751	0.780	0.978
8	0.996	0.902	0.865	0.994	0.987	0.920	0.840	0.996

<sup>1</sup>Data from linear regression analysis comparing slab temperature at various depths with longitudinal steel strain.

<sup>2</sup>Gages 6 and 11 were located at the preformed crack in the NBL.

defined as follows:

$$S_s = S_o - K_s T_a \quad \dots \dots \dots (6.2)$$

where:

$S_s$  = stress in the longitudinal steel for any given temperature,  $T_a$  psi.

$S_o$  = stress in the longitudinal steel at  $0^\circ$  F, psi.

$K_s$  = rate of change in the longitudinal steel stresses due to temperature change, psi/ $^\circ$  F.

$T_a$  = average temperature of slab,  $^\circ$  F.

Table 6.2 gives the values of the constants " $S_o$ " and " $K_s$ " for each of the cycles during which steel strain measurements were taken. Values of these constants are presented for gages at the transverse cracks in both the northbound roadway (0.5 per cent) and southbound roadway (0.6 per cent). It is pointed out that these constants only apply to the cycle under consideration. The reason for the omission of values for the southbound roadway during the first several cycles is that this roadway was not placed till five days after the northbound roadway. Figure 6.4, which shows the relation between stress and temperature for a typical cycle, can be referred to for a graphic illustration of the meaning of these constants. The value of " $S_o$ " is obtained by simply projecting the regression line to the intersection of the  $0^\circ$  F temperature line, whereas the value of " $K_s$ " simply reflects the slope of the regression line.

If the first three cycles after placement were deleted, it was found that the coefficient of determination for each regression analysis is generally in excess of 0.90. The majority of the coefficient values fall between 0.95 and 0.99. This is an excellent degree of correlation between the two variables. As pointed out earlier, these values mean that 95 per cent to 99 per cent of the change in steel stress within a cycle can be attributed to a change in slab temperature.

TABLE 6.2

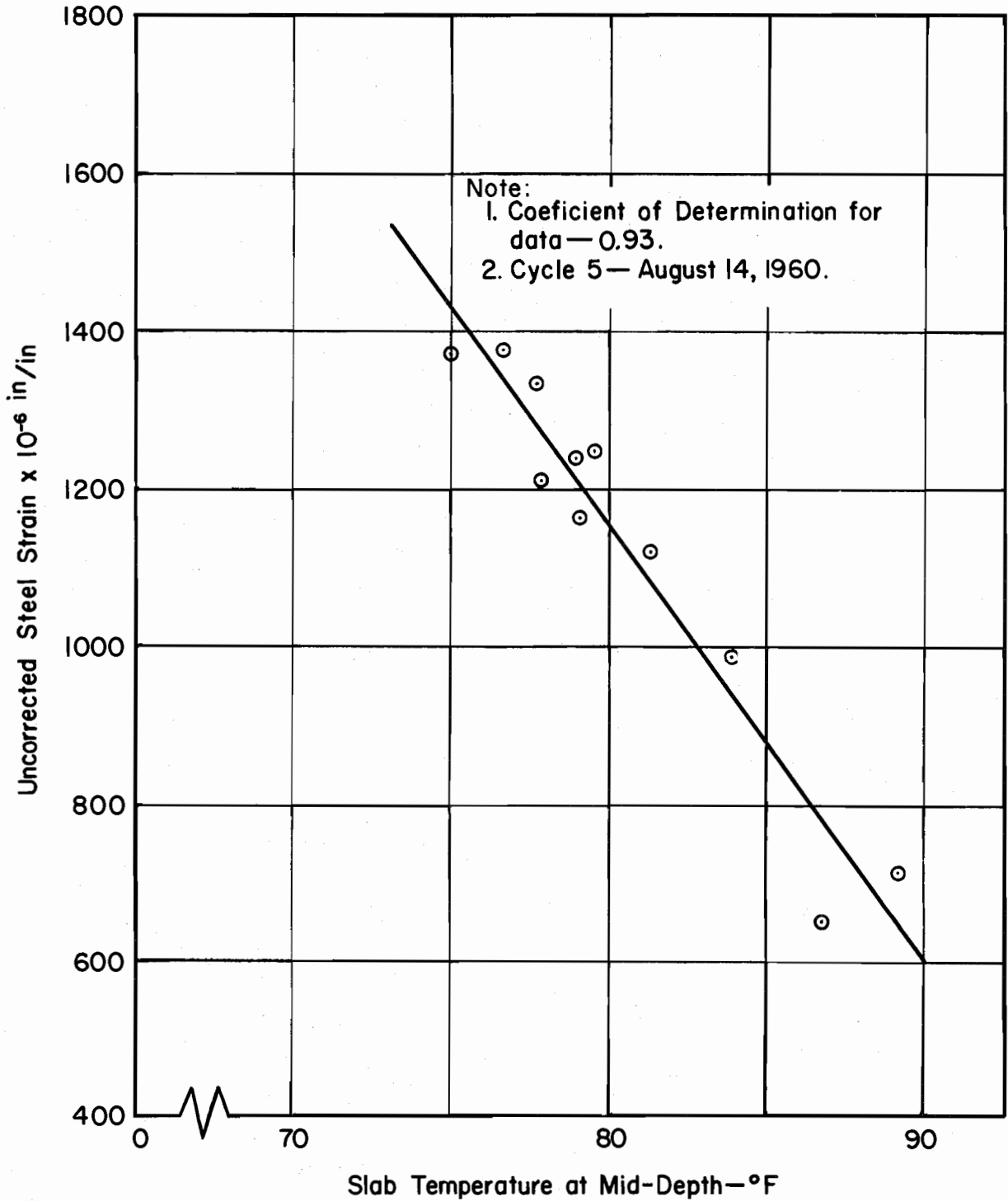
VALUES OF REGRESSION CONSTANTS FOR STRESS EQUATIONS FOR GAGES AT TRANSVERSE CRACKS

Linear Regression Analysis

CYCLE	NBL GAGES				SBL GAGES					
	6A		11A		8B		10B		3B <sup>1</sup>	
	S <sub>O</sub> <sup>1</sup>	K <sub>S</sub> <sup>1</sup>	S <sub>O</sub>	K <sub>S</sub>	S <sub>O</sub>	K <sub>S</sub>	S <sub>O</sub>	K <sub>S</sub>	S <sub>O</sub>	K <sub>S</sub>
1	11,170	103	--	--	--	--	--	--	--	--
2	13,530	132	--	--	--	--	--	--	--	--
3	131,180	1315	127,230	1266	--	--	--	--	--	--
4	159,240	1629	200,700	2126	--	--	--	--	--	--
5	125,000	1239	164,410	1681	--	--	--	--	--	--
6	143,210	1480	169,650	1763	6,510	69	3,170	51	--	--
7	159,950	1674	187,480	1959	86,800	889	90,320	945	14,040	147
8	164,990	1716	202,370	2153	89,000	892	88,630	903	--	--
9	101,530	1005	125,960	1282	73,020	684	73,870	707	59,180	553
10	94,130	941	112,030	1152	74,580	729	77,080	780	58,890	580
11	99,350	1065	95,200	1045	56,820	504	46,520	473	80,650	945
12	71,600	626	61,140	457	49,080	377	53,590	629	--	--
13	73,650	912	75,010	992	48,210	486	37,740	459	36,090	421
14	42,170	386	51,910	584	42,770	410	29,130	330	--	--
15	71,420	892	72,600	967	37,180	299	25,810	292	31,100	312

$$^1S_S = (S_O - K_S T)$$

<sup>2</sup>Crack did not form over this gage until the 9th cycle.



RELATIONSHIP BETWEEN STEEL STRAIN AND MID-DEPTH SLAB TEMPERATURE—WALKER CO.—NBL (0.5%)

Fig. 6.4

Therefore, it is concluded that within any given cycle the primary factor affecting the change in steel stress at a transverse crack is the magnitude of the slab temperature.

The low values for the coefficient of determination obtained during the initial cycles after concrete placement can partially be attributed to the fact that the initial transverse crack did not form in the pavement until the middle of the first cycle in the northbound roadway. An additional factor to consider is the fact that the concrete properties, such as tensile strength, modulus of elasticity, thermal coefficient, etc. experience their most rapid change during the initial 72 hours (9). During these initial cycles the curing of the concrete plays an important part in determining the stress level of the steel.

Referring again to Table 6.2, it is apparent that the values of the constants are decreasing with each successive cycle. In other words, a specific temperature apparently produces a smaller stress with each succeeding cycle.

Stress Variations Between Cycles. The effect of age on the average crack spacing was presented previously, and it may be recalled that the average crack spacing decreased with age. Therefore, following a logical line of reasoning, the average crack spacing was correlated with the values of the linear regression constants " $S_0$ " and " $K_s$ " for each cycle. Attention is directed to the fact that these constants now become variables dependent upon the average crack spacing which in turn becomes the independent variable. Figures 6.5 and 6.6 portray the relation for this project between " $K_s$ " and the average crack spacing for 0.5 per cent and 0.6 per cent longitudinal steel, respectively, while Figures 6.7 and 6.8 present the relation between " $S_0$ " and the average crack spacing for each steel percentage. The regression constants for each gage at a transverse crack are combined on the appropriate graph

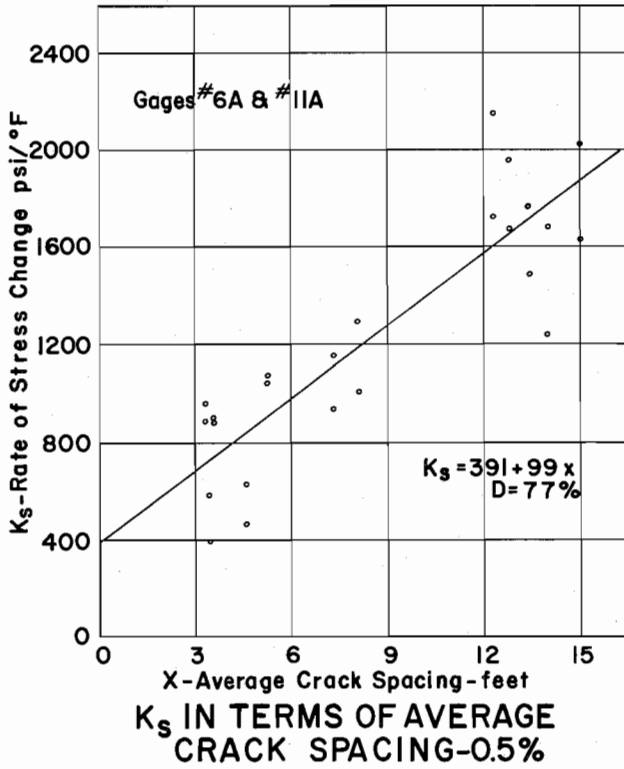


Fig. 6.5

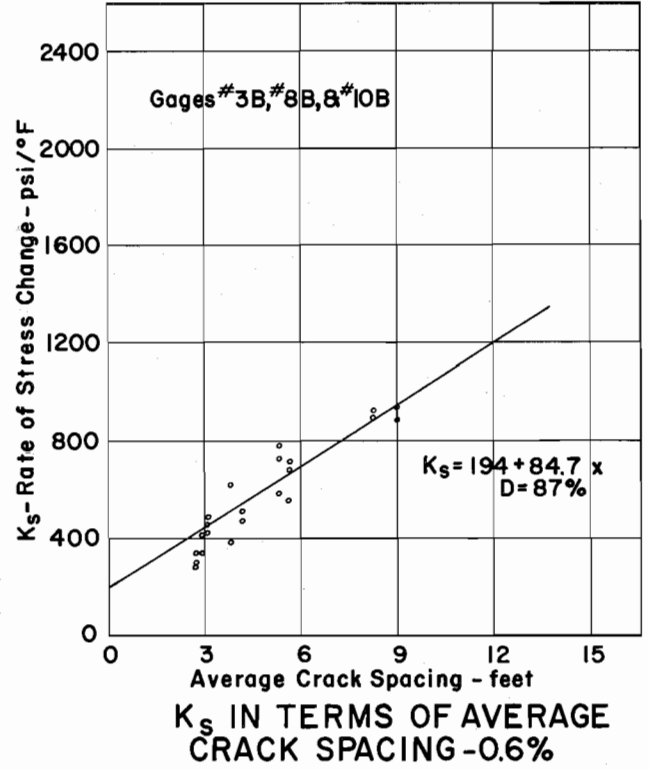


Fig. 6.6

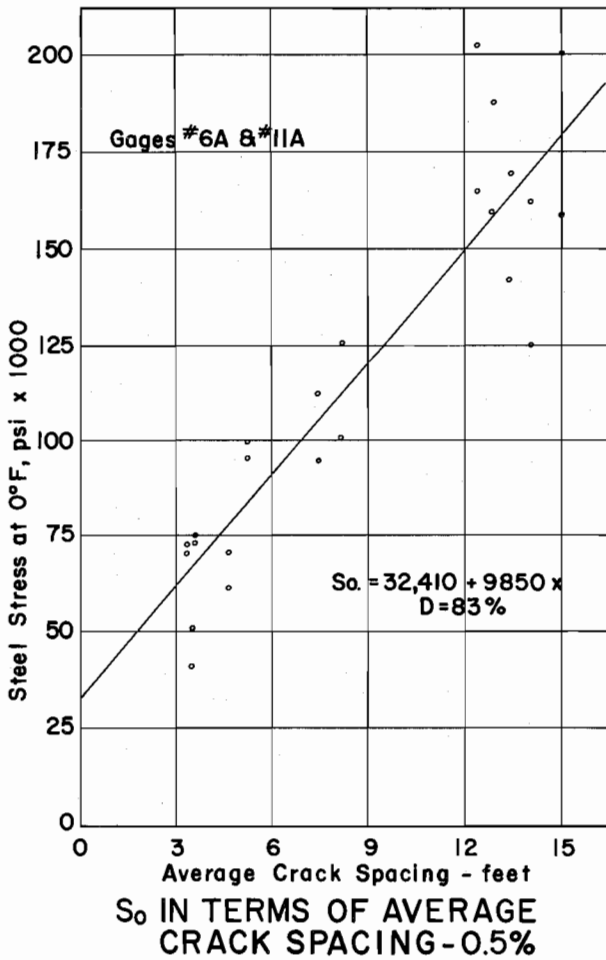


Fig. 6.7

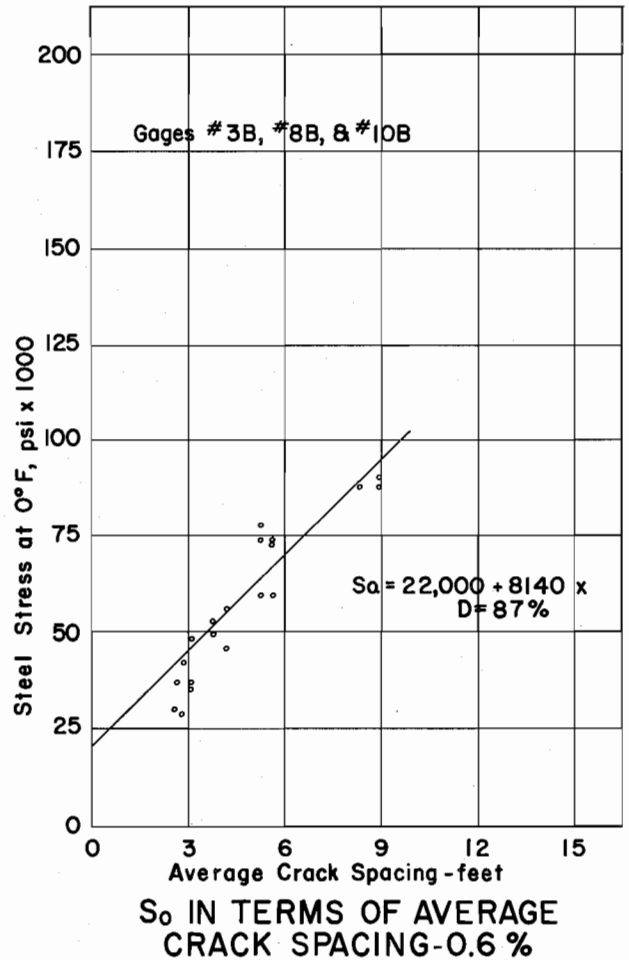


Fig. 6.8



for its steel percentage. One interesting point here is that the data for Gage No. 3B which was at an uncontrolled crack fits the same pattern as those at the controlled crack. Note both constants are directly related to the average crack spacing. This simply means the steel stress - for any given temperature condition - will decrease as the average crack spacing decreases. There is scattering of points on the graphs, but it is pointed out again that the data was taken during a wide variety of weather conditions. Using the regression analysis, the equation for each of these relations can be derived. This analysis results in equations similar to the regression format of Equation 4.1.

$K_s$  in terms of average crack spacing:

$$\text{for 0.5 per cent - } K_s = 391 + 99 X \dots \dots \dots (6.3) \\ D = 77\%$$

$$\text{for 0.6 per cent - } K_s = 194 + 84.7 X \dots \dots \dots (6.4) \\ D = 87\%$$

where  $X$  = average crack spacing in feet.

$S_o$  in terms of average crack spacing:

$$\text{for 0.5 per cent - } S_o = 32,410 + 9850 X \dots \dots \dots (6.5) \\ D = 83\%$$

$$\text{for 0.6 per cent - } S_o = 22,000 + 8140 X \dots \dots \dots (6.6) \\ D = 87\%$$

These equations express the basic relationship experienced during the first year for each steel percentage. It is of interest to note that the coefficient of determination for the regression equations ranges from 77 per cent to 87 per cent. While these are not excellent correlations they are fairly good considering the variety of conditions. For the purpose of analysis, these four graphs or equations could be compared from either viewpoint of steel percentage or from the standpoint of each constant.

First, considering the figures and equations from the standpoint of steel percentage, one logical observation becomes apparent. The slope of regression lines for both constants " $K_s$ " and " $S_o$ " is greater for the roadway with 0.5 per cent longitudinal steel than the one with 0.6 per cent longitudinal steel. This observation along with consideration of temperature explains the earlier observation, where it was found that the 0.5 per cent steel had a lower minimum as well as a higher maximum stress than the 0.6 per cent steel. The higher rate of change allows a much greater change in stress between the maximum and minimum temperature with a given crack spacing.

Next, considering the graphs for  $K_s$  (Figures 6.5 and 6.6), it is interesting to note that lines cross the zero ordinates for " $K_s$ " at values of 390 psi/° F and 195 psi/° F for 0.5 per cent and 0.6 per cent longitudinal steel respectively. This of course is in the range of the value of thermal coefficient for steel (around 190 psi/° F). A rational analysis of the stress system verifies this observation, since it is obvious that the "tied" steel would build up thermal stresses in proportion to its own thermal coefficient if no concrete was present - which is equivalent to zero crack spacing. This supposition indicates the slab segment, including the concrete, is fluctuating or moving along its length with changes in temperature. Therefore, it may be concluded that the rate of change in thermal stresses at a crack in continuously reinforced concrete pavement is some function of the steel's thermal coefficient plus the length of the slab segment.

Considering the graphs for " $S_o$ " versus crack spacing, it may be observed that the regression lines cross the ordinate at values of 32,300 psi and 22,000 psi for 0.5 per cent and 0.6 per cent longitudinal steel respectively. In connection with this observation, it is pointed out that the temperature of the concrete at the time of final set was approximately 95° F. By using the relations mentioned previously

and considering the setting temperature, the magnitudes of " $S_o$ " can be explained. Without the presence of the concrete - zero crack spacing - the restrained steel would develop a stress of approximately 18,000 psi with a temperature drop from 95° F to 0° F.

Combination of Slab Temperature and Crack Spacing. The relations found for stresses within a cycle can be combined with the relations for stress between cycles to predict the stress at any period in the life of the pavement (for a given set of conditions for slab temperature and average crack spacing). Equation 6.2 can be combined with the expressions presented in Equations 6.3 through 6.6 to arrive at an expression for steel stress at any given slab temperature and crack spacing.

Combining Equations 6.2, 6.3, and 6.5 for 0.5 per cent relation:

$$S_o = 32,410 + 9850 X - (391 + 99 X) T \dots\dots\dots(6.7)$$

Combining Equations 6.2, 6.4, and 6.6 for 0.6 per cent relation:

$$S_s = 22,000 + 8140 X - (194 + 84.7 X) T \dots\dots\dots(6.8)$$

where:        positive number denotes tension.  
              negative number denotes compression.

### Steel Stress Distribution

This phase of the study primarily considers the longitudinal distribution of stress along the reinforcing steel. As a point of interest, mention is also made of the transverse distribution of stress along a crack on this project. Refer to Figures 2.2 and 2.3 for the positioning of the strain gages in the pavement.

An examination of the stress magnitudes experienced with the gages located at the transverse cracks indicated the gages nearest the edge of the pavement had slightly greater stresses than those nearer the longi-

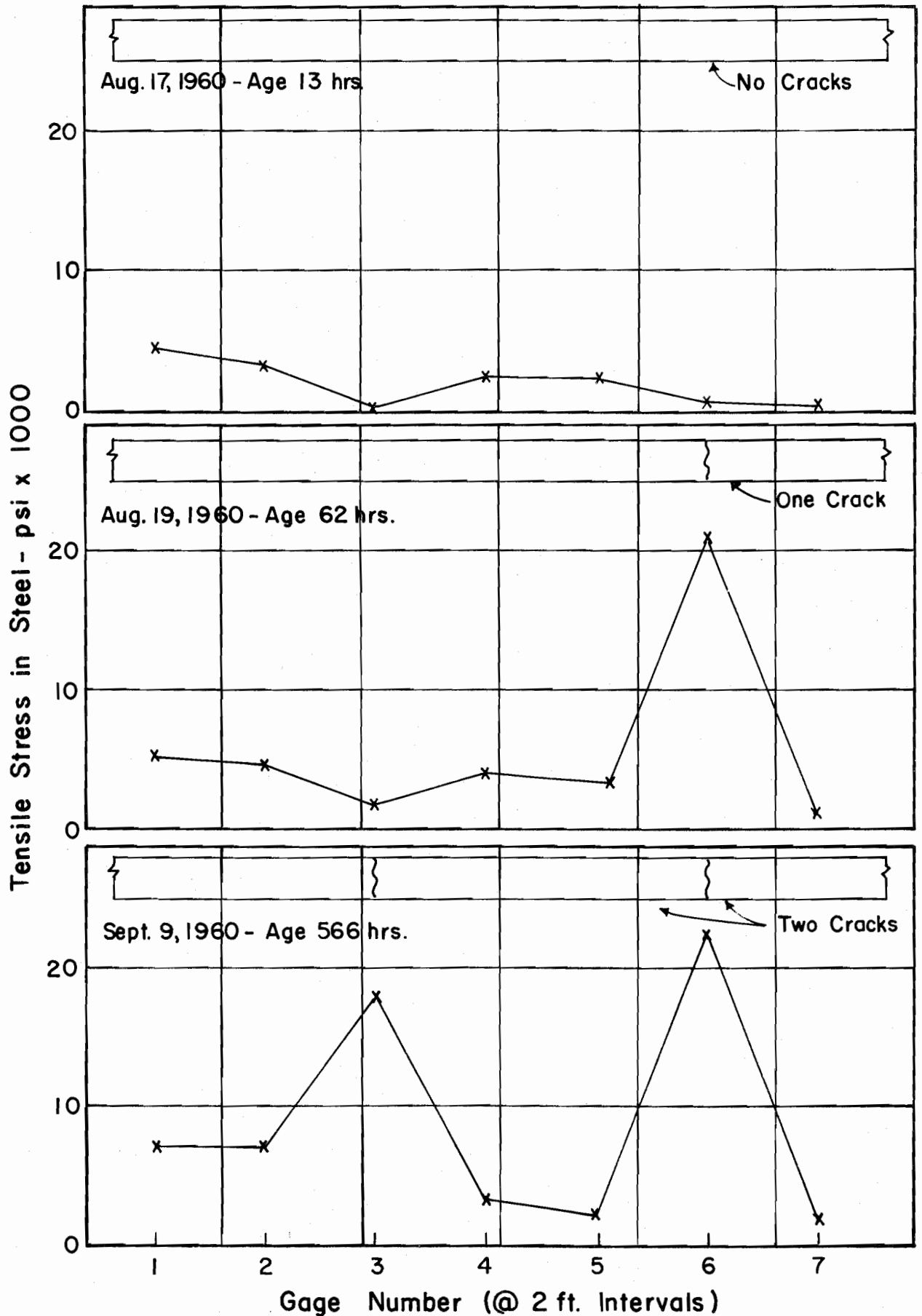
tudinal centerline. In contrast, those gages located in the interior of the slab segment did not show any pattern of stress difference in a transverse direction.

Considering the longitudinal distribution, the stresses in the steel were measured at two foot intervals over a span of twelve feet. The investigation found, as would be expected, that the maximum steel stress is located at a transverse crack while the interior area between cracks experienced less steel stress. The magnitudes of stress experienced were a function of crack spacing and temperature as previously noted. In this section, the stress distribution is studied from the standpoint of crack spacing and variation within a cycle.

Variation with Crack Spacing. Figure 6.9 represents the steel stress distribution in the southbound roadway (0.6 per cent) at three different intervals during the pavement's early age. The top of the figure portrays the steel stress distribution immediately before the first crack occurred. The middle and bottom part of the figure portray the distribution after the first and second cracks developed in the test area. The position of the cracks in relation to the gages is shown by the inset at the top of each portion of the figure.

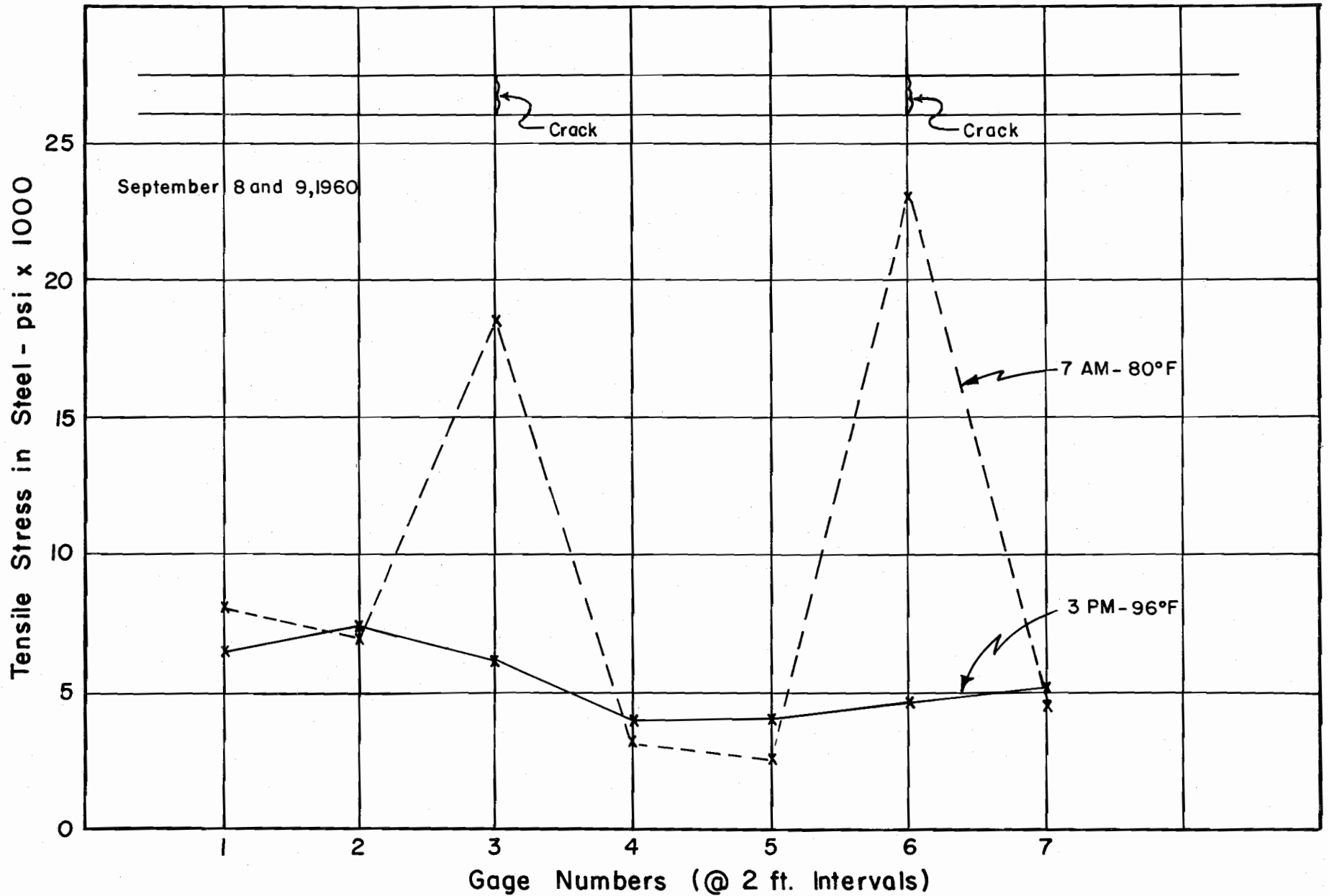
Generally, the ratio of stresses at the cracks are in the order of four times the magnitude of those in the interior. The distribution is very similar to those theoretically proposed by earlier investigations (11). One interesting observation is that both Gages 3 and 6 had stresses of a lower order of magnitude than the adjacent gages before cracking occurred. Both of the gages were located at points where cracks came into the pavement. A plausible explanation of this observation cannot be given at the present time.

Variation Within a Cycle. Figure 6.10 contrasts the longitudinal stress distribution in the southbound roadway at the maximum and minimum temperature in a typical



VARIATION IN STEEL STRESS DISTRIBUTION WITH CHANGE IN CRACK SPACING - 0.6%

Fig. 6.9



COMPARING STEEL STRESS DISTRIBUTION BETWEEN  
MINIMUM AND MAXIMUM TEMPERATURE 0.6%

Fig. 6.10

cycle. This graph is a typical representation of the steel stress distribution relations other than the changes in the stress magnitude attributed to changes in temperature. The dashed line represents the steel stress distribution at the minimum temperature experienced in the cycle, and the solid line is for the distribution at the maximum temperature.

The maximum stress is experienced at the crack during the minimum temperature - as would be expected. Note the stress level along the bar is approximately the same at all locations during the period of maximum temperature. Looking at the interior area between cracks, it is pointed out that the stress in this area has its smallest magnitude during the period of minimum temperature. If the stress level of the steel was solely a function of the temperature, then the stress level in the interior area would be greater during the period of minimum temperature.

This points out that a compressive force is applied to the steel by the slab in the slab segment interior, then the slab attempts to contract due to a temperature drop. The compressive force applied to the steel by the contracting slab then cancels out the additional internal tensile stress that would have developed in the steel as a result of the temperature drop. Hence, a smaller stress is recorded in the slab segment interior during the period of minimum temperature than during a period of maximum temperature.

This study of stress distribution points out that each individual slab segment is a fluctuating body. These segments expand and contract with temperature changes although the center of the slab segment is fixed in relation to the ground. Any opening movement that occurs at a crack must be balanced by a closing movement in the area between cracks. Any study of continuous pavement to develop theoretical stresses should take this fact into consideration. In drawing a comparison, it might be pointed out that a continuous pavement

is similar to jointed pavement except that the movement is severely restricted by the steel.

### Wheel Load Test

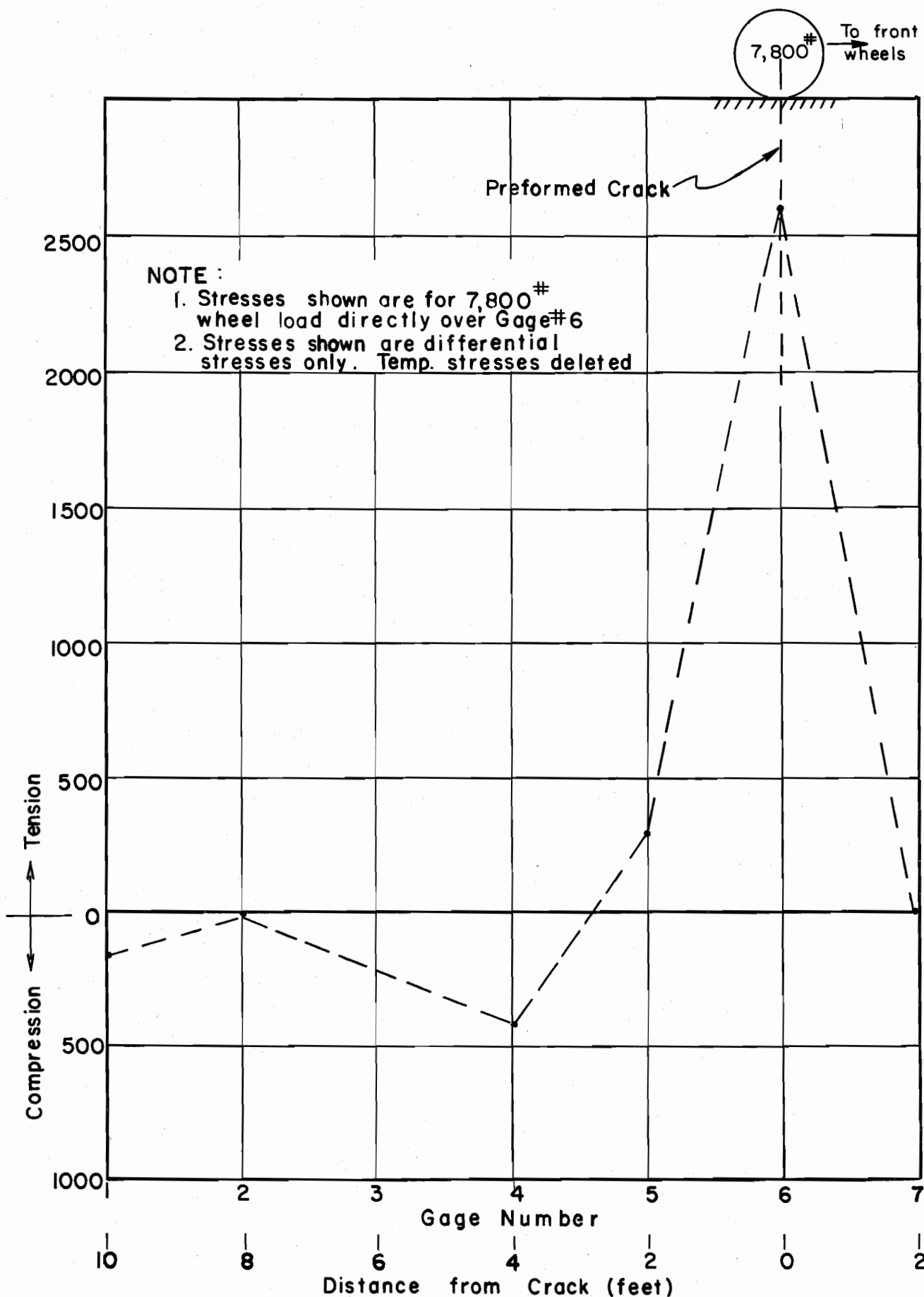
This phase of the study was an investigation into the effect of a wheel load on the steel stresses in a continuously reinforced concrete pavement. The study consisted of two different types of loading - static wheel loading and dynamic wheel loading. Static load tests consisted of determining the longitudinal distribution of the steel stress with the wheel at the crack, and the variation in steel stress at the crack as the wheel moves away from the crack. The dynamic load test consisted of measuring the steel stress at the crack with a vehicle moving over the crack at varying velocities.

The wheel load used in the test was the left rear wheels of a single axle dual wheel dump truck loaded with sand. Table B.1 and Figure B.3 in Appendix B give pertinent data concerning the test and the vehicle used. An important point in relation to this phase of the test is that the readings were taken in the morning hours when the crack was at or near its maximum opening. Therefore, these tests represent the most critical loading period for the cycle.

Static Load. Figure 6.11 shows the longitudinal distribution of stress due to the wheel load being placed directly over the crack. Note the ordinate is labeled "change in stress due to static load", hence, temperature stresses have been deleted from consideration. This figure indicates that at a distance of approximately three feet from the crack (moving in a direction away from the truck), the steel stress goes from tension to compression. The zero reading at Gage 7 when moving toward the front wheels could possibly be due to the influence of the front wheels. It is pointed out that the steel stresses at the interior points are minor when compared to the stress at the crack being less than one-sixth of the magnitude. Carrying this logic further,



CHANGE IN STEEL STRESS DUE TO STATIC LOAD — psi



EFFECT OF STATIC LOAD ON STEEL STRESS DISTRIBUTION NBL (0.5%)

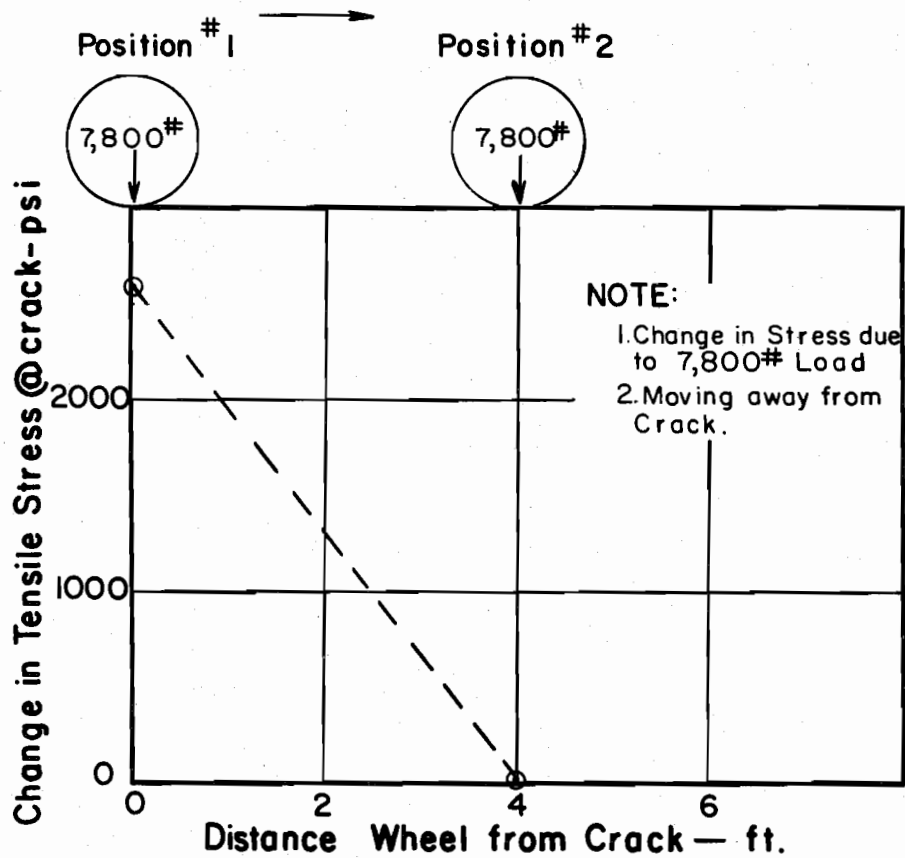
Fig. 6.11

the stress at the crack due to the static wheel load (2,600 psi) appears to be relatively insignificant when the fluctuations of stress due to temperature variations (5,000 - 40,000 psi) are considered. Since small stress variations in steel - such as those experienced with the static load - will not fatigue steel within a practical number of applications, it might be concluded that for this steel ratio, metal fatigue would not occur at the crack for the wheel load applied.

Figure 6.12 portrays the effect of various positions of the wheel load on the magnitude of stress at the crack. Note that the steel stress approaches zero at a distance of approximately four feet from the crack. Although the loading conditions are slightly different, the zero stress point is at approximately the same distance found in the previous relation.

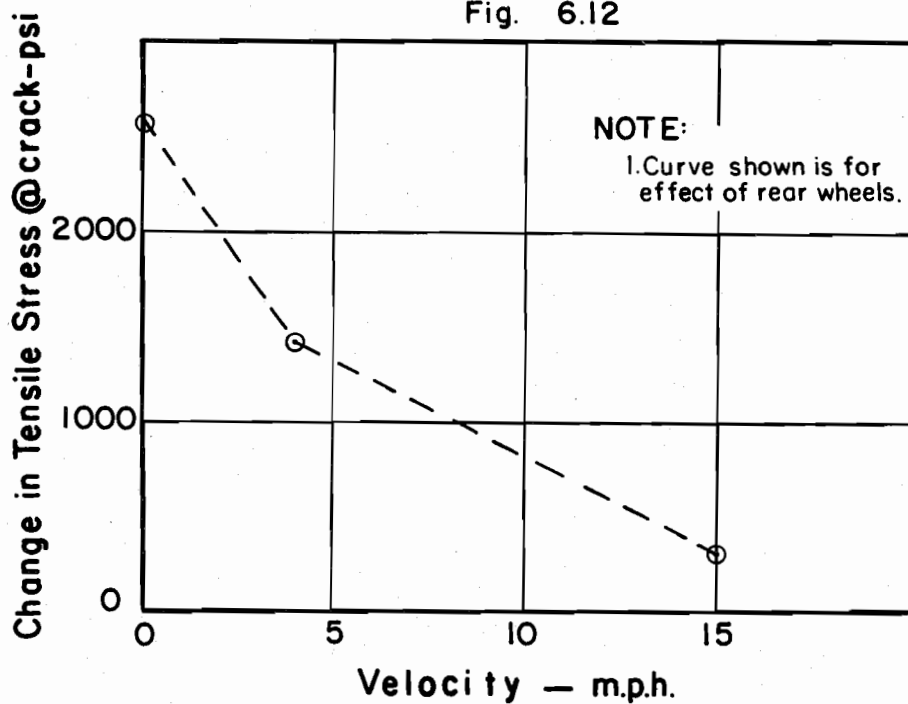
Dynamic. Figure 6.13 infers that within the limits of the data, the stress obtained at the crack is inversely proportional to the velocity of the wheel load. In other words, the stress at the crack decreases as the velocity increases. At the maximum velocity used (15 mph) the stress experienced is approximately 1/8 of the stress experienced with a static load.

These limited tests tend to indicate that external loads such as truck loads do not materially affect the steel stress level when considering the total stress due to other factors. This leads to a tentative deduction that fatigue of steel at a crack due to wheel loads is not a factor to be reckoned with in a properly designed continuous pavement.



EFFECT OF THE DISTANCE STATIC LOAD FROM A CRACK ON STEEL STRESS AT A CRACK. NBL (0.5%)

Fig. 6.12



EFFECT OF VELOCITY OF LOAD ON STEEL STRESSES AT A CRACK. NBL (0.5%)

Fig. 6.13

## VII. CONCRETE MOVEMENT

For the purpose of analyzing the stresses in the concrete, the data were collected in the form of movement. Movement is used in lieu of strain in this investigation, since any measured movement is not due to strain of the concrete, but to relief from restraint stresses developed due to suppressed volume changes of the concrete. The data measurements were made at hourly intervals during the first eight days and three days after placement in the northbound roadway (0.5 per cent) and southbound roadway (0.6 per cent) respectively. In the following analysis, the data were studied from the standpoint of cyclic behavior and longitudinal distribution of movement.

### Movement at a Transverse Crack

Data pertaining to variations in width of a transverse crack were obtained by two different methods. One method was by the use of the Berry Strain Gage and the gage plugs across a crack (see Figures 2.2 and 2.3). The other method was by use of a microscope with a graduated eyepiece. The microscope was located along the line of gage plugs and in the identical spot each time a reading was taken which allowed the duplication of readings.

The first step in this analysis was to determine which slab temperature gave the best correlation with crack width. The linear regression analysis showed that the mid-depth temperature and the average of the three temperatures gave the best correlation, as was the case with steel stresses and temperature. This observation is rather surprising considering that both methods of measurement were made at or near the surface. It might be tentatively concluded that mid-depth temperature or the average slab temperature should be used in any crack width studies.

A comparison of the analysis of the data obtained with the two methods of measurement showed almost identical results. The observation applied to the data from both roadways.

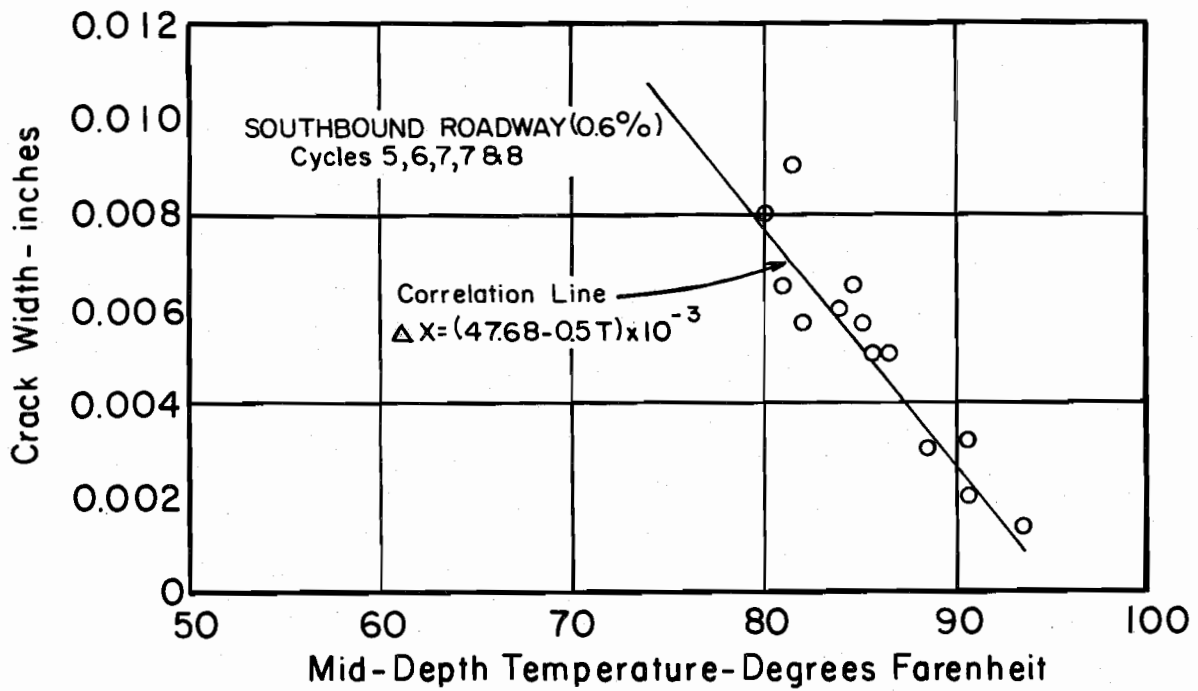
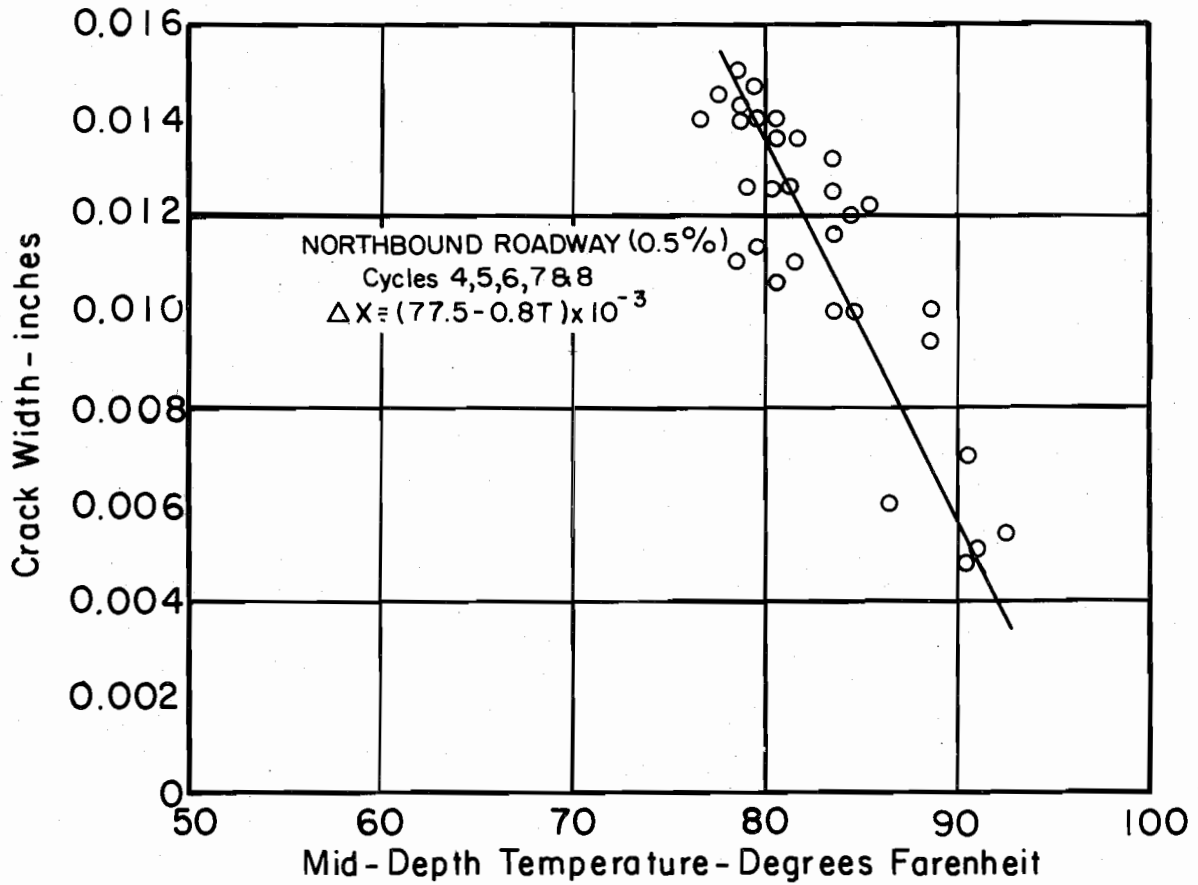
Figure 7.1 portrays a typical relation between crack width and the slab's mid-depth temperature for the control crack in each of the roadways. The top part of the figure is for the northbound roadways and the lower portion is for the southbound roadway. A regression analysis was made for each crack for which data was available which includes the natural formed cracks as well as the control crack. The equations for each of the cracks in a given roadway were equal for all practical purposes. (This observation indicates the method of preforming the cracks did not influence the results.) Therefore, the equations were combined into an average equation. The average equation for each of the roadways is presented below:

$$\text{for 0.5 per cent - } \Delta X = (63.1 - 0.64T)10^{-3} \dots \dots (5.9)$$

$$\text{for 0.6 per cent - } \Delta X = (50.3 - 0.52T)10^{-3} \dots \dots (5.10)$$

where:  $\Delta X$  = crack width, inches.  
 $T$  = mid-depth temperature of the slab, °F.  
 Pavement age less than 20 days.

In comparing the data for the two roadways, a surmise of the equations would indicate that a 20 per cent increase in steel will result in a 20 per cent reduction in crack width. Of course, there are other factors such as cement type that could influence these results. In general, the equations show, as would be expected, that the crack closes as the temperature increases and opens as the temperature decreases. One important point in the considerations of these equations is that the crack widths obtained by the use of the equations are strictly the magnitude at the surface. The crack width near the steel would be less than the magnitudes shown here for any given set of conditions.



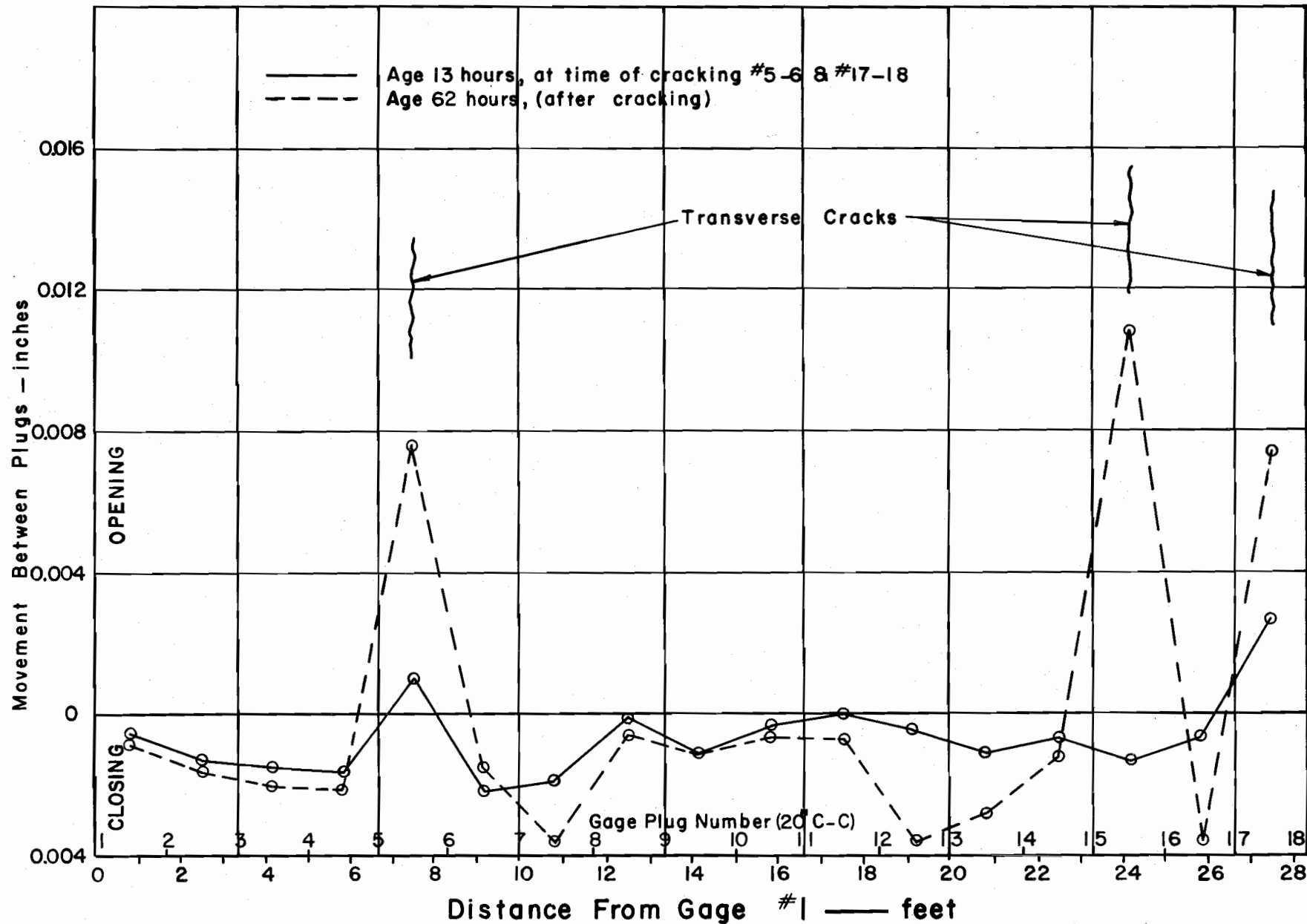
RELATION BETWEEN CRACK WIDTH AND THE MID-DEPTH TEMPERATURE FOR THE PREFORMED CRACK IN EACH ROADWAY

Fig 7.1

### Distribution of Movement

To obtain a better understanding of the meaning of movements between gage plugs, these movements should be studied as a unit. This can be accomplished by plotting the movement between each gage plug versus the distance from gage plug number one to the mid point between the set of gage plugs for a specified pavement age. In this way, the distribution pattern of movements can be investigated in relation to age, slab cracking, and temperature. Figures 7.2 and 7.3 are plots of movement distribution in the southbound roadway at various ages.

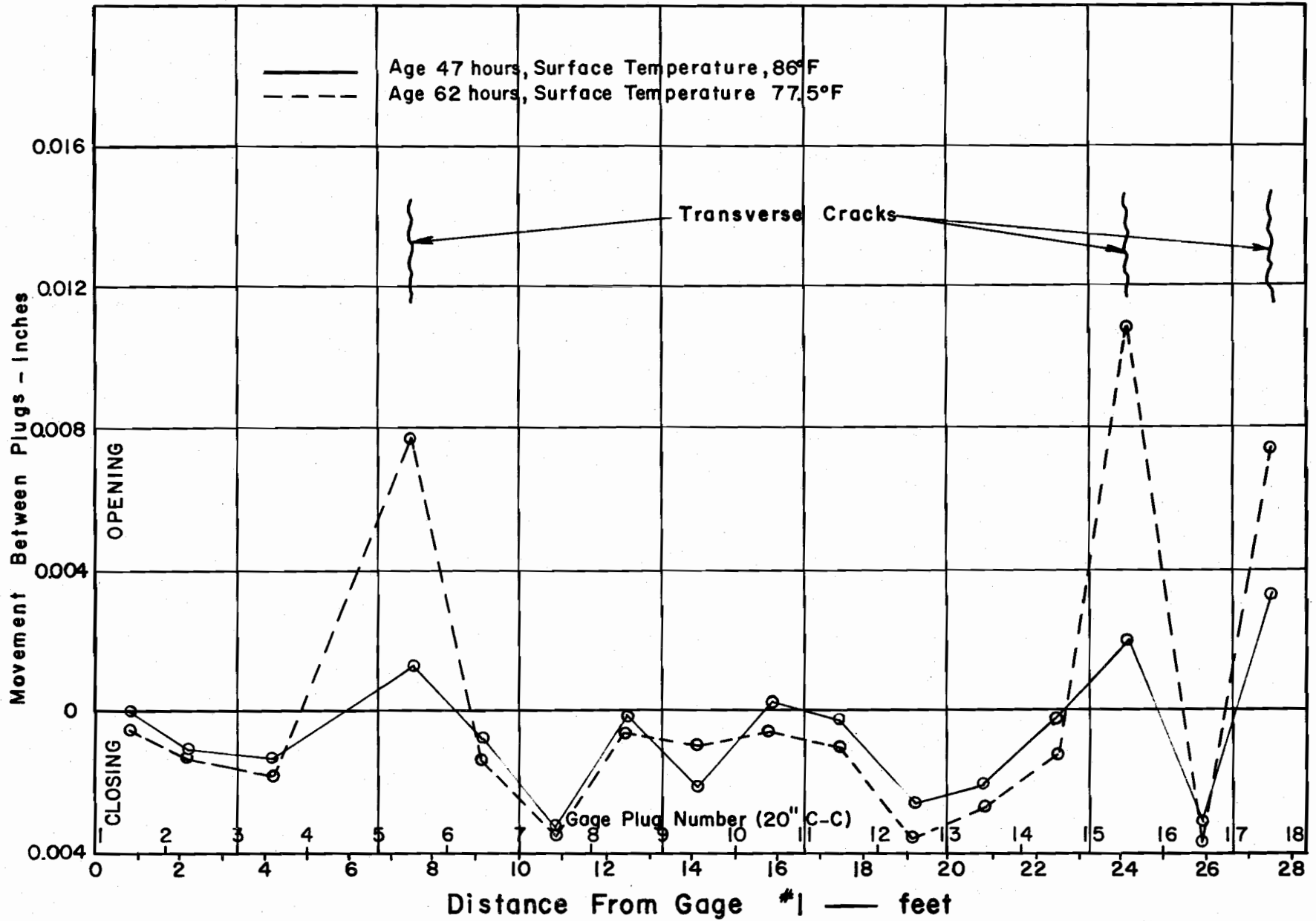
Figure 7.2 compares the movement distribution at minimum mid-depth temperature as the crack spacing changes. The distributions shown on the graph are for a pavement age of 13 and 62 hours respectively which is identical with the periods used for studying steel stress distribution in Figure 6.9. The solid line is for an age of 13 hours which is the period of initial cracking while the dashed line represents a period after the cracks have formed (age 62 hours). Studying the solid line, it is apparent that excessive opening movement in relation to the other gages is beginning to occur between Gages 5 and 6 and Gages 17 and 18. The area between Gages 5 and 6 is at the point of incipient cracking since the strain for this movement is  $50 \times 10^{-6}$  in/in based on 20 inch gage length (ultimate strain at time, approximately  $55 \times 10^{-6}$  in/in). The next set of measurements 40 minutes later indicated the slab had cracked. The data shows the slab had already cracked between Gages 17 and 18 at the age of 13 hours. This means an uncontrolled crack (Gages 17 and 18) formed before the preformed crack (Gages 5 and 6). One interesting observation is that although both the steel strains and the concrete movement data indicated the slab had cracked at an age of 13 hours, the cracks did not become visible to the eye until 24 hours later.



COMPARING MOVEMENT DISTRIBUTION AT THE MIN. TEMPERATURE AS NEW CRACKS APPEAR IN SLAB, SLB (0.6 Percent)

Fig. 7.2





COMPARING MOVEMENT DISTRIBUTION AT MAX. & MIN. TEMPERATURE  
SBL (0.6 Percent)

Fig. 7.3

The dashed line is the distribution at an age of 62 hours. At this time, three cracks had developed within the test area. In contrasting the two distributions note that as the crack opens up, the increased width at the crack is offset by an increased closure in the area between gage plugs. (The dashed line is below the solid line in the interior of each slab segment.) As would be expected, the algebraic sum of movements in the slab segments is approximately equal to zero.

Comparing the two distributions, it is evident that approximately 60-70 inches of the slab segment away from the crack is fluctuating or moving. Note the area between Gages 7 and 8 and Gages 12 and 13 are absorbing the bulk of the movement, whereas the slab segment between Gages 8 and 12 is not experiencing movement. This area of no movement indicates that the full restraint stresses due to suppressed volume changes are developed. It is interesting to note that the next crack in the slab segment developed between Gages 9 and 10 which are in the area of full restraint.

Figure 7.3 was inserted to compare the distribution of movement between adjacent plugs that occurs during the minimum and maximum temperature within a cycle. It may be observed here, as shown previously, that cracks close as the temperature is increased. An apparent observation from the data is that the movement at a crack is absorbed over a considerable length of the slab segment. Note that the interior area between cracks experiences more closing movement at the minimum temperature than at the maximum.

## VIII. DISCUSSION OF RESULTS

A fundamental precept in the design of a continuously reinforced concrete pavement is the determination of the optimum percentage for the longitudinal steel. Sufficient steel must be provided to hold the cracks tightly closed and to prevent the steel from being overstressed. Since the study of the distribution of stresses in the longitudinal steel presented in this report show the maximum steel stress to be at the transverse cracks, as rational analysis would indicate, this area becomes one of the controlling factors in design. In the following sections, an attempt was made to logically analyze the factors influencing steel stresses and the formation of transverse cracks in the pavement. An understanding of the interrelation of the influencing factors could serve as a background for a rational design approach.

### Discussion of Factors Affecting Steel Stress

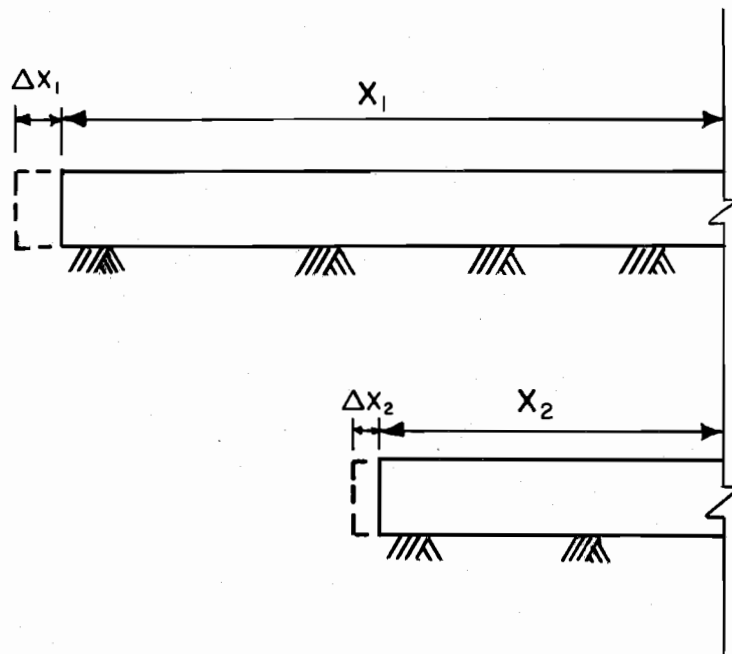
The data obtained from this study have indicated the changes in stress in the longitudinal steel was affected by two factors, these being the temperature and the average crack spacing of the slab. The individual slab segments of the pavement slab are in a constant state of fluctuation in the longitudinal direction. This movement results in an opening and closing of the transverse cracks which in turn results in an induced stress in the steel.

Temperature. The magnitude of stress in the steel due to slab temperature is a direct function of the concrete's and the steel's thermal coefficient of expansion and contraction. The steel would naturally develop stresses due to restraint of volumetric changes even if in an isolated condition, but the internal stress of the steel would amount to only a small part of the actual stresses experienced. A temperature drop of  $10^{\circ}$  F resulted in as much as a 20,000 psi change in steel stress in some instances on this project, whereas the

theoretical maximum that would be induced in the restrained steel, if it was in an isolated condition, would be approximately 1700 psi. This enormous difference in stress levels must be attributed to the limited restraint of the attempted movement of the slab segment at the crack by the longitudinal steel. This attempted movement by the slab segment is a direct function of the thermal coefficient of the concrete. The greater the thermal coefficient, the more the change in stress for a corresponding temperature variation. This explanation points out the desirability of obtaining a concrete with a small thermal coefficient.

Average Crack Spacing. The stress in the longitudinal steel was found to be a direct function of the average crack spacing. In attempting to explain this observation, it is pointed out that the previous observation concerning the thermal coefficient and the fluctuating movement experienced as the temperature changes is inter-related with the crack spacing. The magnitude of the attempted movement and the actual movement (crack width) is a function of the slab segment length. Figure 8.1 gives a graphic illustration of this statement. The magnitude of the actual movement that would result from a given temperature change would decrease as the length of the slab segment decreases.

With this postulate in mind, the consequence of the attempted movement of the slab segment in relation to the steel is examined. The data presented earlier concerning concrete movement indicated that the closing movement between cracks equals the opening movement at the crack (crack width) for the case of a temperature drop. This opening movement of the crack is a result of steel strain over a short section of the steel bar. The length of the steel bar experiencing movement at the crack is the distance along the bar that must absorb the opening movement, or in essence this length may be considered as the gage length of the tensile specimen. Since unit strain is simply the elongation (or movement) divided by the gage length, an increase



For a Temperature drop of  $\Delta T$ , the movement experienced in two slabs of uniform materials, but of different lengths would be:

$$\Delta X_1 \sim X_1 K \Delta T$$

$$\Delta X_2 \sim X_2 K \Delta T$$

$X_1$  and  $X_2$  represents the only variance in the two formulas.

## STUDY OF SLAB MOVEMENT IN RELATION TO SLAB LENGTH

Fig. 8.1

in the attempted movement will result in an increase in strain, i.e. stress. It was shown previously that this attempted movement was a function of slab length, hence, the stress in the steel for a given temperature drop is a direct function of the slab length.\* Consequently, the stress in the steel for a given temperature drop decreases as the average crack spacing decreases.

Combination of Temperature and Crack Spacing. The postulates discussed above point out that the stress in the steel is a complex interaction problem that involves slab segment length, thermal coefficient, and temperature change. A temperature drop results in an attempted movement by the slab segment which is resisted by the longitudinal steel.

An increase in the steel stress results in elongation of the steel, which in turn tends to relieve the restraint forces developed in the concrete. Since the force system for the structure would be a static one, rather than a dynamic one even though movement is experienced, the force developed by the concrete must be balanced by the forces developed in the steel and by the frictional force developed between the slab segment and the subbase. In addition to the preceding hypothesis, the relief movement experienced by elongation of the steel bar at the crack due to the strain developed is balanced by closing movement in the interior of a slab segment—reduction of tensile stresses in slab.

---

\*The function would not be a linear one as might be tentatively concluded; the area of bond failure (gage lengths) would increase with age. This increase in gage length would also reduce the steel stress in addition to the decreasing average crack spacing.

### Formation of Cracks

The relationship between the pavement age and the average crack spacing for the test sections is presented in Figure 5.1, and in Figures 7.2 and 7.3, the longitudinal distribution of movement between adjacent gage plugs along the pavement is portrayed for various ages. An analysis of the data presented in each of these figures indicates that temperature is a prime factor influencing both the movement in a slab segment and the average crack spacing during any period. The purpose of the following discussion is to analyze the interaction among the movement in a slab segment, the change in the average crack spacing, and the change in air temperature. In explaining this interaction, an approximation of the magnitudes of the longitudinal stress distribution will be presented along with the effect of concrete properties on this stress distribution.

Stress Distribution. Stress distribution in a concrete slab is related to movement. A slab segment completely restrained and subjected to a decrease in temperature would develop a uniform tensile stress in the slab. Any contractive movement occurring in the slab segment results in stress relief, and the magnitude of the stress relief is directly proportional to the movement. The partial restraint of movement that occurs at a transverse crack is due to the resistance of the steel and of the subbase, hence, a variation in the magnitude of movement is experienced in the area adjacent to the transverse crack. The magnitude of movement is inversely proportional to the distance from the transverse crack; therefore, the magnitude of the stress increases as the distance from the crack increases.

A relatively long slab would have: (1) a central portion that is completely restrained, consequently, an area of constant stress, and (2) an area at each end of the slab segment that experiences a stress build-up as the distance from the crack increases. As long as the

concrete is of relatively uniform strength, the central portion of a slab segment experiences a greater degree of cracking than the areas of the slab segment adjacent to the crack.

As the relative length of the slab segments decrease, as a result of the new cracks appearing in the slab, the slab segments will no longer have an area of constant stress. If the temperature differentials remain approximately equal during the daily cycles, the pavement will attain a stable crack pattern, since the summation of the flexural and tensile stresses in the pavement will not rupture the concrete.

Figure 8.2 portrays the longitudinal distribution of stresses in the northbound roadway at the age of 13 hours and 62 hours which are periods of minimum temperature for each cycle, hence, the period of maximum tensile stress. The magnitudes of stresses are only rough approximations arrived at by use of elastic theory, movement data, and concrete properties on this project, therefore, they were included only to serve as a basis for comparison.

Effect of Material Properties. The two basic components of the pavement, concrete and steel, exhibit certain physical properties, but the steel's properties are relatively static whereas some of the concrete properties are in a constant state of change. This change and the rates of change have pertinent effect of the formation of cracks and hence, the stress level in the steel. The initial ten days of pavement life is the period when the concrete properties are undergoing the greatest rate of change. The strength, the modulus of elasticity and the thermal coefficient are increasing at various rates as the concrete ages. In general, the thermal coefficient and the modulus of elasticity are changing at a greater rate than the tensile strength especially during the first few cycles. The rate of change of the thermal coefficient tends to stabilize within 20 to 50 hours, while the rate of change for the tensile strength continues over a much longer period.



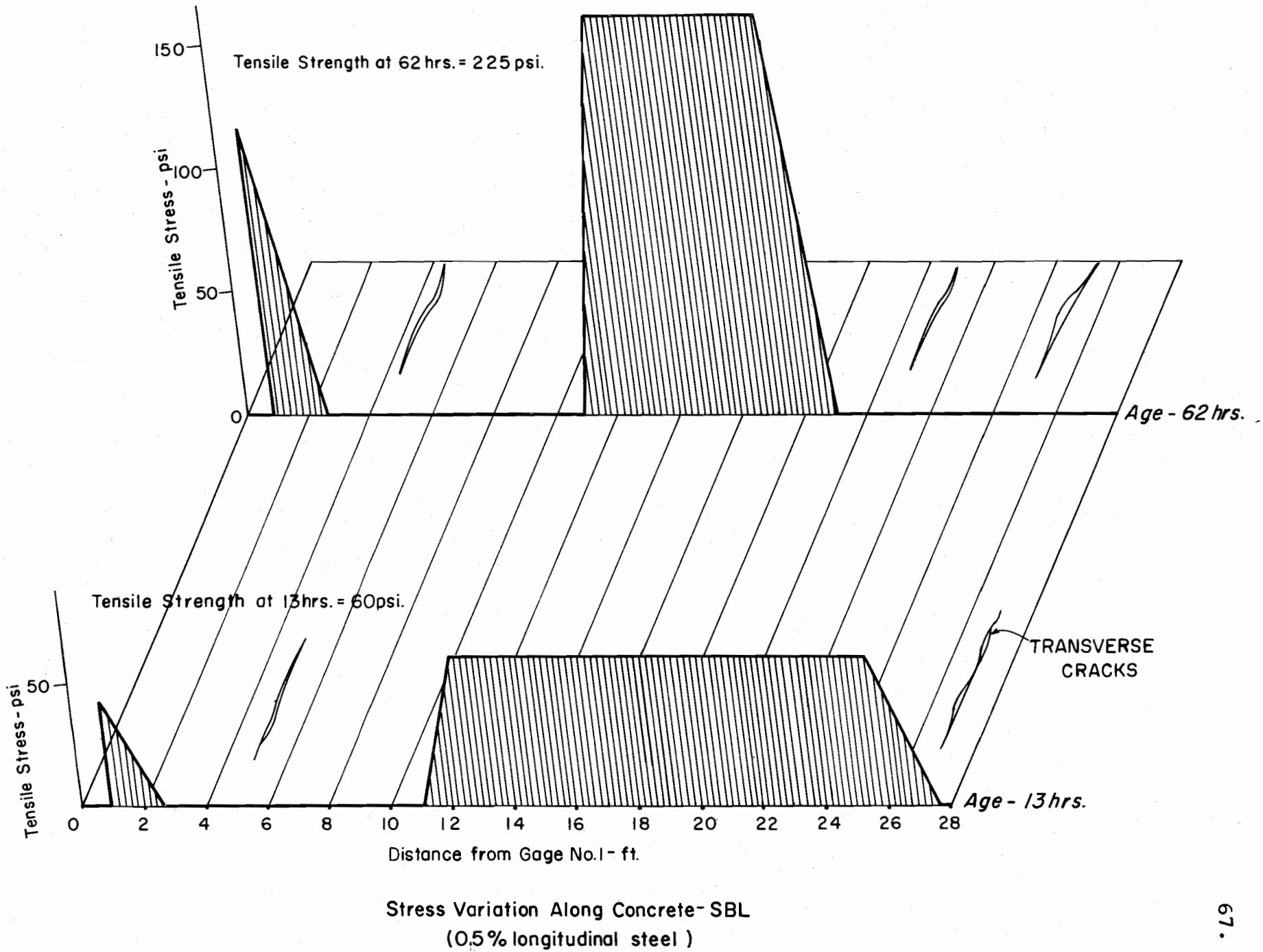


Fig. 8.2

The effect of these various rates of change in concrete properties is demonstrated in Figure 8.2. At an age of 13 hours the combination of the relatively high thermal coefficient and the temperature drop (approximately  $10^{\circ}$  F) has produced sufficient tensile stresses in the concrete to be at a level of the tensile strength. This, of course, is the period when the initial cracking of the slab occurred. In comparison, at an age of 62 hours the tensile strength is of such magnitude that an even greater temperature drop (approximately  $15^{\circ}$  F) does not produce a stress level that is near the tensile strength. This is one of the reasons why the pavement with the Type III cement resulted in a much greater average crack spacing than the pavement with the Type I cement. The Type III (high early strength) has such a high increase in strength during the initial few days that a much greater temperature drop is required before cracking occurs. Therefore, the wide crack spacing results in large stress levels at the crack, and this condition remains until sufficient temperature drops are experienced to produce tensile stresses in the concrete to exceed the tensile strength of the concrete. If the wide crack spacings resulted in the development of stresses that exceeded the yield point of the steel, the crack would open excessively and slab continuity would be lost.

The observations indicate that some of the desirable characteristics of concrete to be used in continuously reinforced concrete are a low thermal coefficient and a slow gain in strength.

## IX. CONCLUSIONS

The research conducted on this project revealed that the design of the required longitudinal steel percentage for a continuously reinforced concrete pavement is more complex than the ratio of the tensile strength of the concrete to the yield stress of the steel. Carrying the observation to its logical conclusion, the selection of a minimum steel percentage based on the performance of a pavement in one section of the country and applying it to another section is an erroneous approach. With the materials and environment in one section of the country, a fixed steel percentage might result in over-design while in another area the percentage will be insufficient.

The findings reported in this paper indicate that the design procedure should encompass crack spacing, temperature drop, and concrete properties, in addition to those presently considered. Two of the more important concrete properties are the modulus of elasticity and the thermal coefficient. In general, the magnitude of these two concrete properties should be as low as possible.

The inclusion of the crack spacing in a design method points out an area where additional information is urgently needed. The factors influencing the crack spacing must be determined and evaluated. (The reason why one percentage of steel results in various crack spacings under different conditions should be pursued.)

In addition to the above hypothesis, the data from this project leads to these additional conclusions and recommendations:

- (1) Any future study of the factors influencing the crack spacing of continuously reinforced concrete pavement should heed the effect of pavement age.

(2) Both the 0.5 and 0.6 per cent design performed satisfactorily on this project. Other factors influence steel stress and the average crack spacing more than steel percentage as long as slab continuity is maintained.

(3) Each slab segment within a slab is in a continual state of fluctuation after the initial transverse cracks occur.

(4) The primary factor influencing steel stresses in a given cycle is the slab temperature. The primary factor influencing the stress temperature relation between cycles is the change in crack spacing.

(5) Type III cement (high early strength) will result in much higher steel stresses than Type I cement (normal) during the early life of a slab.

(6) The average slab temperature gives the best prediction of steel stress and crack width.

(7) The data infers that wheel loads would not be a critical factor from a steel stress fatigue standpoint as long as the slab continuity is maintained and the slab is in contact with subgrade. This observation applies solely to the design of the longitudinal reinforcing steel.

## A C K N O W L E D G M E N T S

The research reported in this paper was conducted on an experimental project in Walker County, Texas, on Interstate Highway 45 constructed by the Texas Highway Department and the U. S. Bureau of Public Roads. The research was under the supervision of Mr. T. S. Huff, Chief Engineer of Highway Design and general supervision of Mr. D. C. Greer, State Highway Engineer.

The authors wish to acknowledge with thanks the able assistance of C. J. Derdeyn of the Highway Design Division and W. B. Ledbetter formerly of the Highway Design Division and presently Instructor in Civil Engineering at the University of Texas.

Also acknowledgment of the help of Willard Moore and other members of the Materials and Tests Division under the supervision of Mr. A. W. Eatman for cooperation in the use of equipment and advise on instrumentation.

Thanks is also given to personnel of Highway District 17 under the direction of Mr. C. B. Thames, District Engineer, who assisted in the planning of the research phase of the project and especially to Jerry Nemec, Supervising Resident Engineer, for the splendid cooperation he arranged for with the contractor during the construction and the testing program.

## BIBLIOGRAPHY

1. Shelby, M. D. and McCullough, B. F. "Experience in Texas with Continuously Reinforced Concrete Pavement", Highway Research Board Bulletin 274, 1960.
2. AASHO Interim Guide for the Design of Rigid Pavement Structures. AASHO Committee on Design, April 1962.
3. McCullough, B.F. and Ledbetter, W.B. "LTS Design of Continuously Reinforced Concrete Pavement", Journal of the Highway Division, Proceedings of the ASCE, Vol. 86, No. HW4, December 1960.
4. Gersch, B.C. and Moore, W.H. "Flexure, Shear, and Torsion Tests of Prestressed Concrete I-Beams", Paper presented at 41st Annual Meeting of the Highway Research Board, 1962.
5. McCullough, B. F. "An Investigation of Continuously Reinforced Concrete Pavement in Comal County, Texas". Unpublished Thesis, University of Texas, 1962.
6. Simpson, George, and Kafka, Fritz. Basic Statistics: A Textbook for the First Course. W. W. Norton and Co. Inc., New York, 1957.
7. Lindsay, J. D. "A Ten Year Report on the Illinois Continuously Reinforced Concrete Pavement", Highway Research Board Bulletin 214, 1959. Washington.
8. Klieger, Paul. Studies of Concrete Made With Texas Cements and Aggregates. Portland Cement Association, Skokie, Illinois.
9. Jones, Truman R. and Hirsch, T. J. A Report on the Physical Properties of Concrete at Early Ages. Texas Transportation Institute, College Station, Texas, 1961.

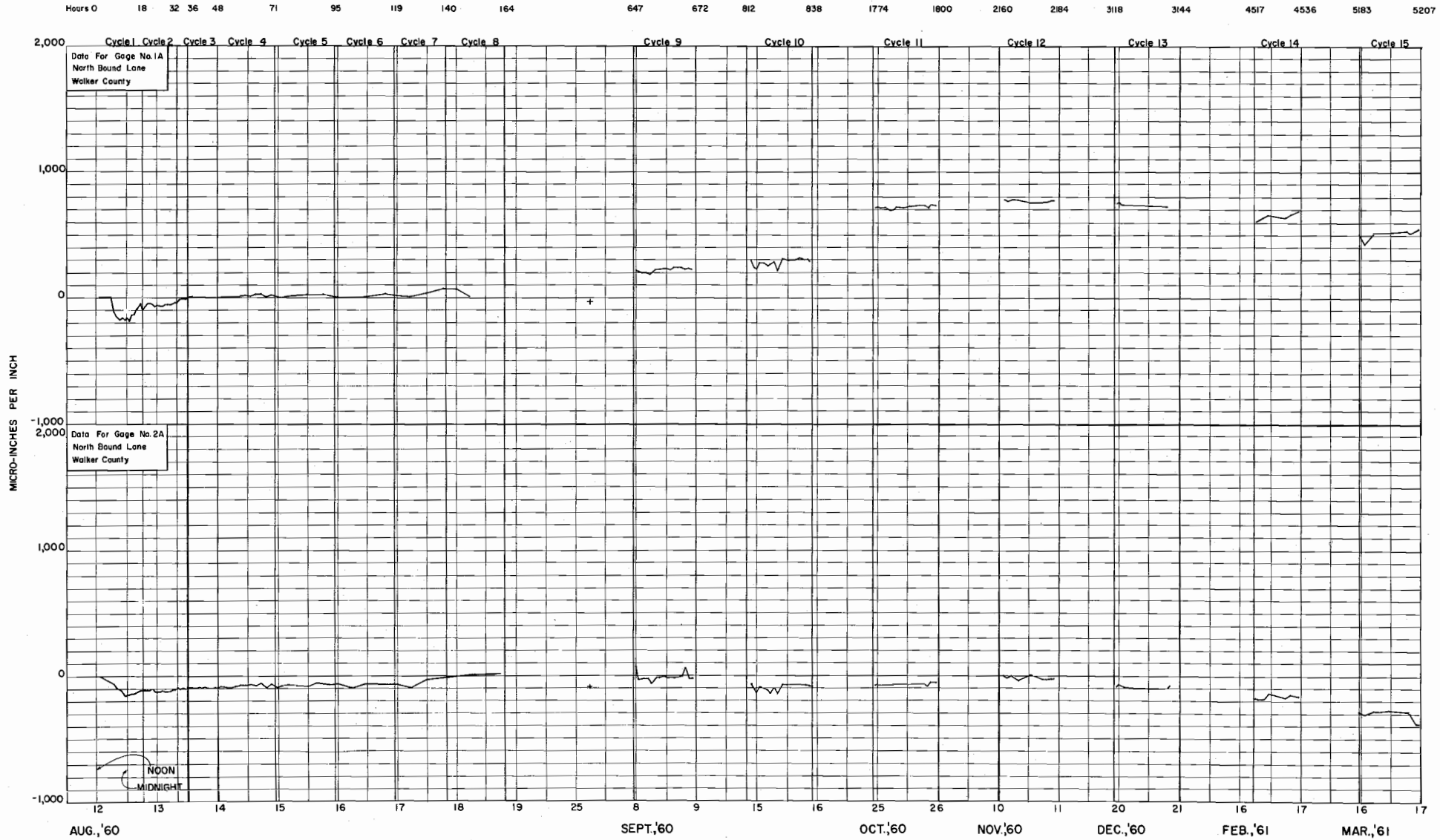
10. Lepper, Henry A. and Garber, Daniel L., Jr. "Maryland Continuously Reinforced Concrete Test Pavement - First Year Strain Observations", Highway Research Board Proceedings, Vol. 40, 1961.
11. Vetter, C. P. "Stresses in Reinforced Concrete Due to Volume Changes", Transactions, A.S.C.E., Vol. 98, 1933.
12. Perry, C. C. and Lissner, H. R. The Strain Gage Primer, McGraw-Hill, 1955.

## A P P E N D I X    A

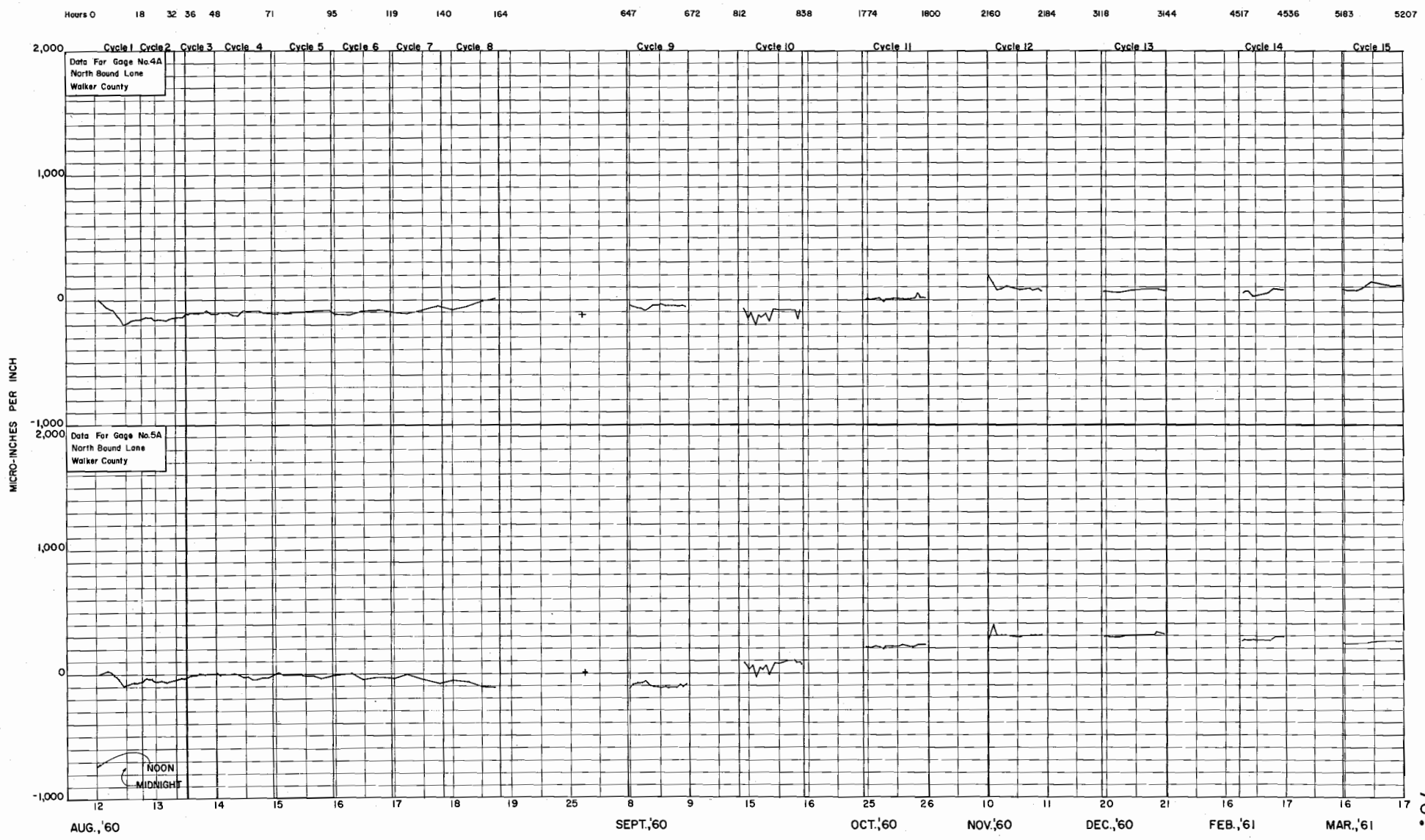
## Stress-Time Plots



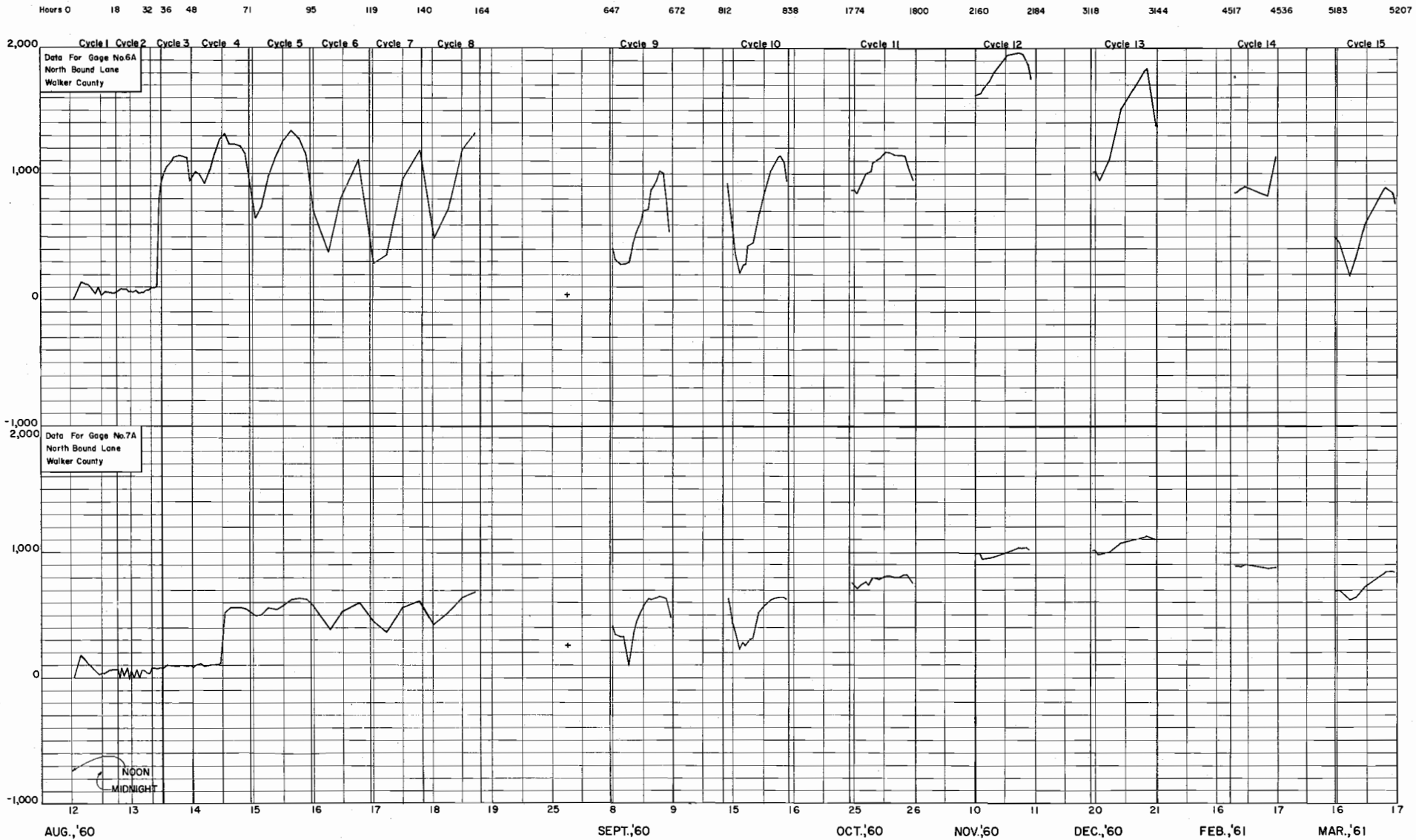
STEEL REINFORCEMENT STRAIN



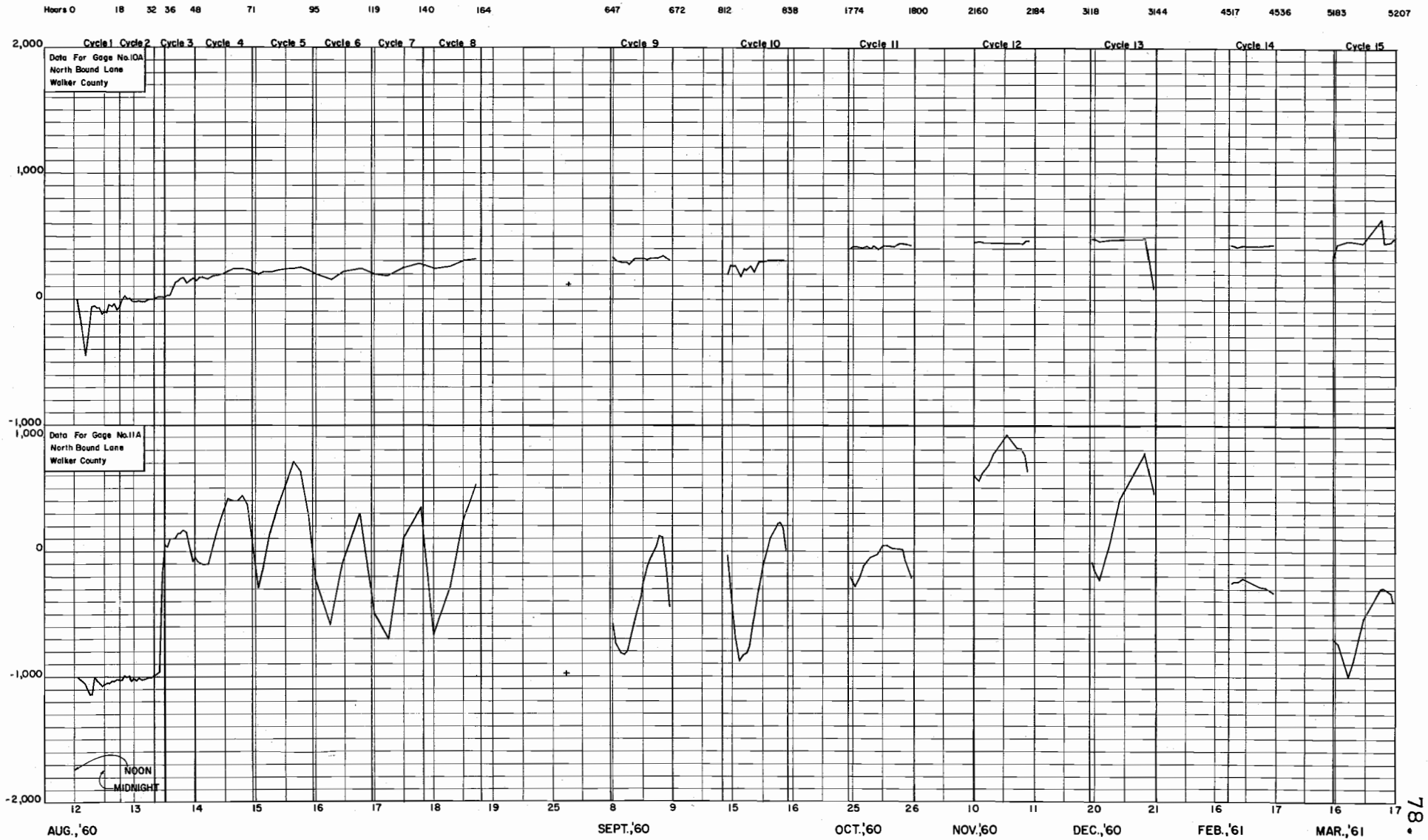
STEEL REINFORCEMENT STRAIN

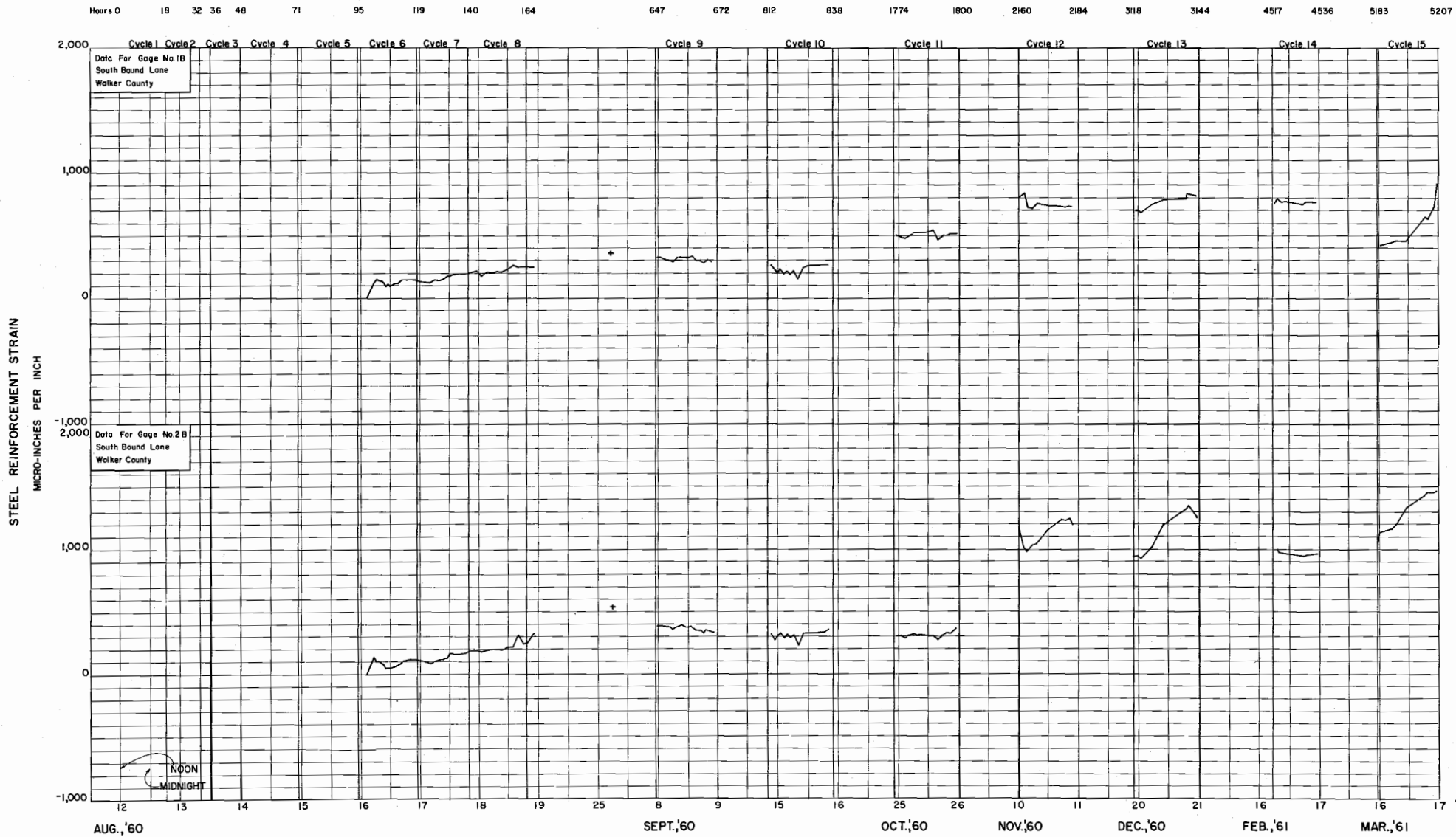


STEEL REINFORCEMENT STRAIN  
MICRO-INCHES PER INCH

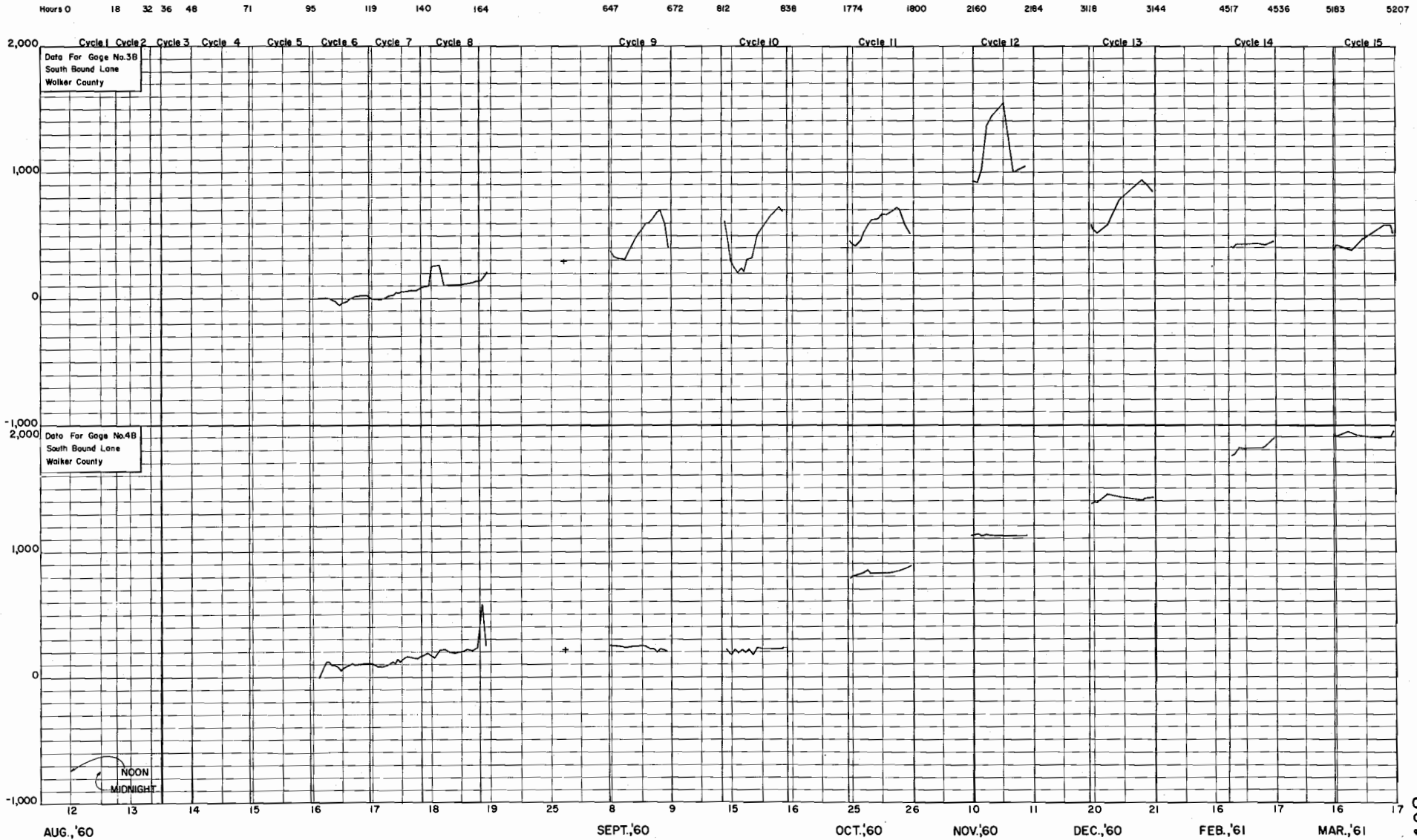


STEEL REINFORCEMENT STRAIN  
MICRO-INCHES PER INCH

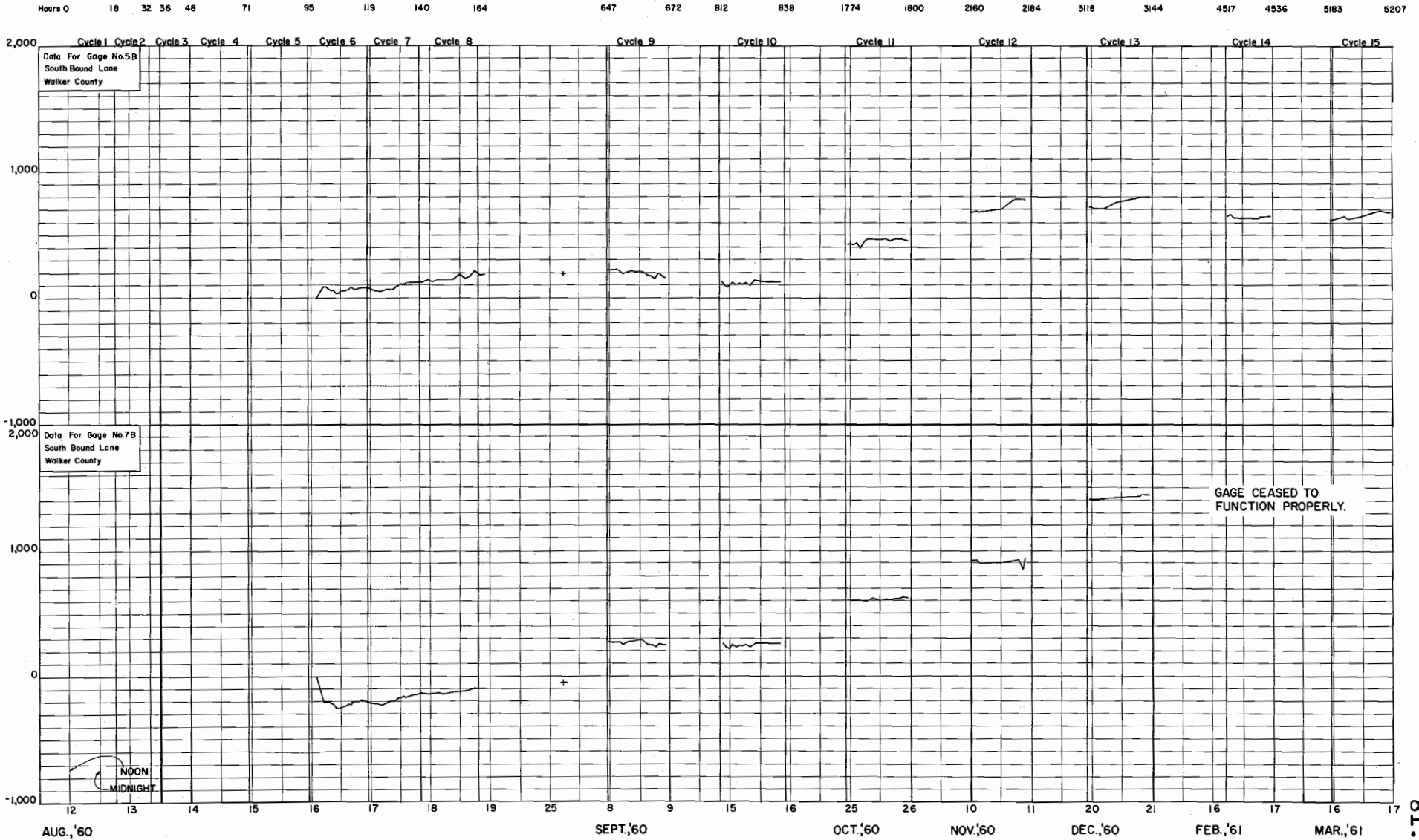


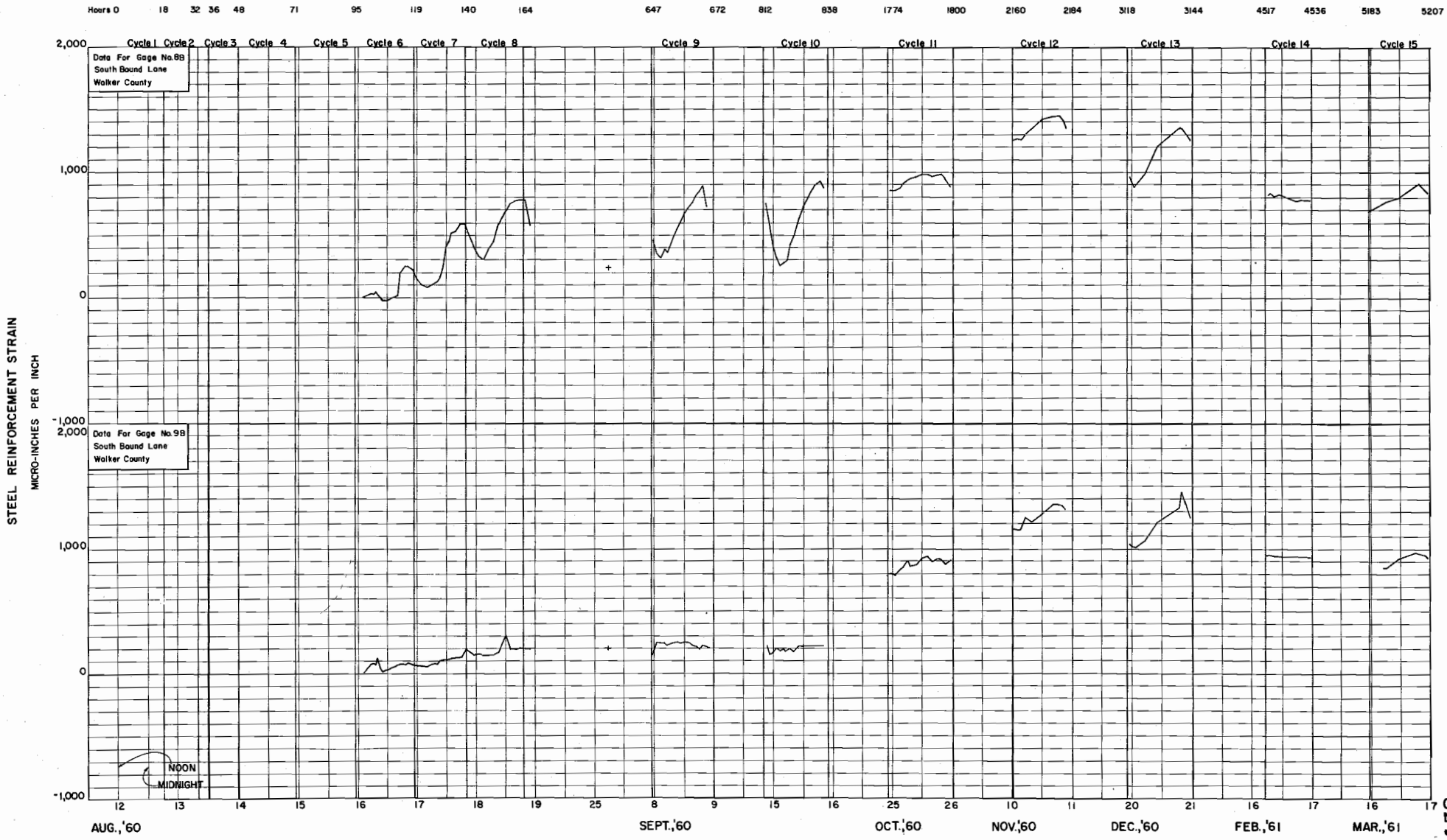


STEEL REINFORCEMENT STRAIN  
MICRO-INCHES PER INCH



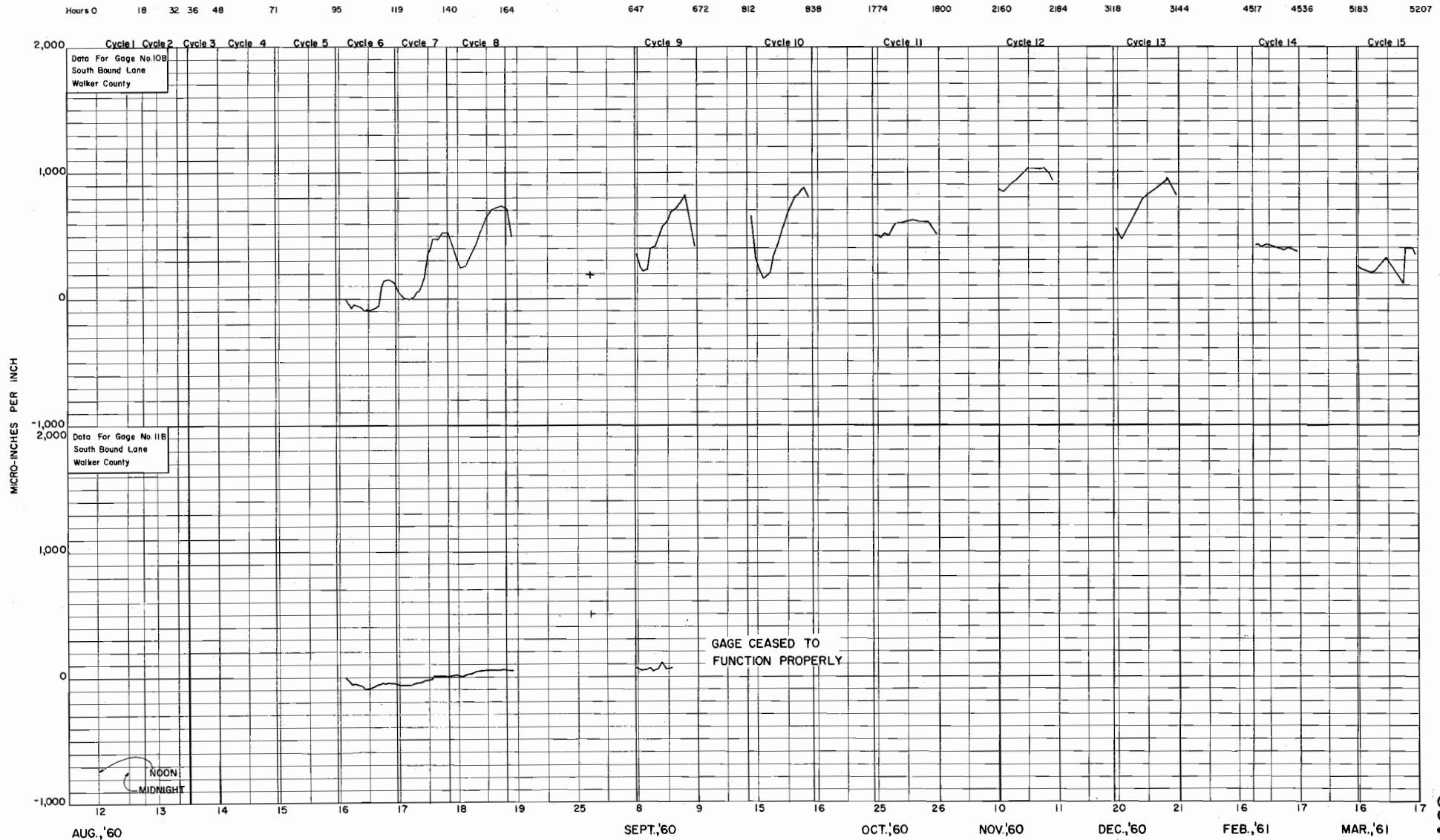
STEEL REINFORCEMENT STRAIN  
MICRO-INCHES PER INCH







STEEL REINFORCEMENT STRAIN



A P P E N D I X    B

Instrumentation and Wheel Load Test Data

REPORT ON THE STEEL STRAIN GAGE CEMENTING  
AND WATERPROOFING PROCEDURES

The SR-4 Strain Gage, Type A-5, 1 inch long, paper backed, was cemented to standard number 5  $\emptyset$  deformed steel reinforcing bars. Prior to attaching the gages, the bars were "turned down" on a lathe to a uniform diameter over a length of four inches. A total of 22 gages were attached to six reinforcing bars on 2'-0" centers along the bars. After the bars were prepared on the lathe each area was sandblasted with a fine sand and cleaned with acetone to remove all grease.

An epoxy adhesive, Armstrong Type A-1, was used to adhere the gages to the bar. A uniform layer of adhesive, approximately 1/2 inch by 1 1/2 inches by 1/32 inch thick was placed on the prepared bar area and the strain gage carefully pressed onto the adhesive. Care was exercised to insure that the longitudinal axis of the bar and the gage coincided, and that complete contact between the gage and the adhesive was obtained with no trapped air bubbles. The gages were then clamped in place and the adhesive was allowed to set for 24 hours. After 24 hours, the gages were all checked and a dyke of adhesive approximately 1/8 of an inch high and 1/8 of an inch thick was formed around the gage. This was done to form a reservoir to hold the waterproofing wax. Figure B.1 shows the gage and dyke installation.

The gage and dyke assembly were then allowed to set for a minimum of 24 hours before further treatment. After sufficient time had elapsed for the adhesive to harden, lead wires were soldered to each of the two gage resistance wires and grouped together into groups of eight lead wires to a cable and sealed in the protective plastic insulation material.

Each gage was then covered with a coating of sealing and waterproofing wax that was heated to a liquid form and applied with a small brush. The wax served the purpose of breaking any bond that might develop between

the strain gage and the material used for waterproofing the gage. Any bond would result in false strain readings.

Upon completion of the wax coating the entire assembly was covered with a flexible type epoxy coating to seal and waterproof the entire assembly. Figure B.2 shows a cross section sketch of the entire gage assembly.

The flexible epoxy was basically an epoxy resin containing a large portion of Thikol that provided the resilient properties. The epoxy covering gained a consistency or hardness comparable to an art gum eraser and again, a minimum of 24 hours was allowed to let the coating set up. The finished product for the waterproofing material was an impact and chemical resistant material possessing adhesion qualities to concrete and steel.

The application of the flexible epoxy coating completed the procedure, and the reinforcing bars were ready for installation in the pavement slab.

TABLE B.1

## PERTINENT DATA CONCERNING WHEEL LOAD TESTS

## A. Loads

1. Gross Load = 20,880#
2. Rear Axle = 15,570# - rear wheels = 7,785#
3. Front Axle = 5,310# - front wheels = 2,655#

## B. Tires

1. Dual tires
2. Total contact area for duals = 138 in<sup>2</sup>
3. Contact pressure = 56.8 psi
4. Size = 9 x 22.5 x 10 ply

## C. Time = September 16, 1960, at 8:00-9:30 AM

## D. Test Procedure - Northbound Lanes (0.5% steel)

1. Static load over crack with readings on every gage.
2. Static load at various positions away from crack with readings taken on gage at crack.
3. Dynamic strains taken for gage at the crack for creep speed and 15 mph.

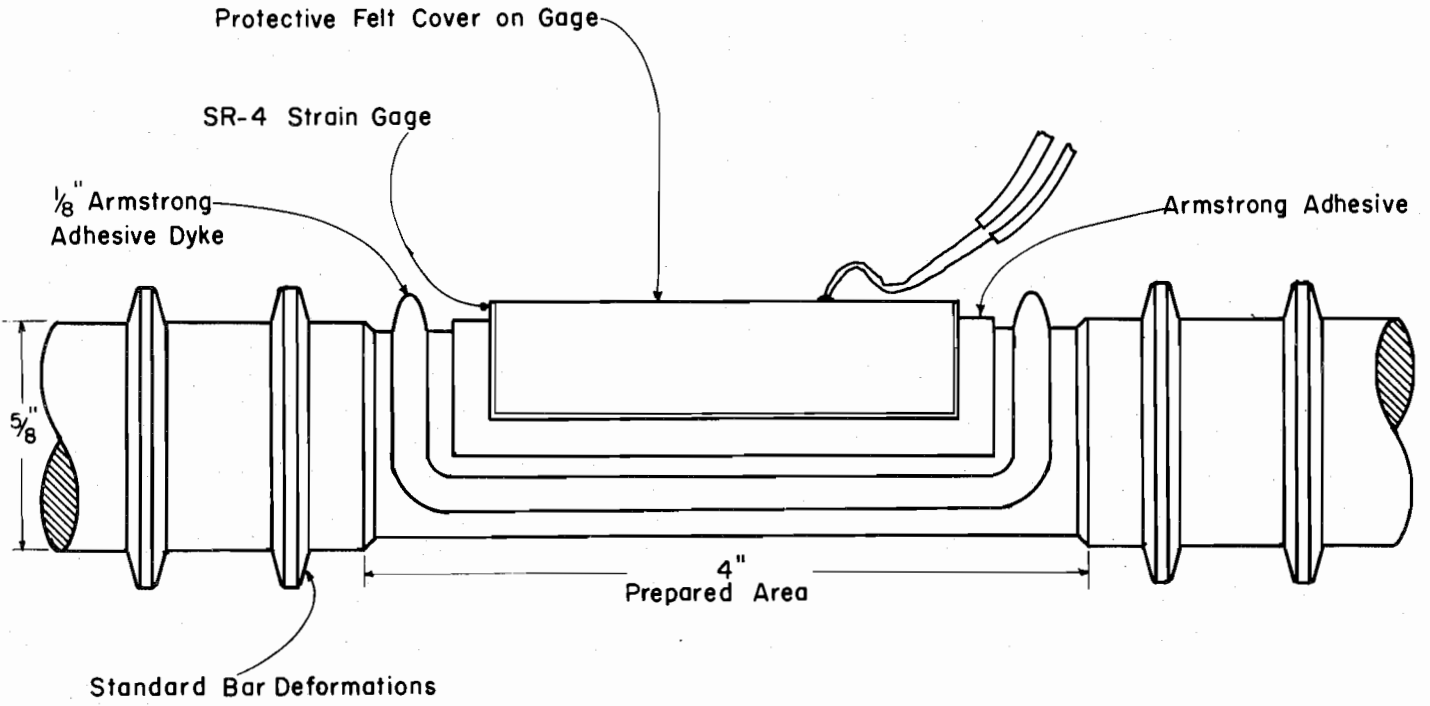


Figure B.1

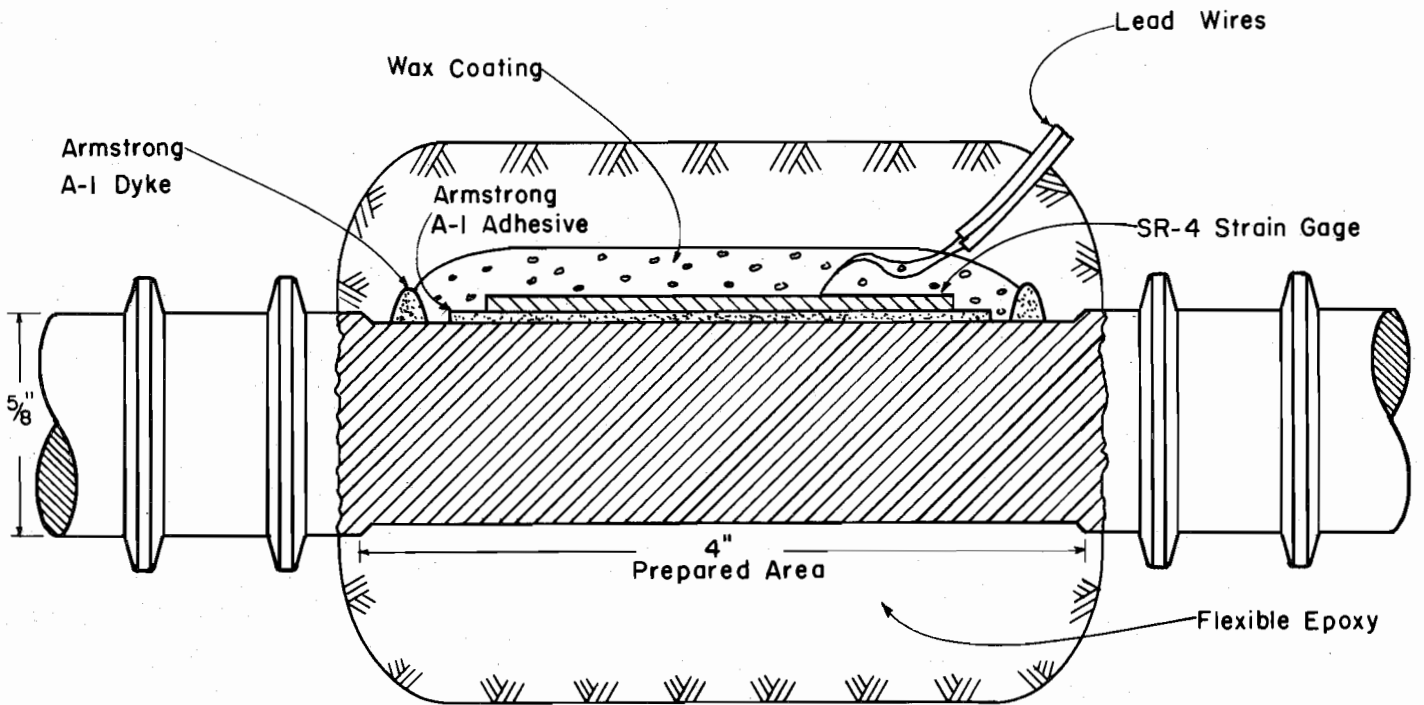


Figure B.2

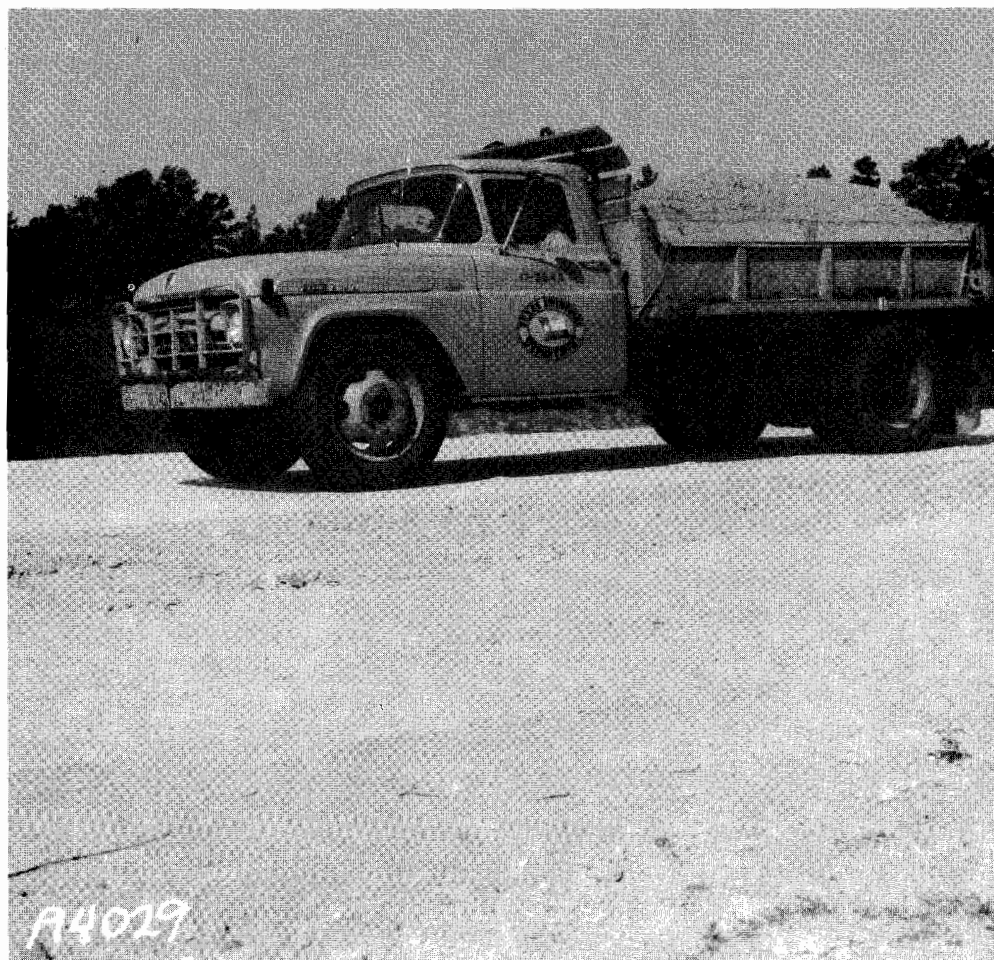
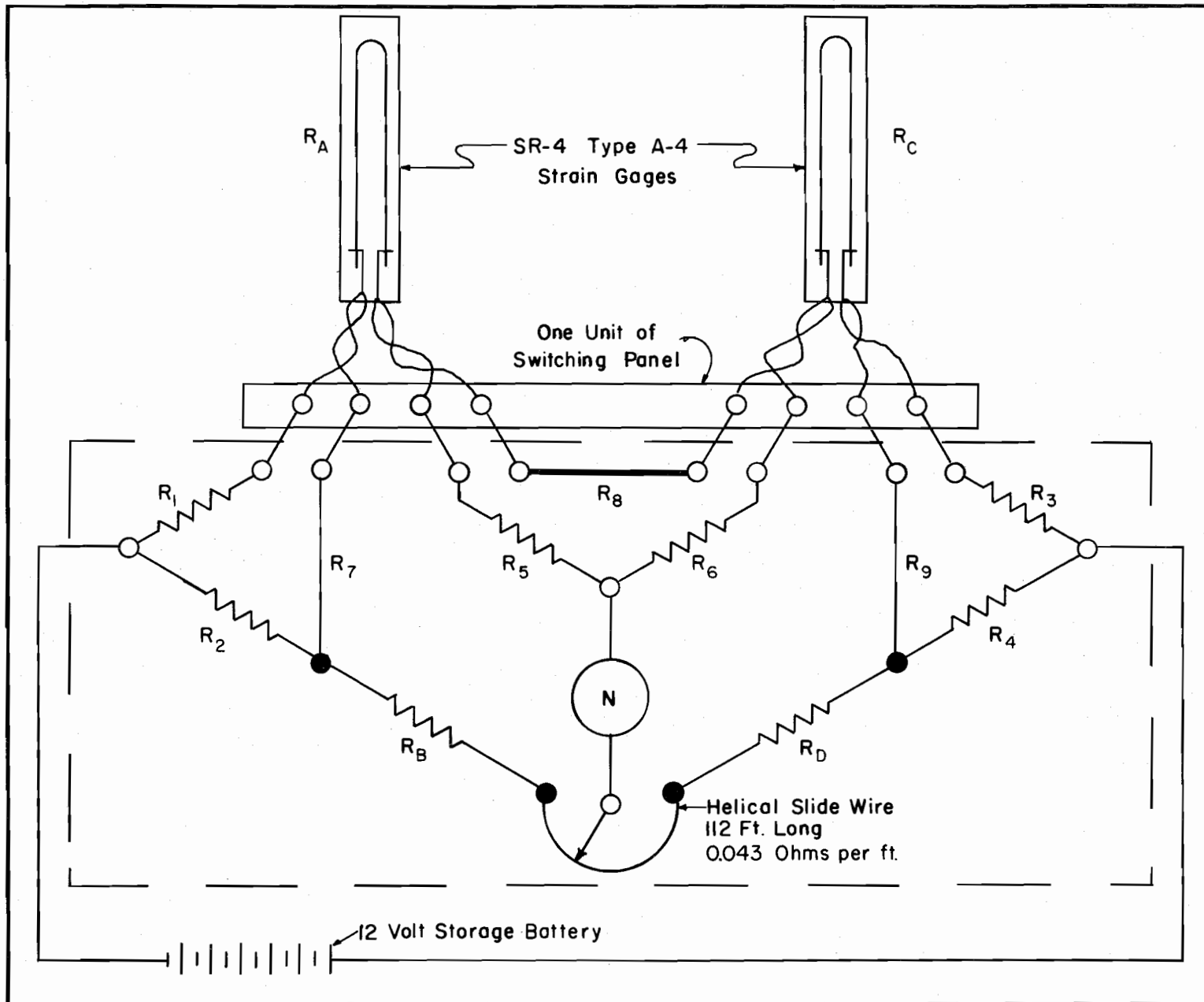


FIGURE B.3 - Vehicle used in wheel load tests.



BRIDGE CIRCUIT USED FOR MEASURING STEEL STRAINS

Fig. B.4



A P P E N D I X C

Stress Calculations

## PROCEDURE FOR STEEL STRESS CALCULATIONS

The measured steel strains are converted to stress in the following manner.

### Between Cracks

$$S_g = 29.14 \epsilon_i \times 10^6 \dots \dots \dots (5)$$

### At Cracks

$$S_t = 22.29 \epsilon_i \times 10^6 \dots \dots \dots (6)$$

### Notations

- $S_g$  = Stress in steel at the gage, psi
- $\epsilon_i$  = Indicated or measured strain in the bar, in/in
- $E$  = Modulus of elasticity of the steel bar, psi
- $F$  = Gage factor of the strain gage being used
- $\epsilon_t$  = True strain in the bar, in/in
- $S_t$  = Stress in a typical 5/8 inch  $\emptyset$  bar, psi

### Development

The variable resistance instrument box used on this project was calibrated to read strain directly. This calibration is based on a gage factor of 2.08. If strain gages with varying gage factors are used, the strain must be corrected by the following formula:

$$\epsilon_t = \epsilon_i \frac{2.08}{F} \dots \dots \dots (1)$$

After obtaining the true strain in the bar, the stress in the steel is calculated as follows:

$$S_g = \epsilon_t E \dots \dots \dots (2)$$

The stress obtained from formula (2) is the stress in the steel at the gages which is in an area of reduced cross section. This elevated stress must be corrected back to what would be experienced in a typical 5/8 inch  $\emptyset$  bar by the following<sup>a</sup>:

$$S_t = 0.765 S_g \dots \dots \dots (3)$$

For simplicity purposes the above formulas could be reduced to one; hence, requiring only one calculation for stress. Within the mass of the concrete only formulas (1) and (2) should be used, whereas all three could be used when calculating the stress at a crack.

Calculating Stresses Between Cracks

$$S_g = \epsilon_t E \dots \dots \dots (2)$$

Combining Equations (1) and (2):

$$S_g = \epsilon_i \frac{2.08}{F} \cdot E \dots \dots \dots (4)$$

Preliminary laboratory tests on the steel showed  $E_s = 27.6 \times 10^6$  psi, and the gage factor for the gages used was 1.97. Substituting these values in the above Equation (4):

$$S_g = 29.14 \epsilon_i \times 10^6 \dots \dots \dots (5)$$

Calculating Stresses at the Crack

$$S_t = 0.765 S_g \dots \dots \dots (3)$$

Combining Equations (3) and (4):

$$S_t = 22.29 \epsilon_i \times 10^6 \dots \dots \dots (6)$$

---

<sup>a</sup>See the treatise on Steel Stress Correction for Gages at transverse cracks for development procedures.

## STEEL STRESS CORRECTION FOR GAGES AT TRANSVERSE CRACKS

Prior to attaching the SR-4 Strain Gages to the longitudinal steel bars, each bar was "turned down" on a lathe to a uniform diameter over a length of four inches. The "turning down" operation was required in order to obtain a smooth surface for cementing the gages to the bars. Therefore, each of the areas was "turned down" to approximately the same diameter for the sake of uniformity. This operation procedure resulted in a net reduction in the effective cross sectional area of the bar.

An examination of the stress conditions in the steel bars reveals the problem created by this operational procedure. Figure C.1 portrays a free body diagram of force conditions in the longitudinal steel at the crack. The forces in each of the bars are approximately equal, therefore, the average strain between points of bond rupture (loss of bond) of the concrete to the steel must be equal. The necked down area must transmit the force, hence a higher stress results in this area due to the reduced cross-sectional diameter of the bar. Correspondingly, an increase in stress results in an increased strain, therefore, the measured strain is of excessive magnitude even though the average strains in all bars between points of bond rupture are equal. With this in mind, it is proposed that the measured strain be corrected by multiplying the ratio of the cross-sectional area at the gage to the normal cross sectional area of the bars.

This correction is based on the following assumptions:

- (1) The point of bond rupture is outside the reduced cross-sectional area of the bar.
- (2) The forces in each of the bars are approximately equal.

Numerous papers on bond of concrete to steel portray the phenomenon of bond development. These papers

should be referred to for the concept of bond development used in this paper. The first assumption is quite plausible since the waterproofing agent extended outside the necked down area. If the point of rupture extended a finite distance outside the necked down area in proportion to the force applied, the second assumption would be valid.

Obtain correct stress as follows:

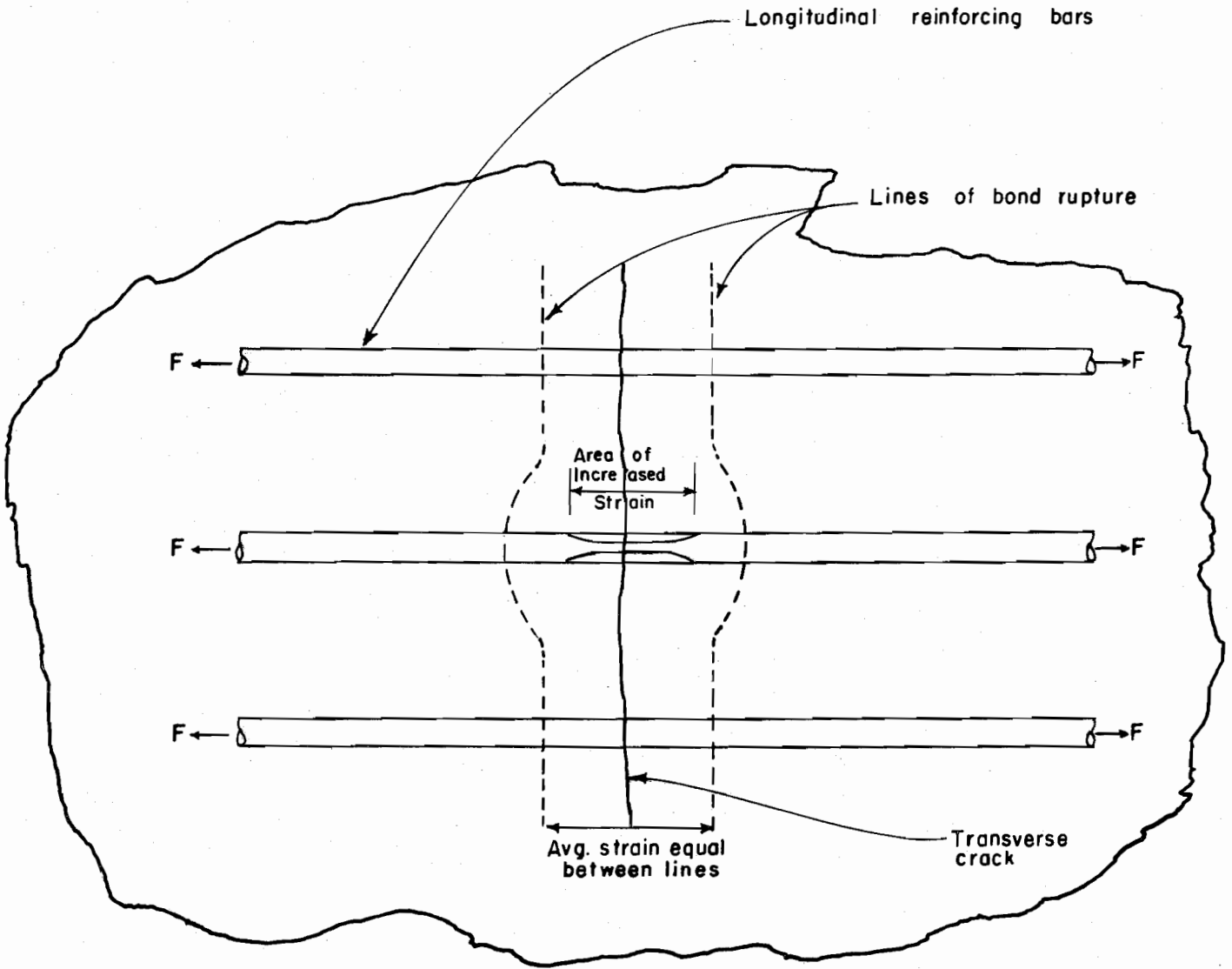
$$S_t = S_g \frac{A_g}{A_n} \dots \dots \dots (1)$$

- where:  $S_t$  = correct steel stress in normal bar, psi.  
 $S_g$  = stress in steel at the gage, psi.  
 $A_g$  = cross sectional area of bar at the gage, square inches.  
 $A_n$  = cross sectional area of a normal bar, square inches (0.31 square inches).

From preliminary measurements the average diameter of the neck down area was equal to 0.549 inch (maximum departure from the average is 0.005 of an inch - less than one per cent) substituting in Equation (1):

$$S_t = S_g \frac{\left(\frac{0.549}{2}\right)^2 \pi}{0.31} = \frac{0.237}{0.310} S_g$$

$$S_t = 0.765 S_g$$



FREE BODY DIAGRAM OF FORCES PRESENT  
AT A CRACK IN  
CONTINUOUSLY REINFORCED CONCRETE PAVEMENT

Fig. C. 1